TRANSIENT PHENOMENA IN FALSE TWIST TEXTURING

by

CHARLES E. BELL

B.S., Lafayette College
(1974)

S.M., Massachusetts Institute of Technology
(1976)

SUBMITTED IN PARTIAL FULFILLMENT
OF THE REQUIREMENTS FOR THE
DEGREE OF

MASTER OF SCIENCE

at the

MASSACHUSETTS INSTITUTE OF TECHNOLOGY

(September 1976)

Signature of Author _____
Department of Mechanical Engineering, August 10, 1976

Certified by _____
Thesis Supervisor

Accepted by _____
Chairman, Department Committee on Graduate Students

TRANSIENT PHENOMENA IN FALSE TWIST TEXTURING

by

CHARLES E. BELL

Submitted to the Department of Mechanical Engineering on August 20, 1976 in partial fulfillment of the requirements for the Degree of Master of Science.

ABSTRACT

This study is concerned with non-steady state behavior of the false twist texturing process used by textile mills for increasing bulk, cover and stretch of thermoplastic continuous filament yarns. In particular, this investigation focusses on unsteady state interactions between the feed yarn and machine components of the texturing process at several machine speeds. The influence on threadline forces and twists of rotational slippage in a pin-spindle twister is observed. Also investigated are draw texturing threadline force responses to oscillating spindle speed and oscillating draw point position. A brief geometric computer treatment, based on a simplified threadline model, is developed for simulating each of the above transient operating conditions and computed results show qualitative agreement with experimental observations. Preliminary threadline tension data obtained during transient operation of commercial pin twister and friction twister texturing machines are also discussed, as well as the effects on texturing parameters of property variation along the length of commercial feed yarns.

ACKNOWLEDGEMENTS

I wish to express my sincere thanks to Professor Backer for his support and guidance throughout the course of my research, and for the encouragement and wealth of information which he has passed along during our many discussions.

I am also grateful to David Brookstein for his help and enthusiasm in the early stages of my work; to Steven Smith and Chris Brogna for their invaluable knowledge and assistance and our many hours of fruitful discussions; to Professor Thwaites, who has provided stimulating concepts and ideas during his stay at M.I.T.; and to all members of the Fibers and Polymers Laboratories for their continuing assistance and moral support.

Special thanks go to Dorothy Eastman for typing the entire thesis manuscript and for all of her helpful suggestions; and to Sharon Joiner for cheerfully preparing the major portions of the thesis illustrations.

The financial and technical support supplied by Burlington Industries, E. I. duPont de Nemours and Company, and the UNIFI Corporation during the course of this research has been greatly appreciated. Support has also been provided from the E. I. Valko Fellowship Fund.

Finally, I thank Karma with all of my heart for her loving patience and encouragement.

TABLE OF CONTENTS

I.A. Texturing of Thermoplastic Yarns

Texturing is a general term used in the textile industry in reference to processes by which crimp, bulk and stretch are imparted to yarns consisting of ordinarily straight filaments or fibers. Most generally, texturing is performed on continuous filament thermoplastic yarns. A yarn to be textured for apparel usage consists of a bundle of individual filaments, each on the order of one mil in diameter, extruded (spun) from polyester or nylon polymer melt. As they leave the spinning operation, these yarns are straight, lean, and relatively inextensible, unlike natural fibers such as cotton or wool which exhibit an inherent crimp. In order to obtain filament properties resembling those of natural fibers, a variety of different texturing processes have been applied to thermoplastic yarns as shown in Fig. 1 from Backer [1].

(a) False Twist. In the false twist texturing process, the yarn is twisted and exposed to heat such that the thermoplastic filaments are "set" into a coiled geometry. The yarn is then untwisted, but the crimp remains in the filaments. (This process will be discussed in greater detail in Section I.B.)

(b) Edge Crimp. A pronounced crimp can also be inserted by running the filaments across a hot sharp edge, which physically deforms one side of each filament, causing the filaments to coil when tension is released. Heat makes the

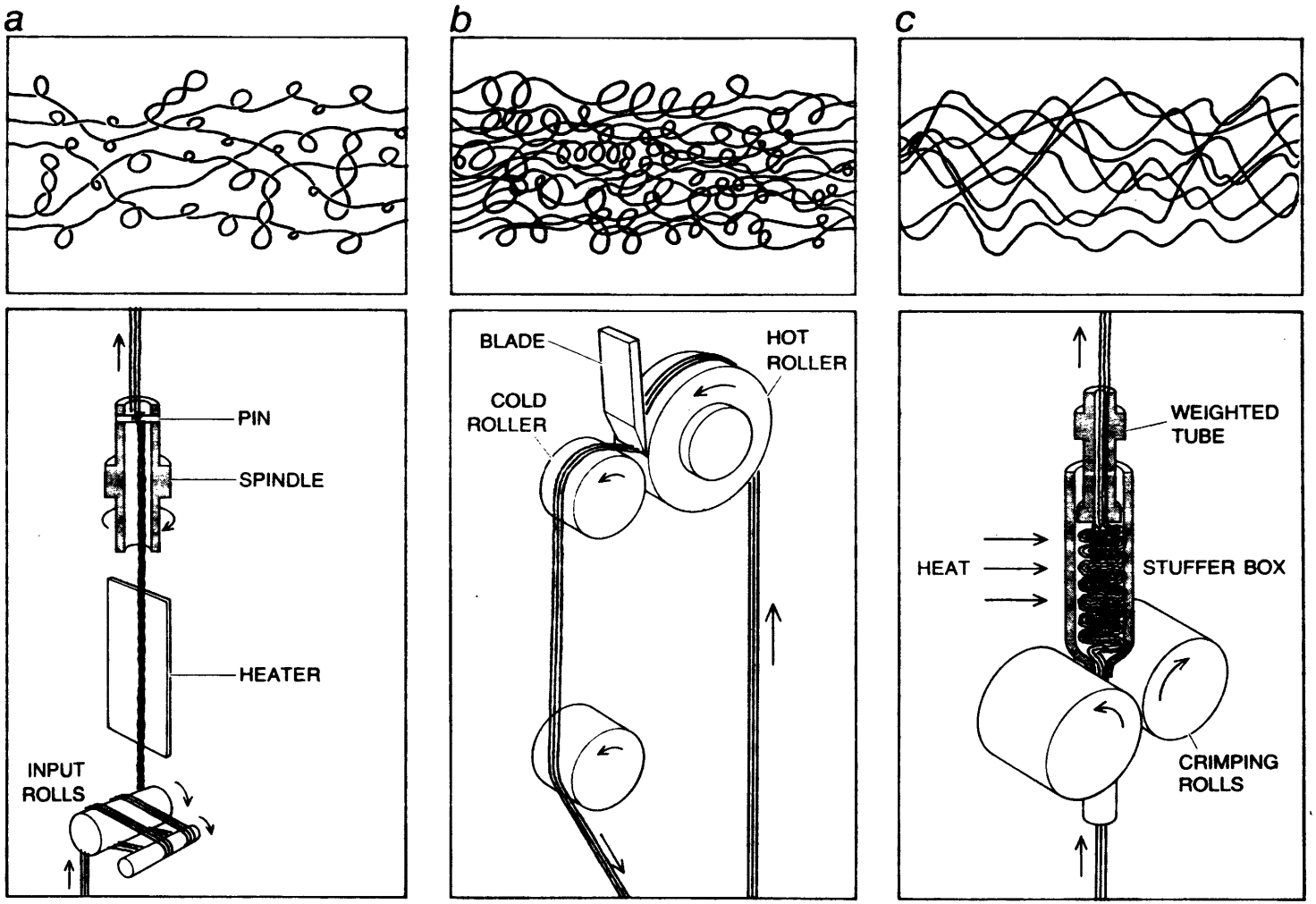

FIGURE 1a METHODS OF TEXTURING

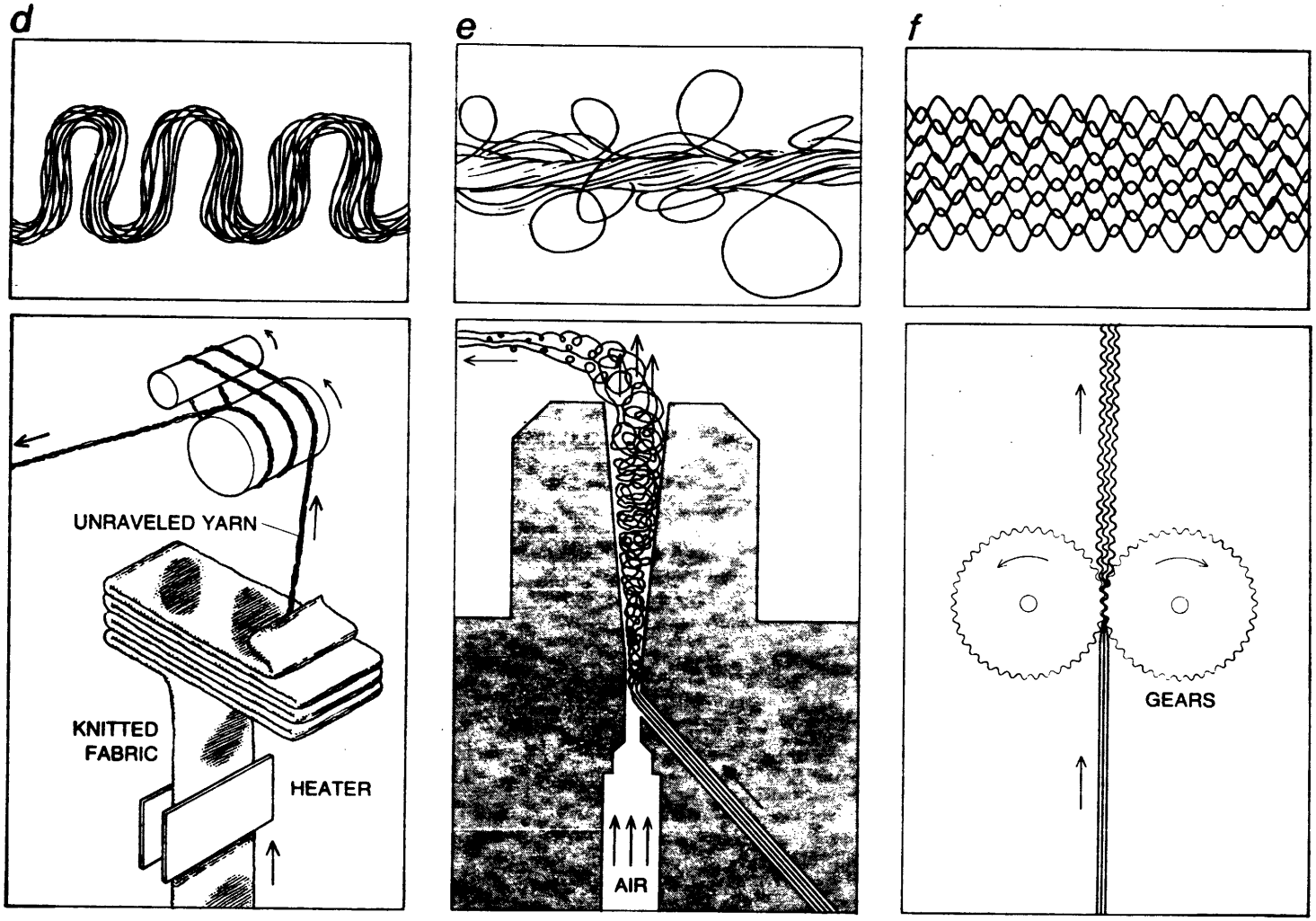

FIGURE 1b METHODS OF TEXTURING

crimp more permanent by establishing new molecular bonds in the deformed material.

(c) Stuffer Box. An effective but less pronounced crimp is imposed by buckling, bending and compressing the filaments and storing them under pressure in a hot chamber. By the time they are pulled out of the output end of the box, the deformed geometry has been heat set into the filaments.

(d) Unravelled Knit. This unusual method of texturing involves knitting a circular tube fabric, heat setting the fabric, and then unravelling the knit structure. A gross, wavy crimp is thus imparted to the entire yarn.

(3) Air Jet. A turbulent airstream can be used to entangle yarn filaments and form open loops on the surface of the bundle. The result is a less extensible textured yarn, but this is often desirable in terms of improved dimensional stability of a fabric.

(f) Gear Crimp. A flat or planar crimp can be obtained by running filaments between hot gear teeth. The lack of a three-dimensional crimp, however, limits the bulk which these yarns can exhibit.

Of all the methods of texturing available, by far the most widely used for continuous filament yarns is the false

twist process.

This thesis examines certain aspects of the false twist texturing system with major emphasis given to non-steady state interaction between the thermoplastic twisted threadline and the mechanical and thermal elements of the texturing machine.

I.B. The False Twist Texturing Process

An idealized schematic representation of the industrial false twist texturing process is shown in Fig. 2. During normal operation, the twister and rollers are rotating at constant speeds. Thermoplastic feed yarn is pulled off the end of a feed yarn package and enters the feed rollers while in a virtually non-twisted state. As the yarn enters the first heater zone, or texturing zone, which lies between the feed rollers and the twister, it twists in response to the torque which has been imposed in the yarn by rotation of the twister. Thus, the yarn is in a twisted state as it passes over the first heater and the filaments in the yarn are heat set into a roughly helical geometry. The yarn is then allowed to cool for a short time before reaching the twister. During steady state operation, the twister imparts a fixed angular velocity to the yarn at a point between the first heater and the intermediate rollers, and as the twisted yarn passes this point, suddenly the direction of rotation of the twister with respect to the direction of twist in the yarn changes sign, and twist is removed from the translating yarn. But even though there is zero twist in the yarn downstream of the twister, the individual filaments remember the coiled geometry in which they were heat set, and the yarn as a whole is bulky and highly extensible as it enters the second heater zone.

The second heater zone may or may not be used, depending on how much extensibility is desired in the textured yarn being produced. Textured yarn taken as it leaves the intermediate

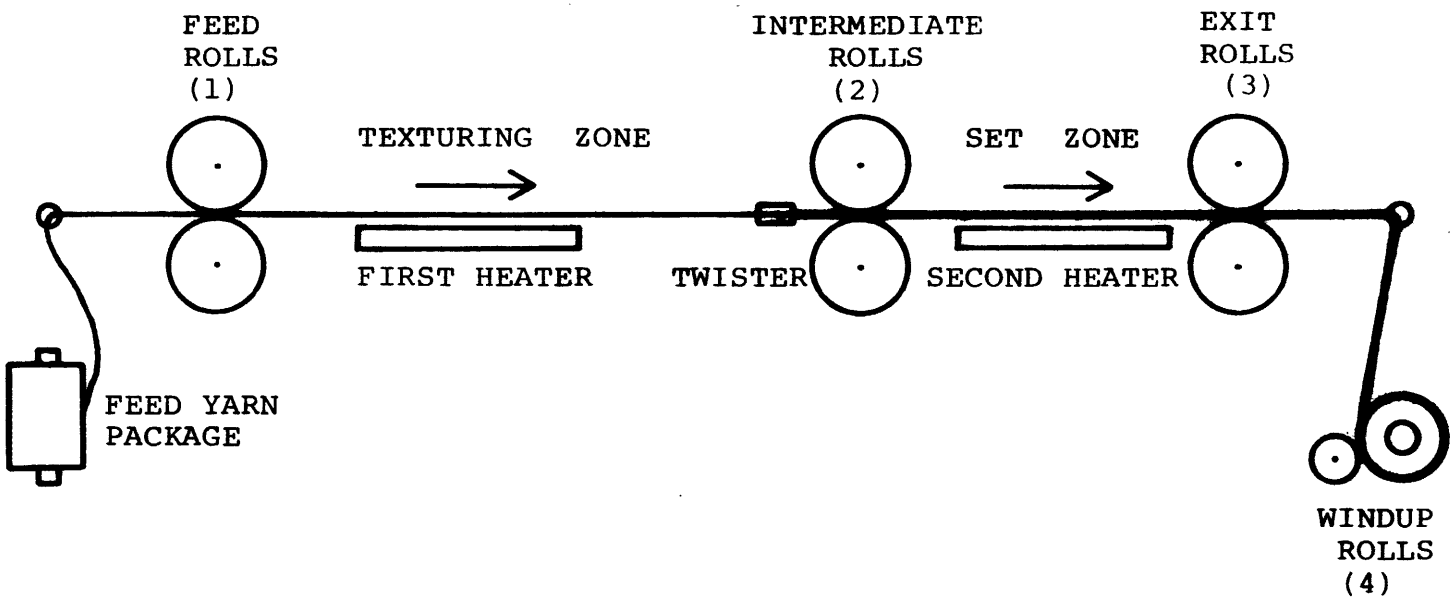

FIGURE 2 THE FALSE TWIST TEXTURING PROCESS

rollers has the ability to retract by about 50% from a straightened configuration, upon release of tension, and this yarn, known as single heater yarn, is used in stretch garments. However, in producing textured yarn to be used in garments requiring greater dimensional stability, some of the liveliness in the yarn is relaxed out using a second heater. The degree of bulk or crimp remaining in the yarn as it leaves the second heater is determined by the relative velocities of the intermediate and exit rollers, and the second heater temperature. Yarns which have been relaxed in this manner, using a second heater, are known as "set yarns", and generally have the ability to retract only about 5-15% from a straightened configuration upon release of tension.

A side view diagram of a typical modern industrial texturing machine is shown in Fig. 3, the yarn path being represented by a dotted line. The hardware responsible for the texturing of any one yarn is known as one position on the machine, and there are often more than 200 side-by-side positions on one texturing machine, all connected through common shafting. In the machine of Fig. 3, three vertically spaced package winding stations accommodate each group of three machine positions. A large flexible belt which runs the length of the machine perpendicular to the page drives the twister units. The tension measuring device shown in the figure is optional, and is not normally supplied on industrial machines.

Texturing machine configurations vary within and between manufacturers, but perhaps the greatest difference between machines is in the design of the twister units. Two distinct

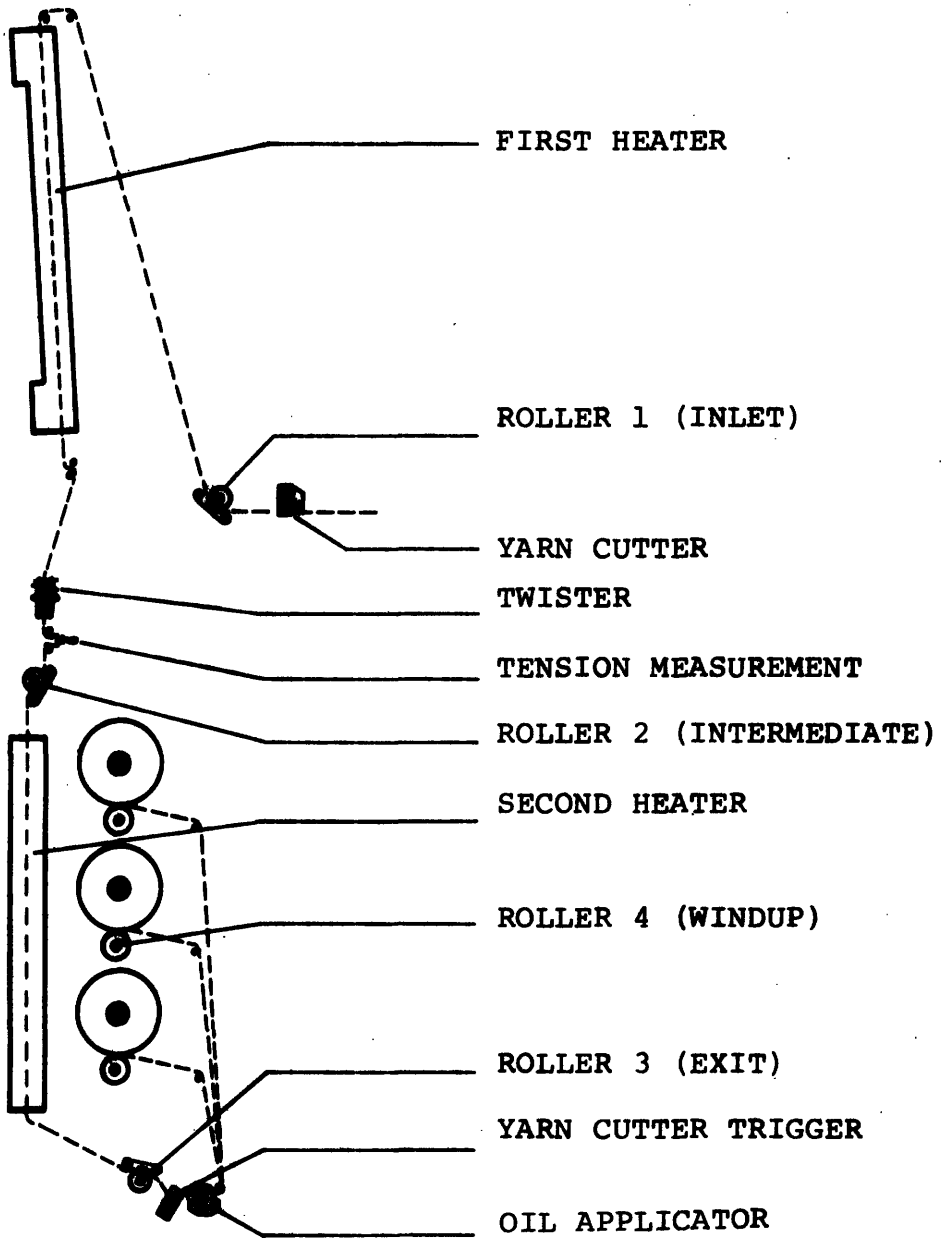

FIGURE 3 A MODERN COMMERCIAL FALSE TWIST TEXTURING MACHINE

twister types are used in texturing machines, "pin" twisters and "friction" twisters. A pin twister, or spindle, is shown in Fig. 4. It consists of a small ceramic pin less than 1 mm in diameter which is fixed inside and normal to the axis of a small metal cylinder. The cylinder, which is mounted in bearings, or held in place magnetically, is rotated about its axis either by belt drive or friction wheel drive. The yarn is wrapped once around the ceramic pin and thereby rotates with the angular velocity of the spindle assembly, while simultaneously translating around the pin. The pin spindle represents an early successful texturing twister and its use still dominates the texturing industry. However, limitations in texturing speed imposed by the pin spindle have led the development of "friction" twisters which do not require a full 360 degree wrap around a driving pin. By going to friction bushings of the type shown in Fig. 5a, and ultimately to the friction disc aggregates of Fig. 5b, textured yarn manufacturers have been able to increase their production speed per position from about 200 meters per minute, using pin spindles up to about 600 meters per minute using the friction disc aggregates. At these highest speeds, in order to attain twist levels of about 90-100 turns per inch of twisted yarn (required for effective crimp development), the angular velocity of the yarn at the twister must be on the order of a million RPM. This speed is attainable by virtue of the high twister-to-yarn-diameter ratio, which is normally on the order of several hundred.

In the last few years, a large portion of texturing machines being produced are equipped with friction twisters,

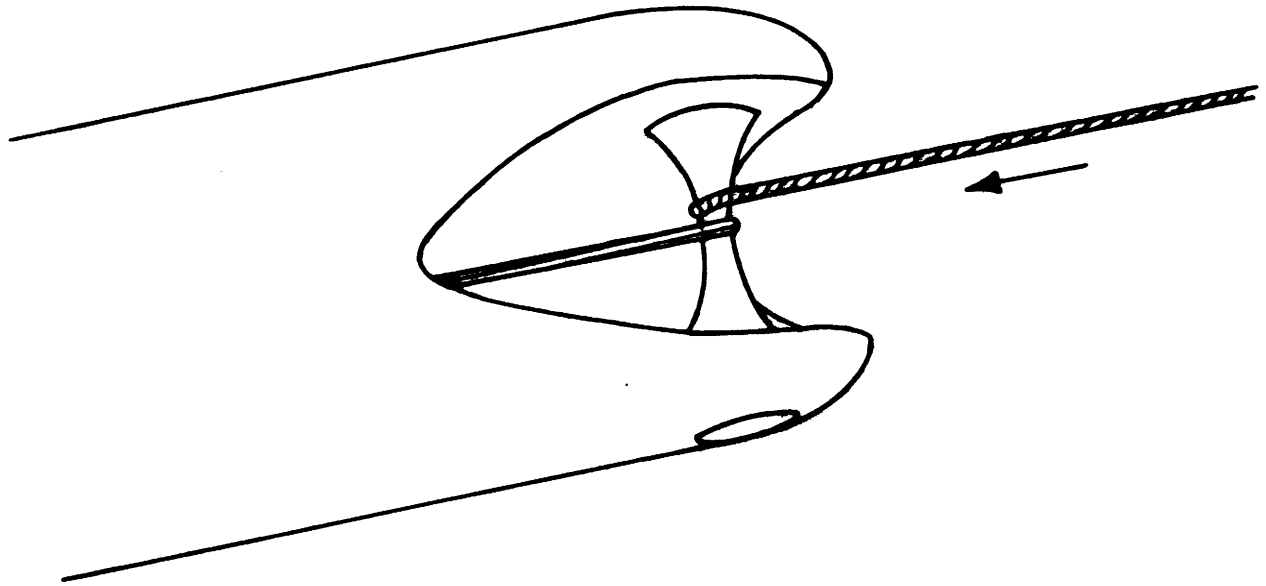

FIGURE 4 A PIN-SPINDLE TWISTER

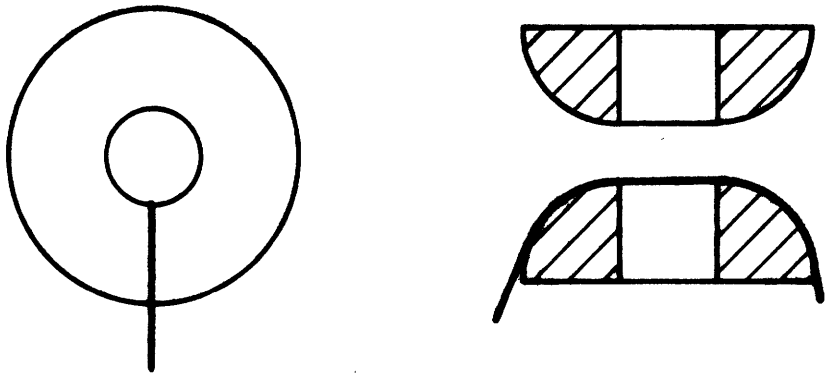

(a) FRICTION BUSHING

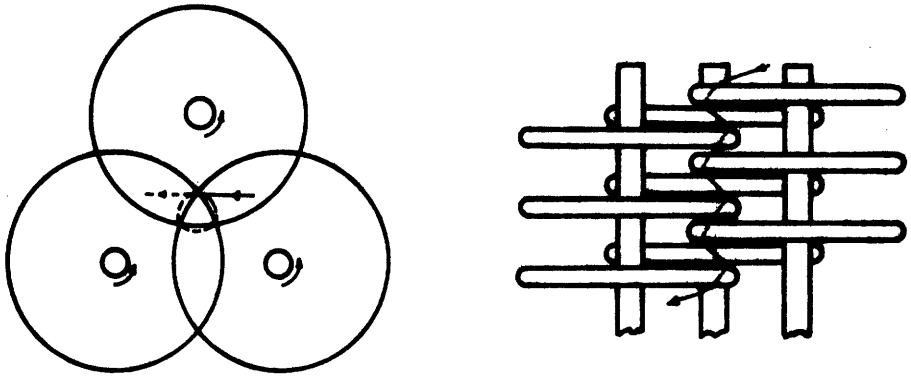

(b) FRICTION DISCS

FIGURE 5 COMMON FRICTION TWISTERS

particularly of the disc variety, and their use is rapidly overtaking that of older pin spindle machines.

Feed Yarns

Two standard types of thermoplastic feed yarn are processed on industrial false twist texturing machines; fully oriented yarn (flat yarn), and partially oriented yarn (POY). Prior to 1972 [2], most feed yarn intended for texturing was extruded and subsequently drawn to maximum orientation by the fiber producers. Thus, no drawing took place when this fully oriented yarn was textured by the textile manufacturer (conventional texturing). Since then, a drawing operation has been combined with the texturing process such that partially oriented feed yarn is either drawn to full orientation prior to texturing in a separate zone on the texturing machine (sequential draw-texturing), or it is drawn where it softens over the heater in the texturing zone of the machine (simultaneous draw-texturing). This combination of the drawing and texturing operations is advantageous for several reasons:

1. The separate drawing operation by the fiber producer is eliminated in the production of partially oriented yarns. Instead, a partial drawing is given to the filaments immediately upon extrusion by increasing the windup speed of the extrusion (spinning) machines.
2. Texturing machines need virtually no modification to convert from conventional texturing to simultaneous draw-texturing.

I.C. Motivation for Study of the False Twist Texturing Process.

As textured yarn manufacturers reach for increasingly higher production speeds, machinery has become increasingly sophisticated and the need for understanding the mechanics of the texturing process has never been greater. The problems of maintaining product quality and uniformity at ever increasing operating speeds has been compounded in recent years by changes in fashion relating to the major textured yarn apparel products. The popular plaid patterns of several years ago have given way to solid colors, creating a paramount importance for textured yarn uniformity and consistency.

In commercial knitting operations, yarns from many packages (often 30 or more) of textured yarn are fed into the knitting machines simultaneously in creating a fabric. If one or more of these yarns is significantly different from the others in terms of dyeing characteristics or bulk, then a marked streak or streaks which repeat(s) periodically could result in the fabric when it is dyed. Such patterns, known as barré, render the fabric inferior and capable of being sold only as second quality merchandise. It is thus crucial to develop a full appreciation of the important variables in the texturing process and their influence on the textured yarn product such that problems with yarn non-uniformity can be detected and corrected in a rapid, efficient manner. Further, once an understanding is reached concerning the effect of various feed yarn parameters on the texturing system, material

properties of machine designs could be modified toward providing improved process consistency and controllability.

With these general goals in mind, studies of stable and unstable transient threadline behavior have been undertaken in an attempt to establish the probable causes of process and hence product variation.

II. EXPERIMENTAL AND ANALYTICAL MODELS OF THE FALSE TWIST TEXTURING SYSTEM

II.A. The MITEX Laboratory Texturing Machine

The MITEX texturing apparatus (Fig. 6) is a bench-size model of a single heater texturing machine which has been designed to operate at slow throughput speeds in the range of 0 to 5 inches per second. In addition to the standard components of a single heater machine, i.e. feed guides, feed rolls, heater, twister (pin spindle), exit rolls, and windup, the MITEX machine is equipped with a pair of torque-tension transducers which provide for continuous monitoring of threadline axial tension and torque before the spindle, and threadline tension after spindle, as shown in Fig. 6. A detailed description of the MITEX torque-tension device is found in reference [2].

The inlet and exit rollers of the MITEX texturing machine are each gear-driven by independent synchronous motors, with roller speeds being incrementally adjustable by changing drive gear ratios. The spindle, however, is belt driven by a DC motor and spindle speed is continuously variable using either of two methods: a variac speed control ($\pm$1% drift), or an amplidyne driven by a variable voltage supply ($\pm$2% drift). A small industrial texturing heater is used on the MITEX machine and temperature is maintained within $\pm$2°C by a Rosemount controller, which includes a temperature readout meter. Any two of the torque, tension, and spindle speed signals can be recorded simultaneously on the two channel DC amplifier strip

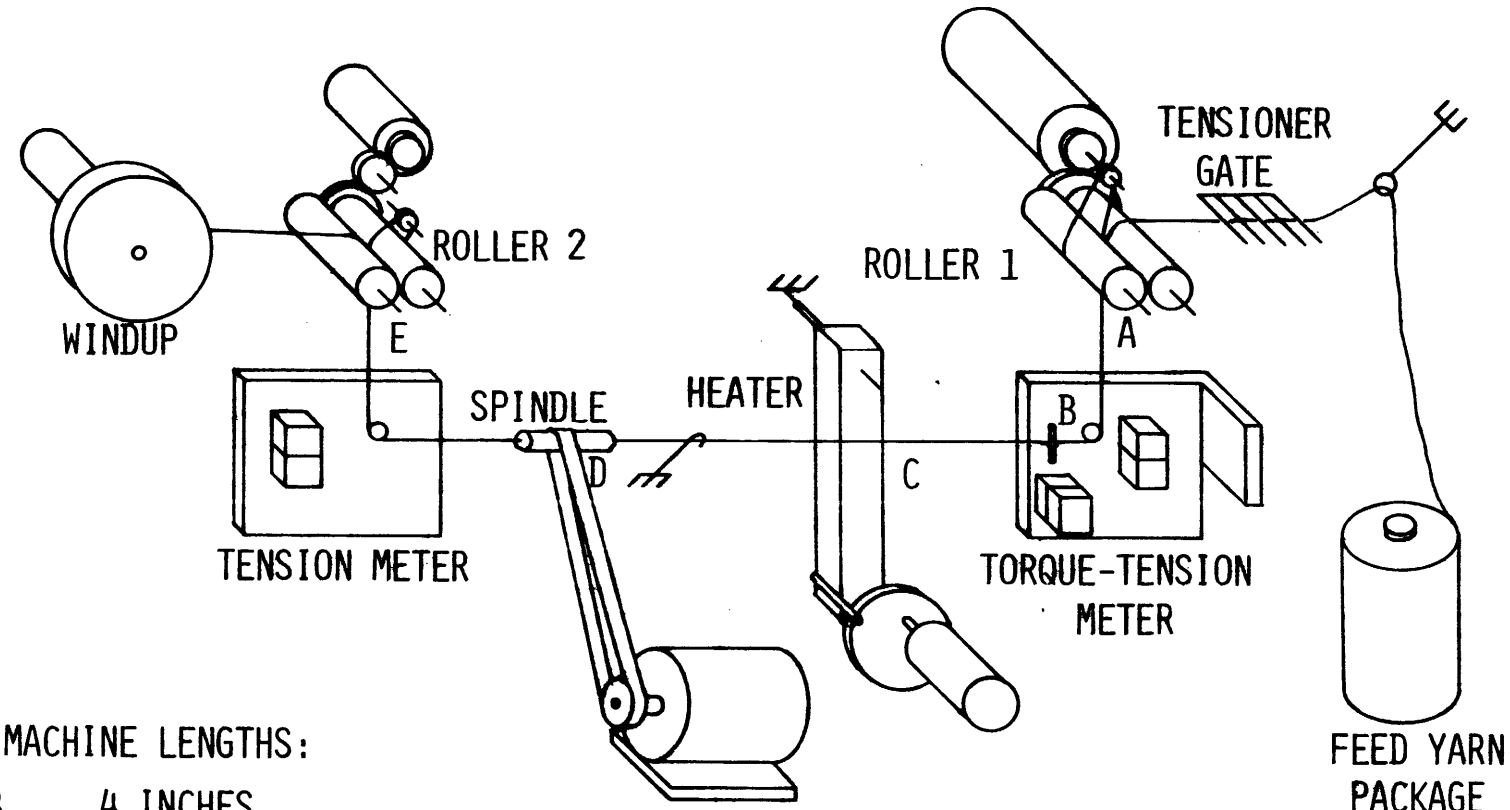

MACHINE LENGTHS:

A-B	4 INCHES
B-C	6 INCHES
C-D	11 INCHES
D-E	9 INCHES

FIGURE 6 THE MITEX TEXTURING APPARATUS

chart recorders used with the above apparatus. Calibration of the instrumentation is done as described in Appendix 6.

The MITEX machine is designed for the texturing of standard industrial feed yarns, and it is intended that observations made on the MITEX will be directly applicable to texturing as performed by industrial machines, although no strict dimensional analysis or scaling of all important variables has been performed to determine dynamically similar machine/material parameters for the case of slow speed operation.

In addition to the question of dynamic similarity between the slow and high speed cases, one must also keep in mind the different machine configurations between industrial texturing machines and the MITEX machine. As was seen in Fig. 3, commercial machines have numerous guides and other threadline interferences which are bound to affect twist and force distributions throughout the system. For practical purposes, these aspects have been left out of the MITEX machine, but their presence will not be forgotten when analytical models and laboratory experimental results are used to predict the performance of commercial machines.

II.B. The Steady State Analysis and Transient Analysis Computer Models

A detailed analytical approach toward modeling of the false twist texturing process undertaken by Brookstein [2] has culminated in the development of a computer program package which can be used to simulate threadline mechanics during steady state or transient draw texturing conditions. The programs were developed with a view toward predicting the performance of an actual texturing system based on a given set of material and machine input parameters. Using the computer models, broad parametric studies of the texturing system can be performed more quickly and efficiently than is possible experimentally, and it is intended that these studies will lead to an appreciation for the important variables in the texturing system, as well as offer valuable engineering guidelines for improvements in feed yarns or texturing machine design.

The program package was developed in two main units, the first being the steady state analysis, which represents a closed form steady state solution to the threadline forces and geometries in the texturing zone and "post-spindle" zone of a theoretical single heater texturing machine. The second unit of the program package is the transient analysis which, when used as an extension of the steady state program, will compute the dynamic behavior of the texturing machine threadline in response to time varying machine and material parameters.

In developing the theoretical texturing model represented by the above computer programs, simplifying assumptions were made based on numerous experimental observations made on the MITEX texturing apparatus. A brief review of these assumptions and other important aspects of the model are listed below, as adapted from Brookstein [2].

(1) The single heater texturing machine is divided into four zones between rollers 1 and 2; the cold zone, the hot zone, the cooling zone, and the post-spindle zone.

(2) Individual filaments making up the yarn in each zone are grouped into three concentric layers around a core filament, and the filaments in each layer of twisted yarn follow right ideal helices.

(3) All filaments are strained equally in the twisted yarn of the cold zone.

(4) The effect of interfiber friction and transverse stresses on threadline torque is considered negligible at the cold zone and hot zone entrances.

(5) The friction between yarn and spindle does not significantly affect linear velocities of the threadline in draw texturing.

(6) Tension and torque in the texturing threadline are uniform from the entry roll to the spindle.

(7) Hot zone threadline, cooling zone threadline, and spindle rotational velocities are equal.

(8) At steady state conditions, the twist in the texturing zone has two uniform levels, one for the cold zone,

the second for the hot and cooling zones.

(9) Inertial effects on threadline mechanics are considered negligible.

(10) Threadline torque at the entrance to the hot zone is primarily due to fiber tension.

(11) Two different models of twist contraction in the cold zone can be used, one based on an averaging over the entire yarn cross section, the other based on averaging over the yarn radius. The model based on an averaging over the entire cross section is used in all other zones.

With these assumptions in mind, steady state equations for threadline twists, filament strain, draw ratio of each filament layer, and threadline forces were derived to formulate the steady state analysis. Computations are carried out in the steady state analysis based on the following input parameters: machine zone lengths, machine speeds, filament layer radii in the threadline of each zone, the number of filaments in each layer of each zone, cold filament rigidities and hot stress strain parameters. The latter parameters were represented by two coefficients of a polynomial expression used to fit data obtained in filament tension vs. draw ratio tests at a given temperature ($T_{fil} = A \cdot DR^2 + B \cdot DR^3$). The steady state program provides good predictions of threadline force and twist values as can be seen in Appendix 2, where computed threadline forces have been included next to experimental values for various POY-PET yarns.

The steady state equations were subsequently differentiated with respect to time in developing the transient analysis, which in its present form is dependent on the steady state program for initial conditions. The transient analysis utilizes the DYnamic SYStems (DYSYS) integration routine available in the Joint Mechanical Engineering-Civil Engineering Computer Facility at M.I.T. to carry out numerical integration of the describing equations.

Only limited usage of the transient analysis was made during the course of the research discussed in this thesis, and the results thereof are reported in Appendix 2. Much effort has gone into understanding the mechanics and solution methods used in the transient model, however, and these concepts have provided a basis for the kinematic computer model presented in the following section, as well as for much of the experimental work discussed in Chapter III.

II.C A Kinematic Computer Model

For use in conjunction with the MITEX texturing apparatus and as an aid toward understanding the basic dynamic behavior of the texturing system, a simple mathematical model was developed, based on the sketch shown in Fig. 7. In this model the threadline consists of a single cylindrical layer of filaments following parallel helical paths.

The texturing process is lumped into six idealized zones as numbered in the sketch, with corresponding small letters designating endpoints of each zone. In Zones 0 through 3, the one layer of filaments is arranged in a helical geometry with a constant radius and a variable but uniform helix angle throughout each zone. The filaments are considered inextensible, except at the interface between Zones 1 and 2 (where drawing and uptwisting takes place) and they are considered to have zero bending or torsional rigidities. The twister is located at the interface between Zones 2 and 3. Zones 4 and 5 represent twist storage zones only, and the filament geometry in these zones is not considered. If the threadline radii for Zones 0 through 3 are known (constant) inputs along with the twister speed (variable), roller speeds (variable), five zone lengths (variable), and the time derivatives of the zone lengths, then the following equations, when combined and integrated, will completely describe the state of the model of Fig. 7 at any time t for a given set of initial conditions:

Equilibrium: Recognizing that axial yarn tension and torque must be equal in Zones 1 and 2 in order to maintain texturing

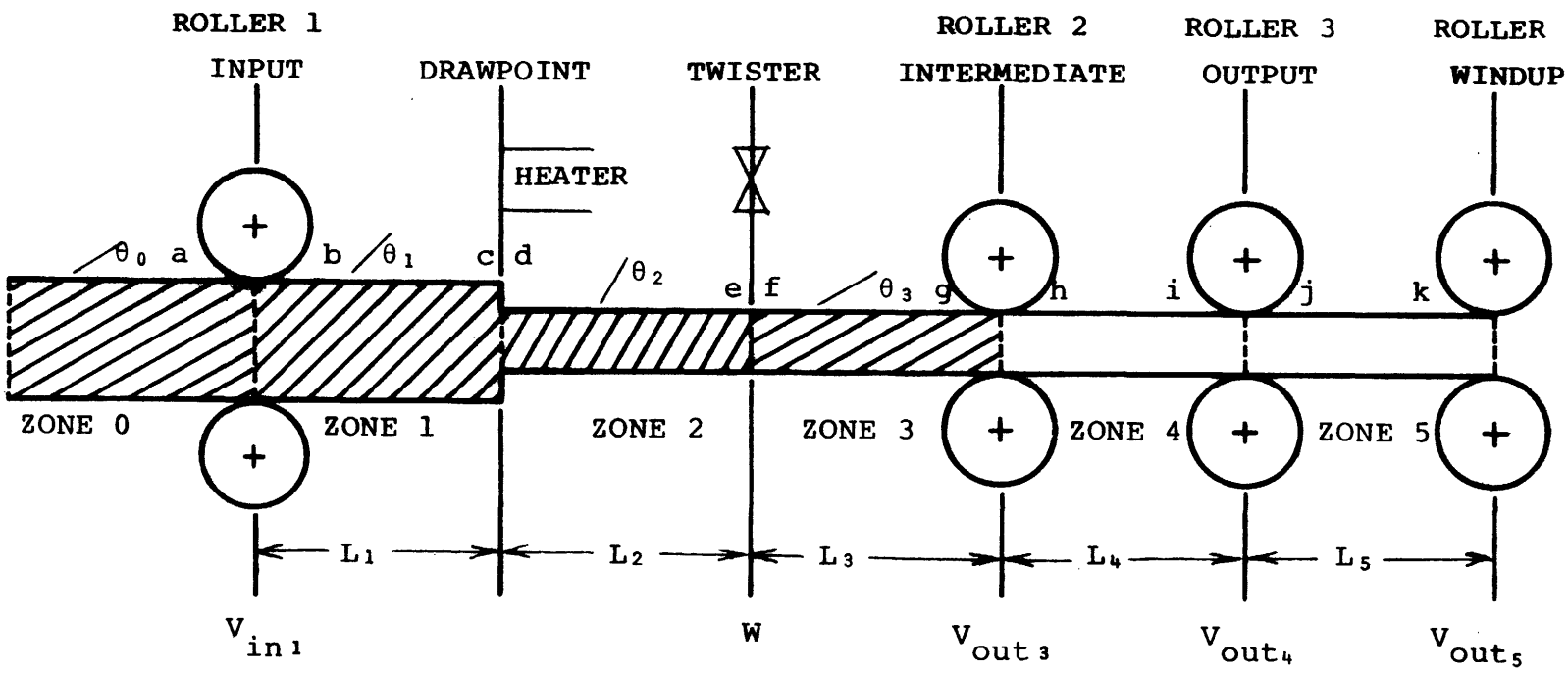

FIGURE 7 MODEL OF THE FALSE TWIST TEXTURING SYSTEM

zone threadline equilibrium, it follows that the geometry of Zones 1 and 2 can be related in this model by the expression shown below (see Fig. 8):

$$R_1 \tan\theta_1 = R_2 \tan\theta_2$$

Filament Length Conservation:

$$\frac{d\,(L\sec\theta)}{dt} = F_{i\ in} - F_{i\ out} \quad (i = \text{Zones } 1, 2, 3)$$

Turn Conservation:

$$\frac{dT}{dt}_i = (P_{in}\, V_{in} - P_{out}\, V_{out})_i + (W_{out} - W_{in})_i$$

(i = Zones 1, 2, 3, 4, 5)

where:

R = zone radius

θ = zone helix angle

L = zone length

F = length of filament per unit time passing a zonal interface

T = total radians of twist in a zone

P = radians of twist per length of twisted yarn

V = linear velocity along yarn axis

W = yarn angular velocity.

By differentiating the Equilibrium expression with respect to time and applying the Length and Turn Conservation expressions to the appropriate zones, the following equations result:

Equilibrium:

$$\theta_1 = \arctan\,[(R_2/R_1)\,\tan\theta_2] \qquad (1)$$

$$\dot{\theta}_1 = \frac{(R_2/R_1)\,(\sec\theta_2)^2\,\dot{\theta}_2}{1 + [(R_2/R_1)\,\tan\theta_2]^2} \qquad (2)$$

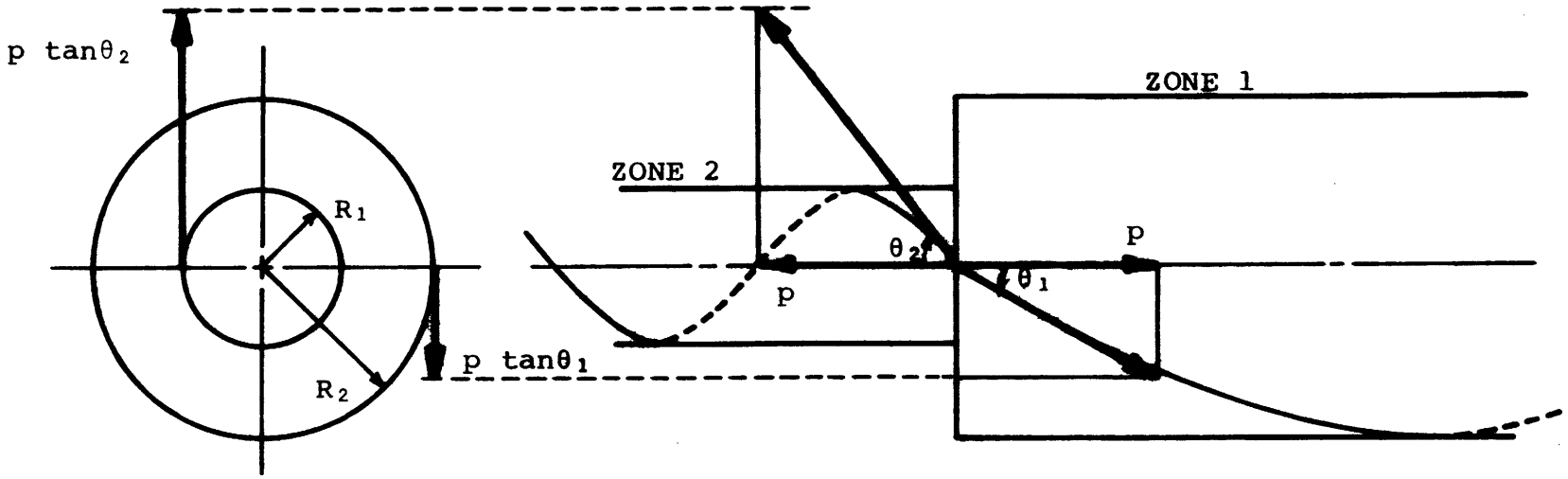

FIGURE 8 THREADLINE FORCE EQUILIBRIUM BETWEEN ZONES 1 AND 2

(p = Axial Yarn Tension)

Filament Length Conservation:

$$F_b = V_{in} \sec\theta_0 \tag{3}$$

$$F_c = F_b - \dot{\theta}_1 L_1 \sec\theta_1 \tan\theta_1 - \dot{L}_1 \sec\theta_1 \tag{4}$$

$$F_d = F_e + \dot{\theta}_2 L_2 \sec\theta_2 \tan\theta_2 + \dot{L}_2 \sec\theta_2 \tag{5}$$

$$F_e = F_g + \dot{\theta}_3 L_3 \sec\theta_3 \tan\theta_3 + \dot{L}_3 \sec\theta_3 \tag{6}$$

$$F_g = V_{out} \sec\theta_3 \tag{7}$$

(NOTE: $F_a = F_b$, $F_c \neq F_d$, $F_e = F_f$, $F_g = F_h$)

Turn Conservation: Zone 3:

$$\dot{T}_3 = (P_{in} V_{in} - P_{out} V_{out})_3 + (W_{out} - W_{in})_3 \tag{8}$$

where:

$P_{in} = \tan\theta_3 / R_2$

$P_{out} = \tan\theta_3 / R_3$

$V_{in} = F_e / \sec\theta_2$

$V_{out} = V_{out}$

$W_{in} = W_e$

$W_{out} = 0$

$T_3 = (L_3/R_3) \tan\theta_3$

$\dot{T}_3 = \dot{\theta}_3 L_3 \sec^2\theta_3 / R_3 + \dot{L}_3 \tan\theta_3 / R_3$

Turn Conservation: Zones 1 and 2: (beginning of 1 to end of 2)

$$\dot{T}_1 + \dot{T}_2 = (P_{in} V_{in} - P_{out} V_{out})_{1\&2} + (W_{out} - W_{in})_{1\&2} \tag{9}$$

where:

$P_{in} = \tan\theta_0 / R_0$

$P_{out} = \tan\theta_2 / R_2$

$V_{in_1} = V_{roller_1}$

$V_{out_2} = F_e / \sec\theta_2$

$W_{in_1} = 0$

$$W_{out_2} = W_e$$

$$T_1 = L_1 \tan\theta_1 / R_1$$

$$T_2 = L_2 \tan\theta_2 / R_2$$

$$\dot{T}_1 = \dot{\theta}_1 L_1 \sec^2\theta_1 / R_1 + \dot{L}_1 \tan\theta_1 / R_1$$

$$\dot{T}_2 = \dot{\theta}_2 L_2 \sec^2\theta_2 / R_2 + \dot{L}_2 \tan\theta_2 / R_2$$

Turn Conservation: Zone 4:

$$\dot{T}_4 = (P_{in}\, V_{in} - P_{out}\, V_{out})_4 + (W_{out} - W_{in})_4 \qquad (10)$$

where:

$$P_{in} = \tan\theta_3 / R_3$$

$$P_{out} = T_4 / L_4$$

$$V_{in_4} = V_{out_3}$$

$$W_{in} = 0$$

$$W_{out} = 0.$$

Turn Conservation: Zone 5:

$$\dot{T}_5 = (P_{in}\, V_{in} - P_{out}\, V_{out})_5 + (W_{out} - W_{in})_5 \qquad (11)$$

where:

$$P_{in} = T_4 / L_4$$

$$P_{out} = T_5 / L_5$$

$$V_{in_5} = V_{out_4}$$

$$W_{in} = 0$$

$$W_{out} = 0.$$

Combination of the above equations yields four first order differential equations which are, in general, non-linear with time varying parameters:

Combining eqs. (6), (7), and (8),

$$\dot{\theta}_3 = \frac{(\sin\theta_2 \sec\theta_3 R_3/R_2 - \tan\theta_3(V_{out} + \dot{L}_3) - W_e R_3}{(1 - \sin\theta_2 \sin\theta_3 R_3/R_2) L_3 \sec^2\theta_3} \quad (12)$$

Combining eqs. (2) and (9),

$$\dot{\theta}_2 = \frac{V_{in} \tan\theta_0 R_2/R_0 - \dot{L}_1 \tan\theta_1 R_2/R_1 - (\dot{L}_2 + F_e/\sec\theta_2) \tan\theta_2 + W_e R_2}{L_2 \sec^2\theta_2 + L_1 \sec^2\theta_2 \sec^2\theta_1/(R_1^2/R_2^2 + \tan^2\theta_2)} \quad (13)$$

From eq. (10),

$$\dot{T}_4 = V_{out_3} \tan\theta_3/R_3 - V_{out_4} T_4/L_4 \quad (14)$$

From eq. (11),

$$\dot{T}_5 = V_{out_4} T_4/L_4 - V_{out_5} T_5/L_5 \quad (15)$$

Equations (12) through (15) can be integrated numerically on a digital computer starting at initial conditions $\theta_2(0)$, $\theta_3(0)$, $T_4(0)$, and $T_5(0)$ to determine the state of the system model as a function of time.

Once the state of the system model is known, other physically relevant values can be computed. For instance, the draw ratio of the filaments between Zones 1 and 2 can be determined by dividing eq. (4) by eq. (5). Then, by inputting the tension vs. draw ratio curve for the filaments in the form of a fitted polynomial curve, tension and torque in Zones 1 and 2 can be computed directly [2]. Similarly, the tension jump across the twister can be computed, using the belt formula assumption $p_3 = p_2 e^{\mu\theta}$ by inputting an assumed coefficient of friction and geometry of wrap of the yarn against the surface of the twister. These physical quantities can be used to study

conditions under which unsteady twister slippage might occur in the real texturing system.

Other physically meaningful conditions can be studied in this model, such as slippage in the feed or exit rollers, or changes in the position of the draw point which might occur in texturing due to varying heater to yarn heat transfer over the first heater. Such perturbations can be introduced into the model through inputting state dependent and/or time varying parameters, as will be discussed later in this thesis.

A step-by-step breakdown of the computer model as prepared in Fortran is provided in Appendix 7. Numerical integration of the differential equations is carried out using the DYnamic SYStems (DYSYS) program available in the Joint Mechanical Engineering-Civil Engineering Computer Facility at M.I.T.

Clearly, this model does not consider most of the physics taking place in the real texturing system. It does, however, include the effect of transient twist contraction and the necessary condition of turn conservation, which appear to be dominating influences in certain modes of transient texturing process operation, as will be discussed in the chapters to follow. This idealized model, therefore, is a useful conceptual tool which is easily understood and which can serve as a basis of comparison when studying the subtle complexities of the real process.

III. STUDIES OF TRANSIENT PHENOMENA

Most of the following discussions pertain to results obtained from the MITEX laboratory texturing machine and from the analytical computer models. Since the MITEX machine is not equipped with a second heater zone and since the second heater zone and the windup zone are included only superficially in the analytical models, the threadline behavior in these zones will not be discussed in depth at this time. Emphasis will be placed, therefore, on threadline force and twist behavior in the texturing and post-spindle zones as influenced by variations in machine and material parameters.

III.A. Threadline Buckling

The degree to which a yarn can be twisted in the yarn texturing process and continue to maintain a straight central axis depends on filament material properties, as well as the physical constraints imposed on the yarn during twisting. Observations have shown that for normal conditions of texturing, using common commercial feed yarns, this twist limit is somewhere around 60 TPI (machine) or, roughly, 80 turns per inch of twisted yarn.

The yarn is said to buckle torsionally when, upon further twisting, it assumes a corkscrew configuration. This buckling effect can be observed in the false twist texturing process when the yarn is subjected to high twist levels, as shown in Fig. 9, taken from Brookstein [2]. The figure shows the effect on the yarn at three points along the texturing zone of different levels of machine twist being inserted into partially oriented feed yarn (POY) during slow speed draw texturing on

DRAW TEXTURING THREADLINES

245·34 POY PET 1.60 DRAW RATIO 210°C. HEATER

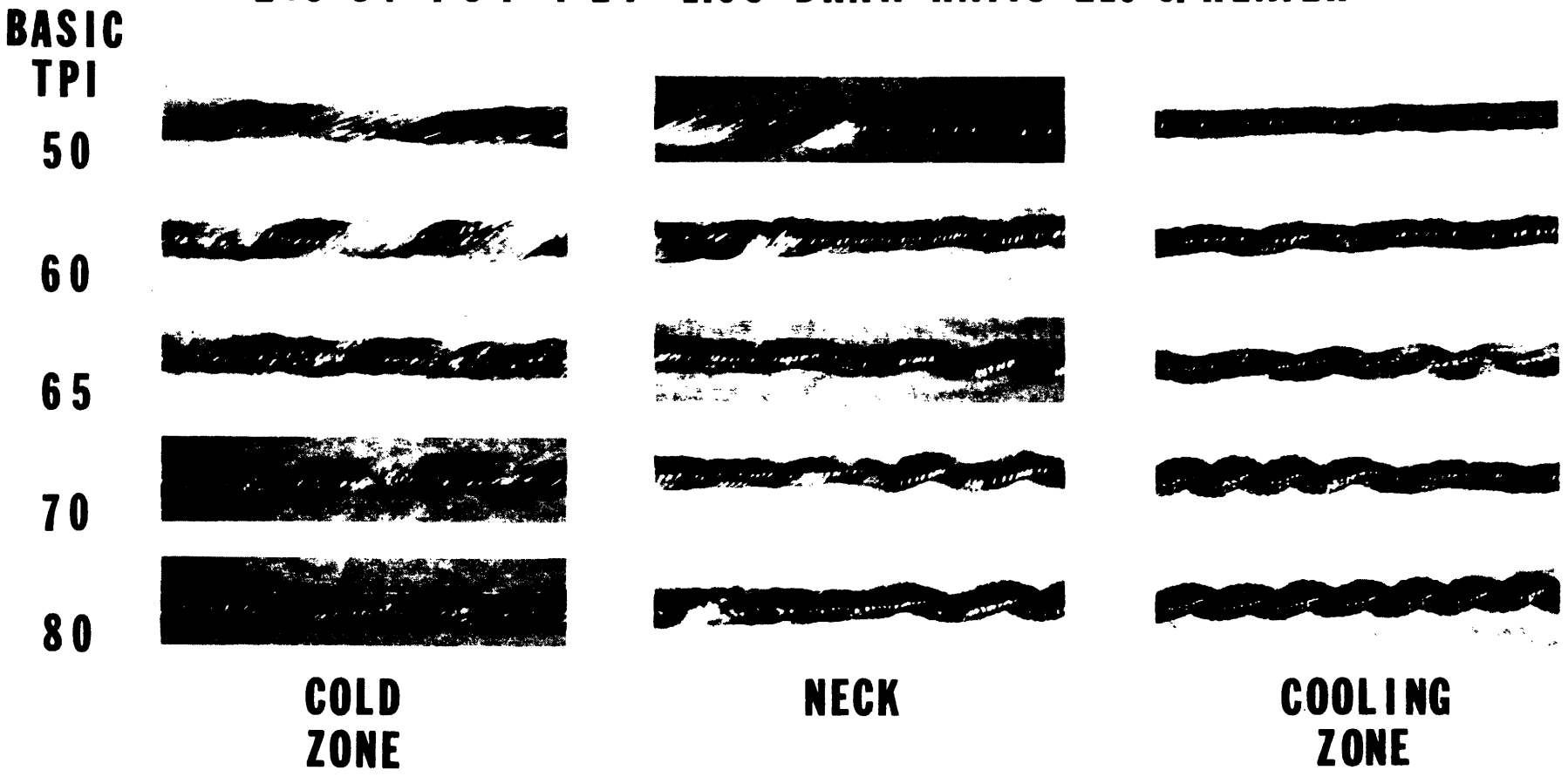

FIGURE 9

the MITEX machine. The heated portion of yarn at the neck zone (or draw point) is the torsionally weakest or softest point along the yarn, and buckles are observed to form there as the yarn up-twists due to its softening and reduction in radius.

At lower levels of machine twist, buckles formed in the neck zone are relatively small and appear in small groups spaced at fairly wide intervals (.5 to 1. inch), while at high twist levels, pronounced buckles form virtually continuously in the neck zone. In conventional texturing as well buckles form over the heater at high twist levels in a manner similar to that seen in draw texturing.

With the aid of a stroboscope, a microscope, and a motion picture camera, several interesting observations have been made about threadline buckling during texturing. Most of these observations were made during draw texturing, but it is felt that buckling behavior will be similar in conventional texturing as well for similar texturing conditions:

(1) On the MITEX texturing machine buckles are observed to form at the softening point in the yarn as the yarn enters the heater. They are then transported, while undergoing seemingly no change, to the pin twister, where they are completely untwisted. Even though the yarn is completely untwisted as it enters the post-spindle zone, however, evidence of the buckles persists after the spindle in the form of visually perceptible irregularities along the length of the untwisted and straightened yarn.

These irregularities have a spacing corresponding roughly to that of the buckles which had existed in the cooling zone.

(2) As an individual buckle reaches the pin twister, the entire cooling zone of the threadline is seen to decrease in translational velocity momentarily, while the buckle is untwisted. This occurrence is not surprising, since a greater length of filaments is contained in a unit length of buckled yarn as compared with a unit length of unbuckled yarn, and since the constant velocity intermediate roller of the texturing machine calls for a fixed rate of filament length to be pulled past the point of untwisting at the pin. Interestingly, at the same instant that a large sized buckle is untwisting at the pin twister, a new buckle similar to the one which is untwisting is seen to be forming at the softening point over the heater. Thus, when operating conditions of the MITEX machine are such that buckles are fairly pronounced (conventional texturing Condition A [1% OF; 65 TPI; 3.9 IPS; 210°C], for example), the buckles can be seen to perpetuate themselves. Similar observations have also been reported in earlier studies [3].

(3) Based on the previous observation, an attempt was made to correlate the random tension and torque fluctuations seen during normal steady state

texturing with the formation of buckles in the threadline. Due to rapid frequency of buckle formation relative to the frequency of the random force variations during these observations at operating Condition B , it was not possible to establish such a relationship. The method used was to blip the marker pen on the recorder at the sight of a forming buckle, while simultaneously recording tension and torque. (see [4] following for details on B).

(4) Another observation of importance was made during the study of buckle formation. By watching the point where the cold yarn enters the neck zone using operating Condition B [1.6 DR; 60 TPI; .34 IPS; 210°C] (mild buckling), it is possible to pick out irregular sections in the cold twisted yarn which turn into buckles as they enter the softening point over the heater. These irregular sections probably represent torsionally weak points in the yarn which result from asymmetric structural development as the yarn is twisted at the entrance to the cold zone.

Thus, there appear to be two causes of buckle formation at the softening point; one being the momentary stoppage resulting from the unwinding of a buckle at the pin, and the other being the collapse of torsionally weak spots in the yarn when they are softened while under the influence of the existing torque field in the threadline. Working together, these two

effects would tend to increase gradually the frequency of buckles in the threadline (and thus the total number of buckles) once buckle formation had begun. In fact, this phenomenon can be observed during conventional texturing on the MITEX machine at operation Condition A [1% OF; 65 TPI; 3.9 IPS; 210°C]. The level of overfeed is quite important, however, and only with positive overfeeds into the texturing zone is the threadline tension low enough to allow the buckles to grow unchecked. In draw texturing, the tension in the threadline is sufficient to keep buckles from progressing past a certain stage of development for a given level of twist. This is also true in conventional texturing when the overfeed is set to provide tensions in the range of those found in draw texturing.

III.B. Controlled Spindle Speed Variations

Precise control of the drive roller and twister speeds in the texturing process is of primary importance if a constant number of turns of twist are to be maintained between the inlet rollers and the twister. Because the twister speed (or more directly, the rotational speed of the yarn at the twister) is one of the more difficult constant parameters to maintain in a real situation, it is interesting and useful to study the effect on the texturing system of certain controlled variations in twister speed. By varying the twister speed in a step or oscillatory fashion using both the experimental and analytical models, insight can be gained as to the overall settling time of the system and the degree of overshoot to be expected in threadline force values.

Step Change in Spindle Speed

A drastic step change in twister speed occurs during machine startup from conditions of zero threadline force, zero threadline twist, and zero machine speeds. If at first the twister remains motionless and all rollers are accelerated to full operating speed (3.14 IPS), the tension in the texturing zone will jump within a few seconds to a value determined by yarn material properties, the translational speed of the yarn at roller 1, and its speed entering the spindle. Simultaneously, the tension in the post-spindle zone will jump to a higher value than the texturing zone tension due to the friction across the spindle. When the spindle is then brought to full speed instantaneously (0-60 TPI change complete within 2-3 sec on MITEX), a longer filament path through the texturing machine is suddenly dictated and threadline torque and tension go through transient peaks before settling down to new steady state values. If one machine length is defined the distance between the twist trap at the torque-tension device and the spindle, one can see in Fig. 10 that the 63% settling time of the draw texturing threadline is about 3 machine lengths during startup conditions (based on roller 2 velocity).

The "step" change seen in the MITEX apparatus has been simulated analytically by the $-\pi/2$ to $\pi/2$ section of a .2 cps sine curve, starting from zero speed at $-\pi/2$. Using input parameters"a"listed in Appendix 3, the kinematic computer model predicts the force and twist curves seen in Fig. 11.

It is also informative to observe the response of the

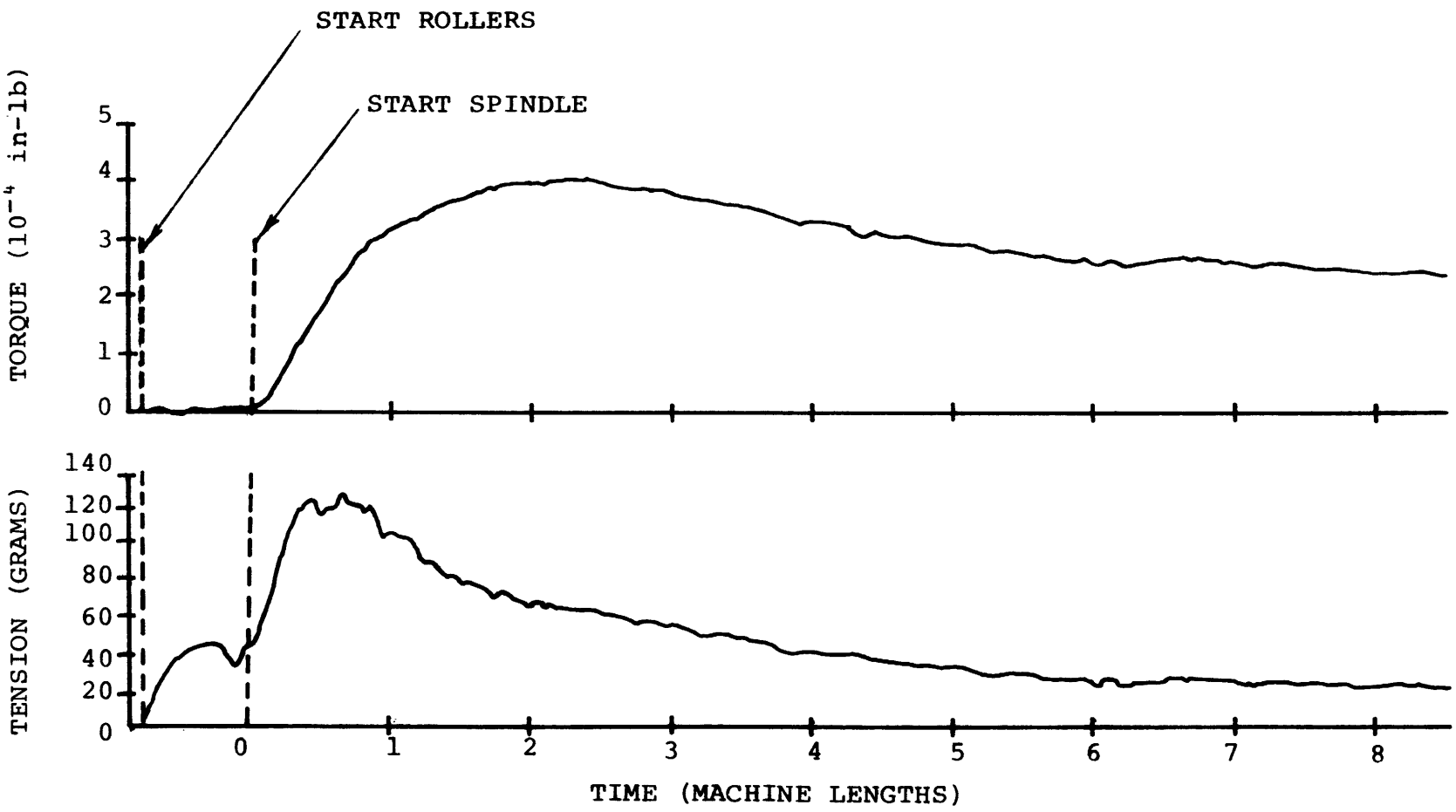

FIGURE 10 THREADLINE FORCE RESPONSE TO MACHINE STARTUP [1.6 DR; 0-60 TPI; 3.1 IPS; 210°C]

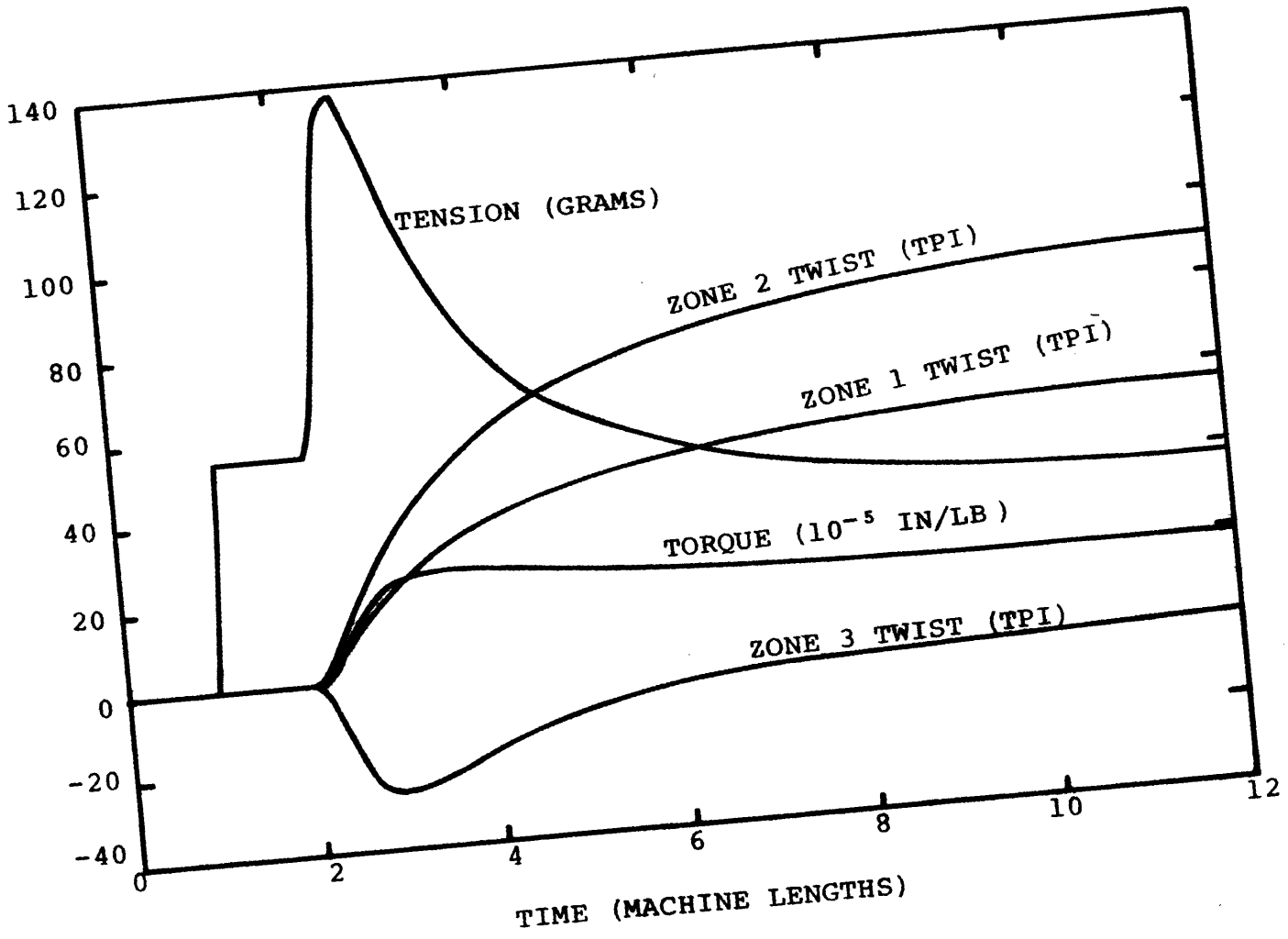

FIGURE 11 COMPUTED THREADLINE BEHAVIOR DURING MACHINE STARTUP
(T = 1, START ROLLERS; T = 2, START SPINDLE)

texturing system to a less severe step change in spindle speed between two operating conditions. This can be accomplished experimentally by using a variac to power the controller for the spindle drive motor. By switching back and fourth between wall power and variac power, the spindle speed can be raised and lowered by a preset amount in a manner which approximates a step change (change complete within 2 sec). The experimental threadline force curves for yarn E are seen in Fig. 12, representing a "step" change from 65 to 55 TPI and back, using operating Condition C [1.6 DR; 3.1 IPS; 210°C]. In order to test the sensitivity of the real texturing process to differences in feed material properties, a number of different POY feed yarns with different properties representing the range of properties seen in commercial feed yarns were tested. The tension vs. draw ratio curves for these yarns as measured in the laboratory are listed in Appendix 5. A summary of the experimental overshoot, rise time, and settling time responses for each yarn is seen in Fig. 13. A "step" change was also implemented on the kinematic computer model using input parameters b and a sinusoidal change complete within 2 sec. The force and twist curves predicted by the kinematic model are seen in Figs. 14 and 15. It is not expected that the kinematic model would provide meaningful differences in behavior between these yarns due to the narrow range of material properties encountered in commercial samples, but good qualitative agreement is manifested in the force response curves; and the computed overshoot, rise time, and settling time predicted by the

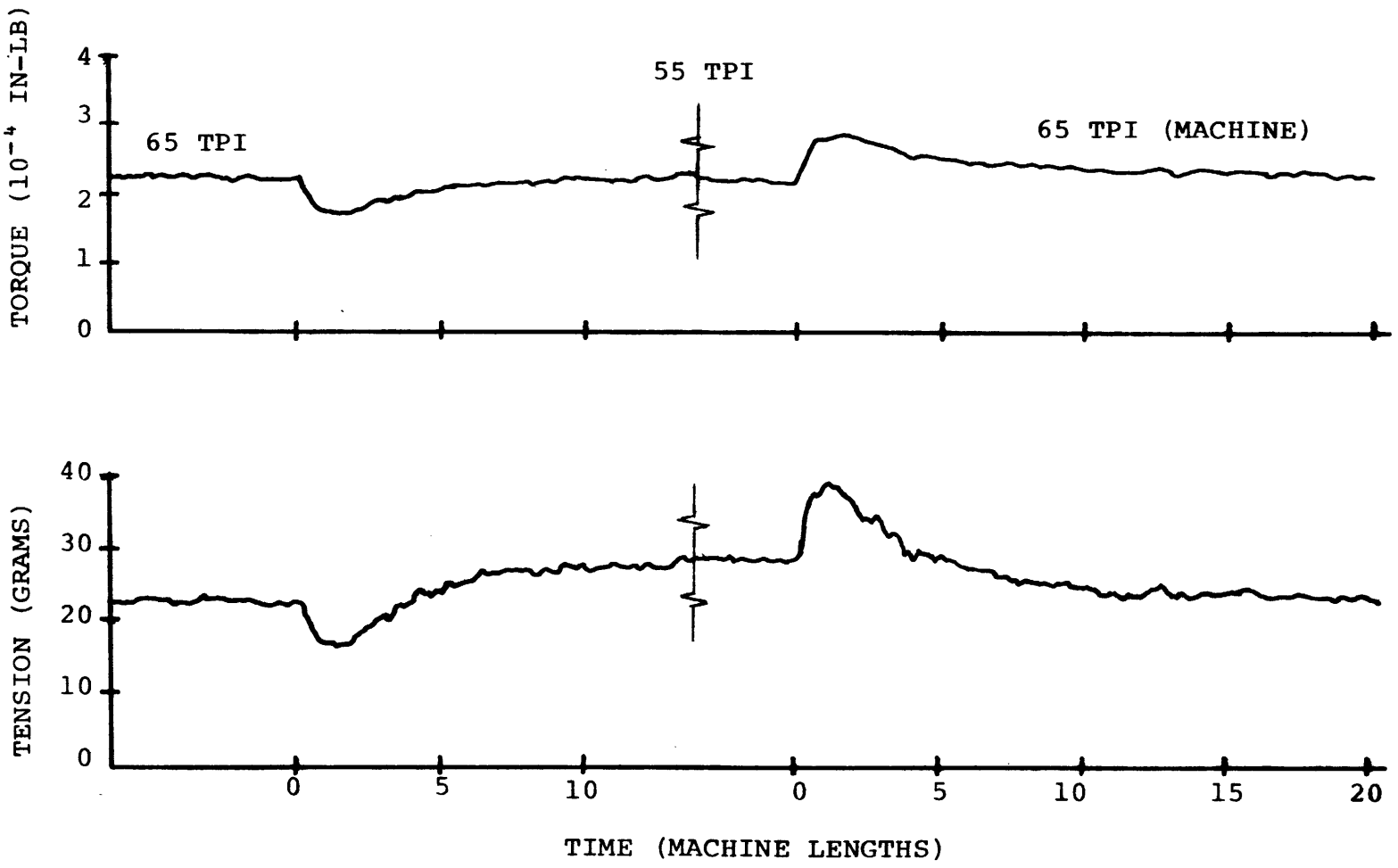

FIGURE 12 THREADLINE FORCE RESPONSE TO A SUDDEN CHANGE IN SPINDLE SPEED [1.6 DR; 65-55-65 TPI; 3.1 IPS; 210°C]

Disturbance Mode-Step Change*	Yarn	Tension g (± .2g)	% of Former S.S. Value	Torque 10^{-4} in/lb (± $.03x10^{-4}$) (in/lb)	% of Former S.S.Value	100% Rise Time (sec) (±1 sec)	63% Decay Time (sec) (±2 sec)	100% Rise Time (sec) (±1 sec)	63% Decay Time (sec) (±2 sec)
65-55	A	-7.2	26.5	-.55	20.8	5	17	4	17
	B	-5.1	23.5	-.50	22.2	6	13	6	14
	C	-5.5	22.0	0.50	22.2	5	13	5	13
	D	-5.1	26.2	-.45	20.3	5	21	5	20
	F	-5.5	20.4	-.50	22.7	5	15	5	19
	H	-5.1	18.9	-.50	23.3	5	16	7	12
	J	-7.2	23.6	-.55	2.12	5	18	7	10
55-65	A	+9.8	36.0	+.75	28.3	5	19	5	24
	B	+9.4	43.3	+.65	28.9	5	15	5	17
	C	+10.2	40.8	-.75	33.3	6	16	6	17
	D	+9.8	50.3	+.75	33.8	6	16	6	16
	F	+9.8	36.3	+.70	31.8	5	13	5	15
	H	+9.4	34.8	+.65	30.2	5	17	7	17
	J	+9.8	38.4	+.70	26.9	5	18	6	23

*Change complete within 2 sec.

FIGURE 13

EFFECT OF SPINDLE SPEED CHANGES ON THREADLINE PARAMETERS

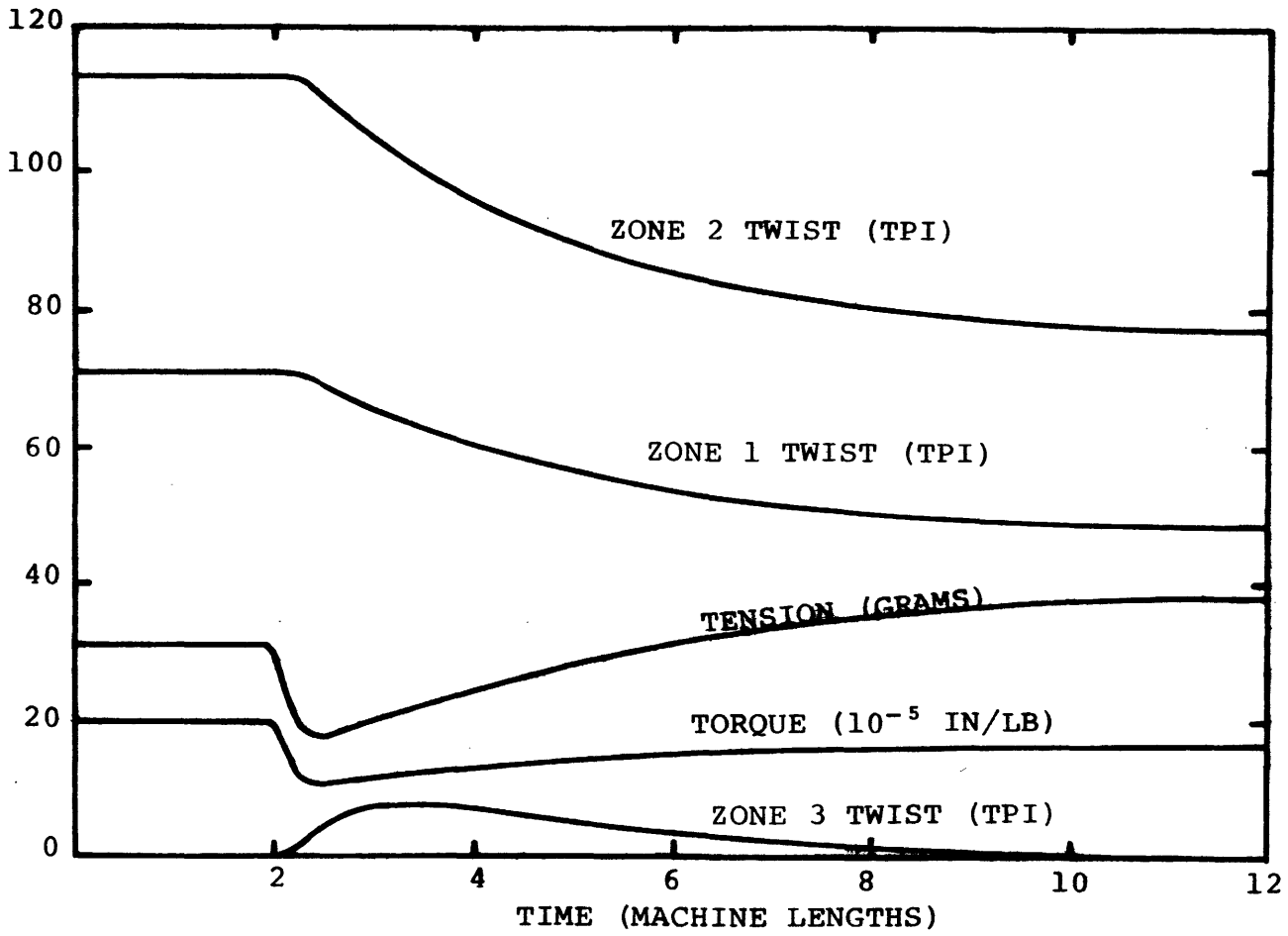

FIGURE 14 COMPUTED THREADLINE RESPONSE TO A SUDDEN DECREASE IN SPINDLE SPEED FROM 65 TO 55 MACHINE TPI

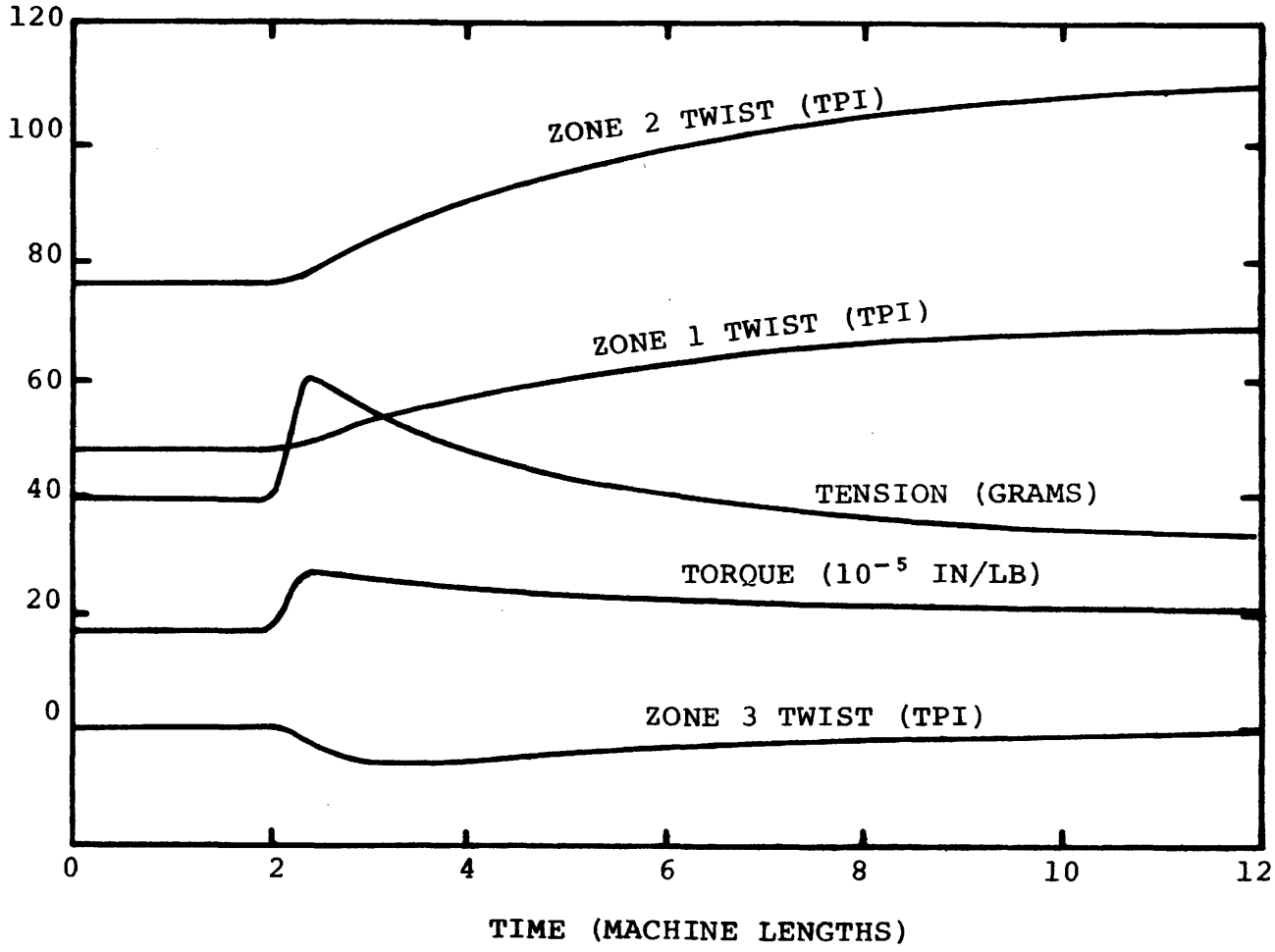

FIGURE 15 COMPUTED THREADLINE RESPONSE TO A SUDDEN INCREASE IN SPINDLE SPEED FROM 55 TO 65 MACHINE TPI

computer model were similar to the experimental values as seen in Fig. 13, vs. Fig. 14 (twist decrease) and Fig. 15 (twist increase).

It is worthy of note that in the real (MITEX) process, the post-spindle twist which develops due to the change in spindle speed manifests itself as clumps of tight spots when the spindle is slowed down from 65 to 55 TPI, but as uniform twist when the change is from 55 to 65 TPI. The distinction between the two types of twist can be observed when the yarn is subjected to negligible tensions as it emerges from roller 2. The tight spots are clumps of twist which were not unwound fully upon passing through the twister while the uniform twist appears in sections of yarn which were untwisted beyond zero twist such that twist in the opposite direction to that in the texturing zone appears. Tight spots are normally easier to notice than sections of uniform twist, since a tight spot diameter is little more than that of twisted yarn in the cooling zone. The production of these non-uniform tight spot sections results from complicated interactions at the pin which have not been considered in the analytical models.

Oscillating Spindle Speed

The overall dynamic response of the texturing system has been observed on the MITEX apparatus by introducing a $\pm$10% sinusoidally oscillating spindle speed varied over several frequency decades while monitoring threadline tension and torque in the texturing zone and threadline tension in the post-spindle zone (Fig. 16). Due to limitations imposed by the two-channel strip chart recorder, only spindle speed and one

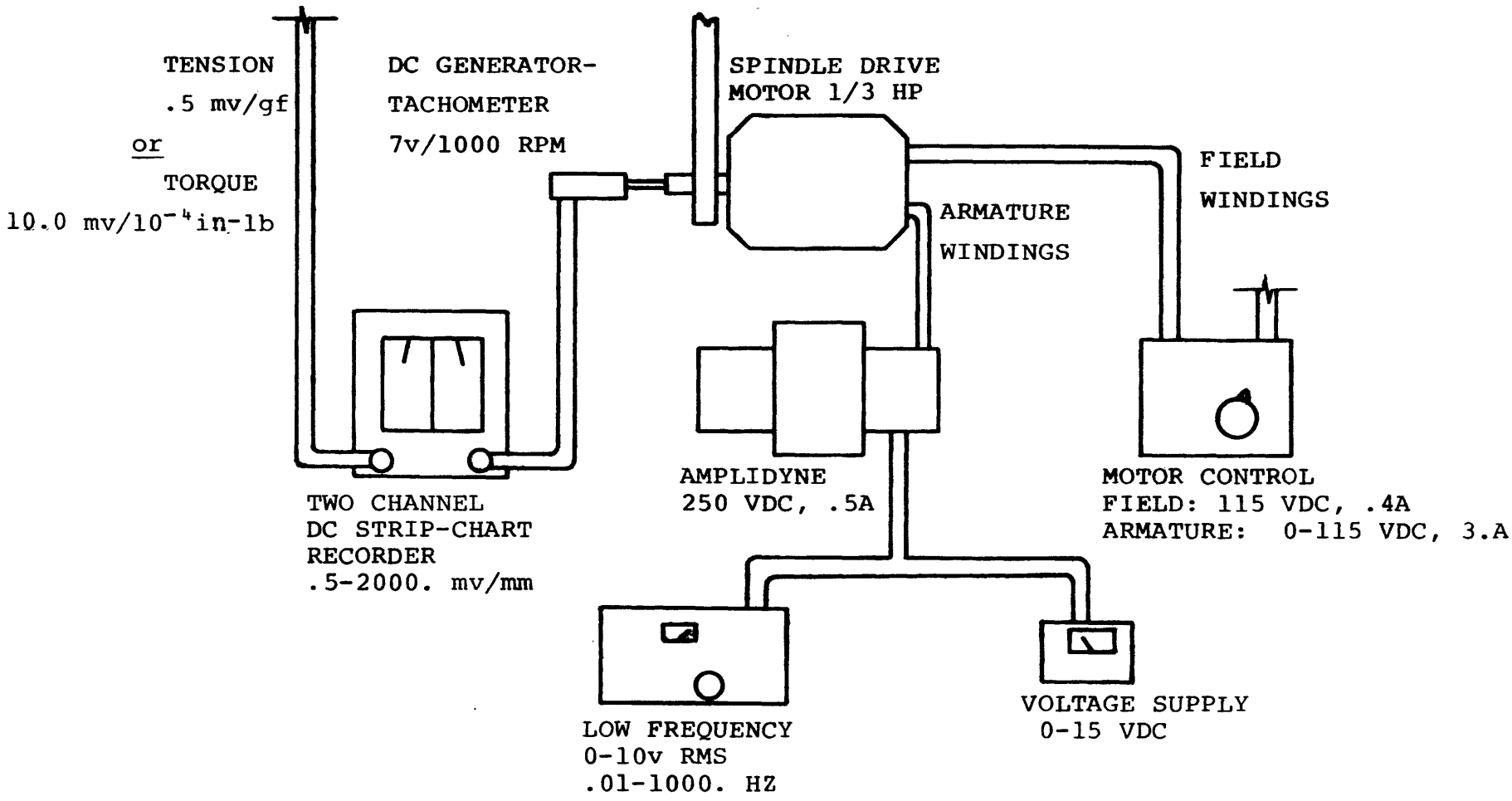

FIGURE 16 APPARATUS USED IN OSCILLATING SPINDLE SPEED TESTS

other signal could be recorded at any one time, which necessitated three separate runs of the same procedure. The apparatus was not changed between the three runs except for the introduction of torque-tension device #2 into the post-spindle zone prior to the third run, requiring a 90° bend in the post-spindle zone threadline, as was seen in Fig. 6. Care was taken to maintain the same total post-spindle zone length as for the two earlier runs.

Using operating Condition O [1.6 DR; 60 TPI; 3.1 IPS; 210°C], the frequency of the oscillating spindle speed was varied incrementally from .01 cps to 2. cps in seven steps while maintaining a constant amplitude. Steady state data were recorded under the same conditions to provide a data point at 0 cps. The resulting amplitudes of tension and torque are plotted against phase in Fig. 17. The steady state tensions were estimated as being 180° out of phase with the spindle speed, while the steady state torque appeared to be directly in phase. Phase in all other cases was determined on the basis of estimating the phase of the sine curve which, to the eye, best fits the output signal*. A sample pre-spindle tension trace is shown in Fig. 18.

An interesting observation can be made concerning the pre- and post-spindle tension amplitudes at .2 cps spindle oscillation. Although an accurate determination of the phase of these force traces is rather difficult to obtain because of

---

*Representation techniques suggested by Thwaites.

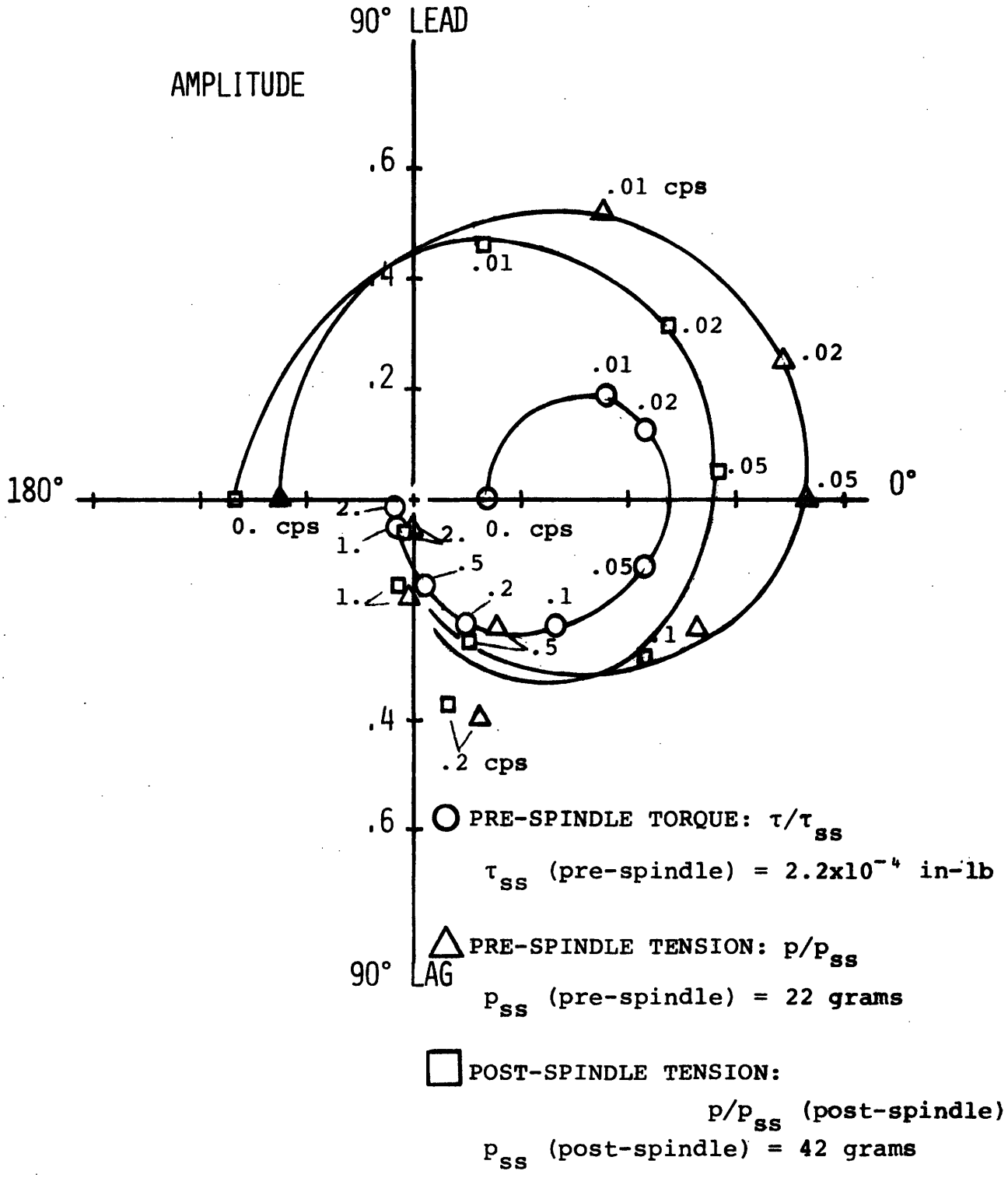

FIGURE 17 AMPLITUDE AND PHASE OF THREADLINE FORCES IN RESPONSE TO OSCILLATING SPINDLE SPEED AS OBSERVED ON THE MITEX MACHINE DURING DRAW TEXTURING

(1.6 DR; 60 ± 10% TPI; 3.1 IPS; 210°C)

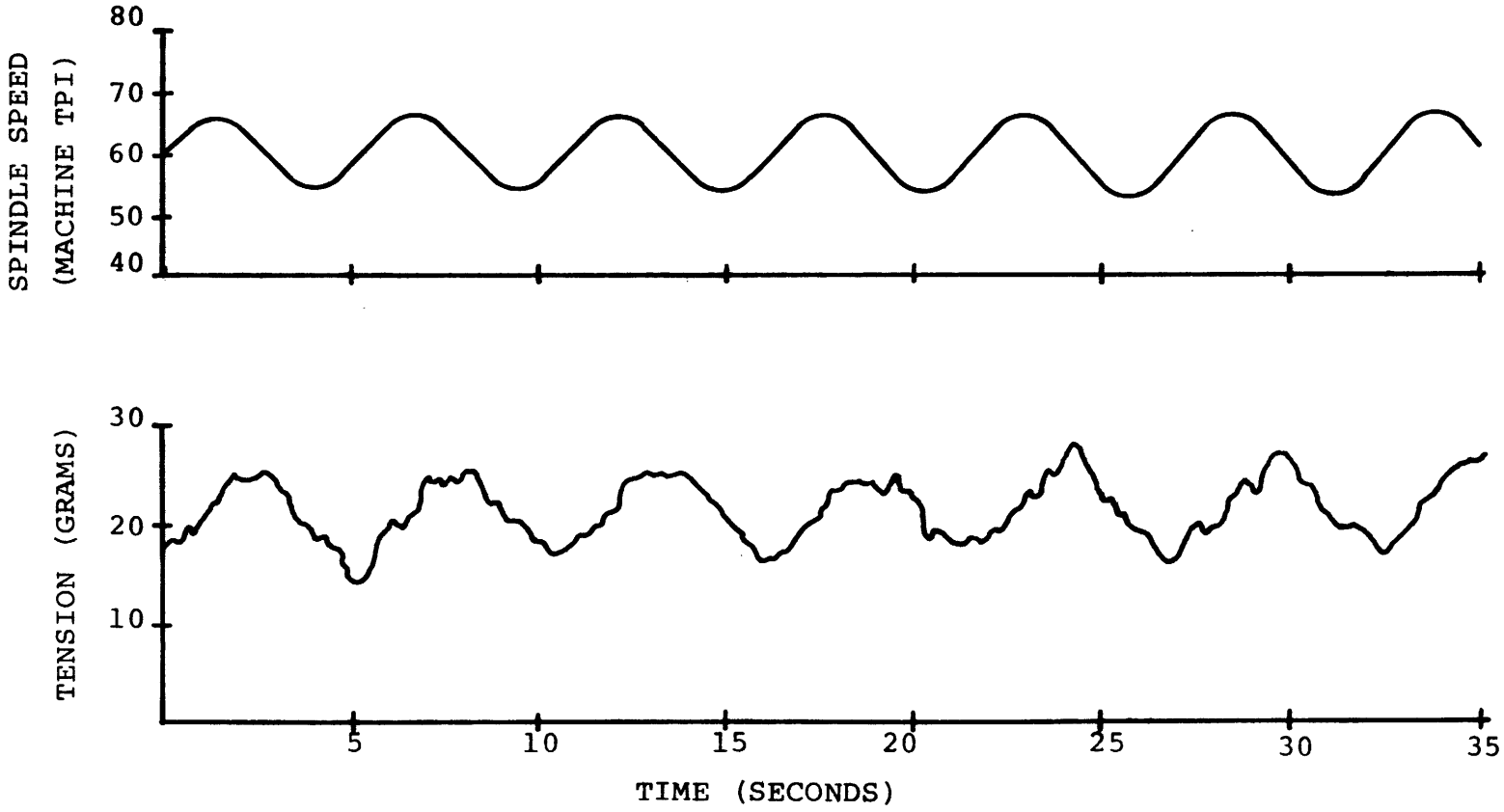

FIGURE 18 TEXTURING ZONE TENSION RESPONSE TO OSCILLATING SPINDLE SPEED
[1.6 DR; 60 TPI ± 10%; .19 CPS; 3.1 IPS; 210°C]

random texturing system noise, especially at the higher frequencies of spindle oscillation, careful analysis of the data indicated that the tension traces lagged the spindle speed excessively in the range of .2 cps relative to the neighboring data points. Later it was noticed that .2 cps (5. secs per cycle) is very nearly the transport frequency of the yarn between the entrance to the heater and the spindle (4.7 secs based on an estimated 1.35 yarn contraction factor), such that buckles being formed during one cycle of spindle oscillation were being unwound at the spindle at the same point in the following cycle. It is not known what the precise effect on the threadline might be of these "in phase" buckles, which have apparently caused a local phase shift in tension readings, but further investigation in the range of this frequency could lead to some interesting findings which would add to our understanding of threadline buckling behavior.

Observations were also made concerning tight spots in the textured yarn resulting from oscillating spindle speed. At lower frequencies of oscillation, tight spots were seen to emerge during the decreasing half of the spindle speed trace, confirming observations made for step changes in spindle speed. But, as frequency was increased to .5 cps and above, the percent of the cycle over which tight spots were observed diminished to zero.

Computer Simulation of Oscillating Speed

Computer simulations corresponding to the above experiment were performed using the kinematic model to determine the

frequency range over which this model is a reasonable representation of the real texturing system as observed on the MITEX machine. Input parameters"b"* were used to produce the results which are plotted in Figs. 19a and b. Although no first hand experimental data are available to confirm the real behavior of twist in the MITEX threadline, the computed curves shown in Fig. 19b are considered reasonable. It can also be seen that at lower frequencies of spindle speed oscillation the computed values of tension and torque and their phase agree qualitatively with the experimental results. At frequencies above .02 cps, however, the computed values of phase of tension and torque lead the experimental values to the extent that they never cross the zero degree or "in phase" axis. Also, at frequencies above .05 cps, the computed tension and torque amplitudes are in error on the high side.

It is evident from the above experimental and computed data that the method of computing tension and torque values in the analytical model do not adequately represent the physical system at higher frequencies of spindle speed oscillation. An alternate method of computing tension and torque can be implemented as described in Appendix 4. Instead of considering the filaments which make up the yarn in the computer model as inextensible, the filaments can be modelled as elastic strands (except at the draw point). The resulting equations shown in the Appendix can be included in the model without changing the state equations for system geometry, and more realistic threadline tension and torque amplitudes and phase offset values can

*see Appendix 3

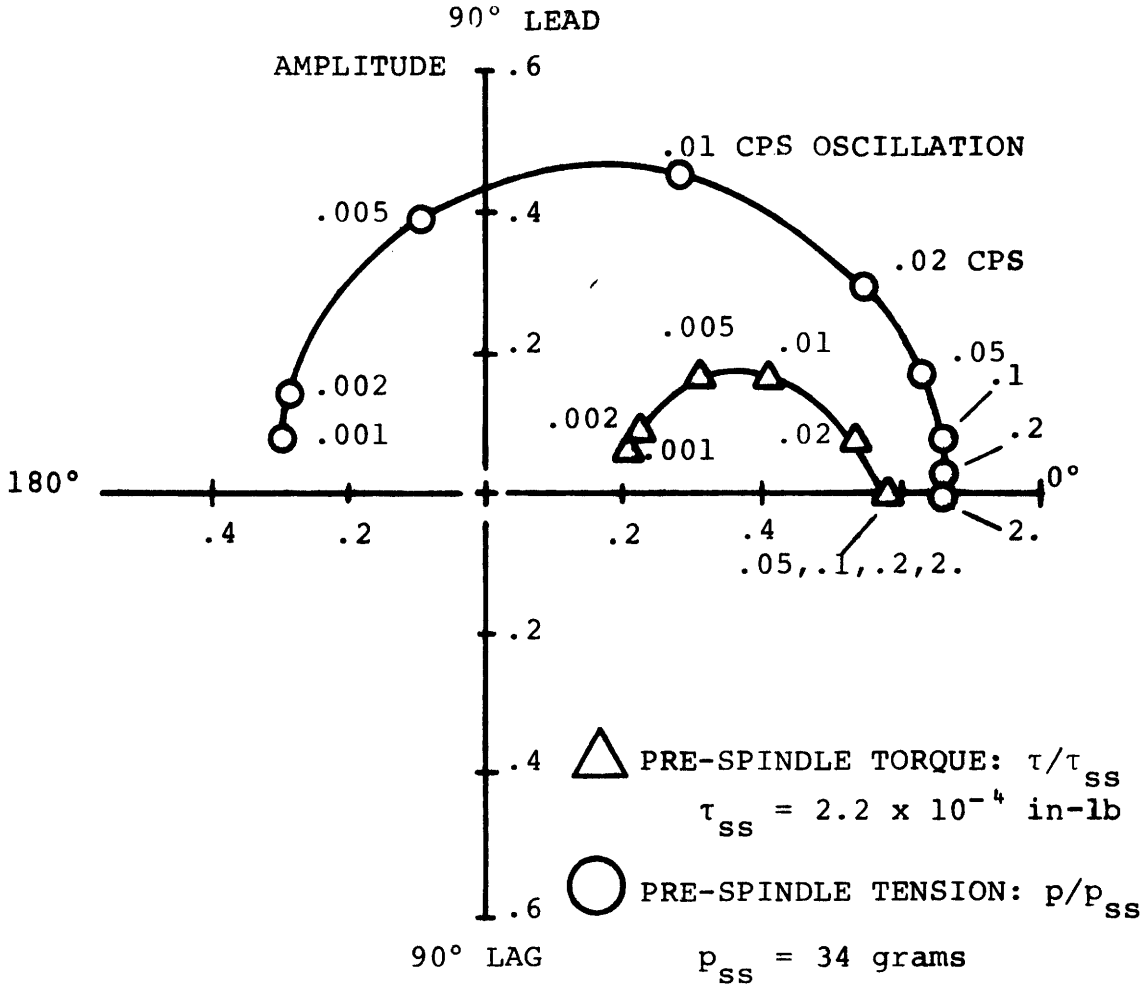

FIGURE 19a COMPUTED AMPLITUDE AND PHASE OF THREADLINE FORCES IN RESPONSE TO OSCILLATING SPINDLE SPEED (60 TPI $\pm$ 10%)

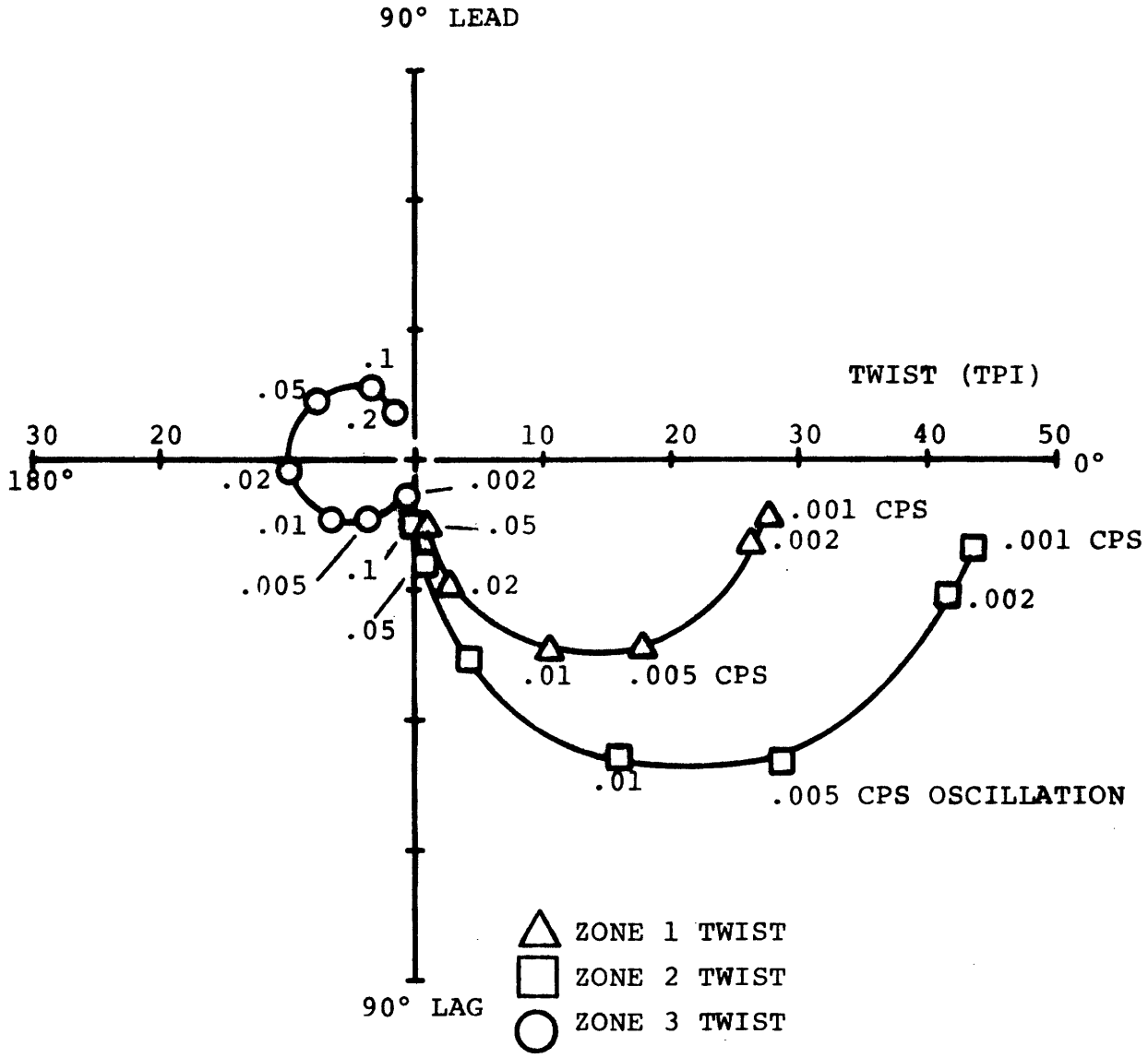

FIGURE 19b COMPUTED AMPLITUDE AND PHASE OF THREADLINE TWISTS IN RESPONSE TO OSCILLATING SPINDLE SPEED (60 TPI ± 10%)

be expected at the higher frequencies of spindle speed oscillation, while little change in the computed values would be expected at low frequencies. This reasoning can be supported through the following argument, which is an illustration of how even a simple model can be used to structure thought and gain insight concerning the mechanics of the texturing process.

The filaments can at one extreme be considered inextensible except at the draw point, where extension would take place like a continuous dashpot (Case 1). This assumption was made in the calculation of tension and torque in Section II.C. At the other extreme, the filaments can be considered as being elastically extensible with no draw point (Case 2). These extreme cases can be represented schematically as shown in Fig. 20, where a filament has been resolved from a helical orientation to a straight line for simplicity. When the period of oscillation of the spindle speed is small compared with the transport time of the shortest machine zone, the geometries of the filaments in the texturing and post-spindle zones remain virtually constant (i.e. only small amplitude twist variations occur). Thus, the post-spindle twist will remain near zero and the filament length per unit time passing in and out of the texturing machine match the roller surface speeds. This is indicated at points x and y in Fig. 20, where F_x is the filament velocity with respect to point x and F_y is the filament velocity with respect to point y. F_x and F_y are constant velocities representing constant roller speeds in this discussion. If the spindle speed were also constant, with a value S_n, then the distance of separation between points x and y could represent the total filament path length

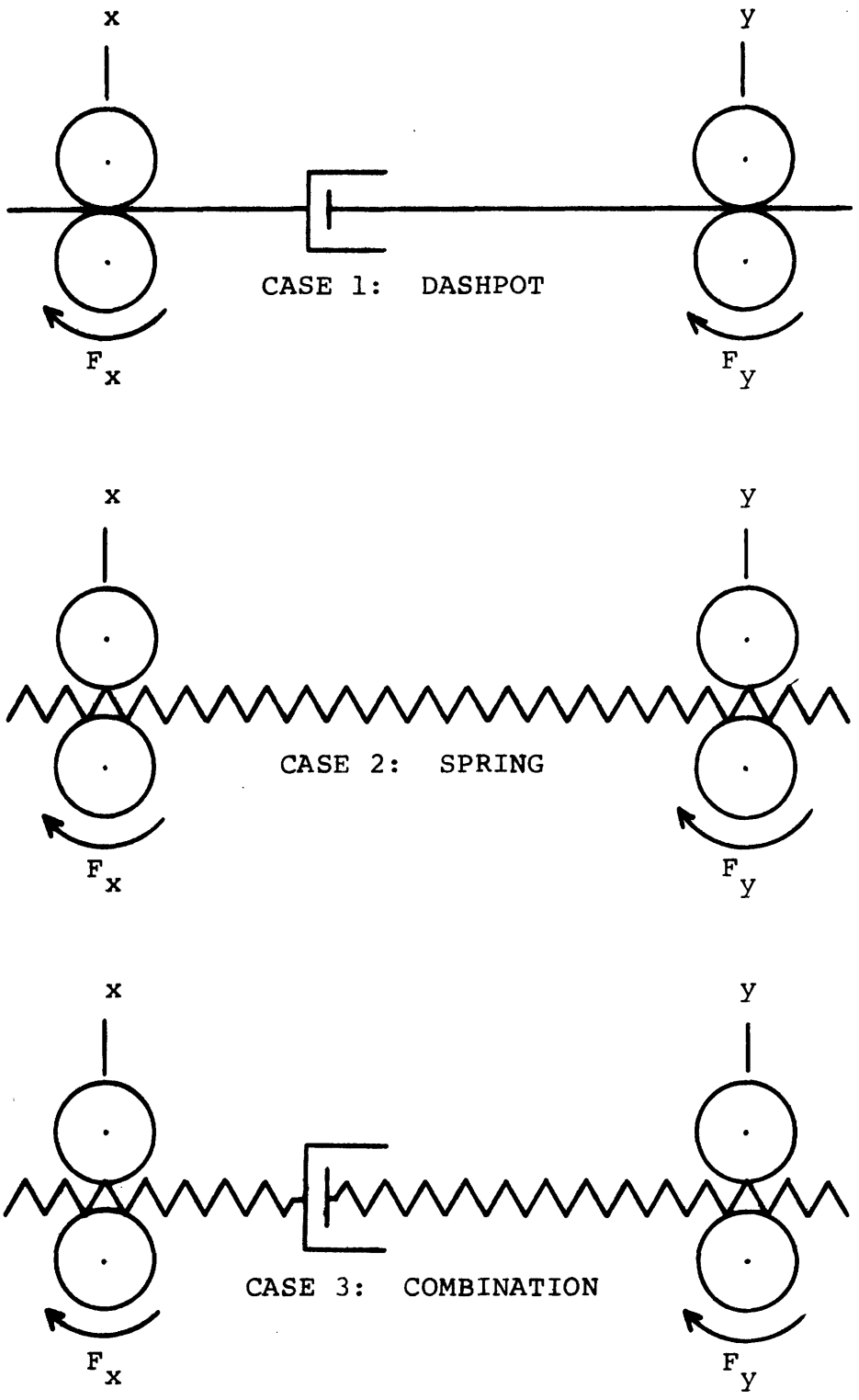

FIGURE 20 TEXTURING ZONE THREADLINE MODELS

between rollers 1 and 2 will vary roughly as the integral of the spindle speed. This variation in filament path length corresponds to a relative velocity between points x and y which will be roughly proportional to the deviation of spindle speed from the nominal value ($S - S_n$). Thus, for the sinusoidal variation in spindle speed shown in Fig. 21, the filament tension variation for Case 1 will be in phase with the spindle speed (dashpot), while the tension variation for Case 2 will lag the spindle speed by 90 degrees (spring). Since the alternate method of computing tension and torque discussed in Appendix 4 is a series combination of Case 1 and Case 2, as shown in Fig. 20 (Case 3), the filament tension would be expected to lag the spindle speed by somewhere between 0 and 90° at the higher values of spindle oscillation frequencies. Also, tension and torque amplitudes would be lower using Case 3, due to the sharing of strain between the spring and dashpot. This behavior would correspond more closely to the experimentally observed data of Fig. 17. At lower frequencies of spindle speed oscillation, however, the changing twist levels in the texturing zone begin to dominate the filament tension amplitude and phase response, and the above arguments become non-applicable.

Since the purpose of the kinematic computer model is merely to serve as an aid toward understanding the mechanics of the false twist texturing process, further indulgence in computer simulation at this stage would have led to neglect of experimental work on topics which follow, and it was decided to leave for a later date the implementation of the Appendix 4

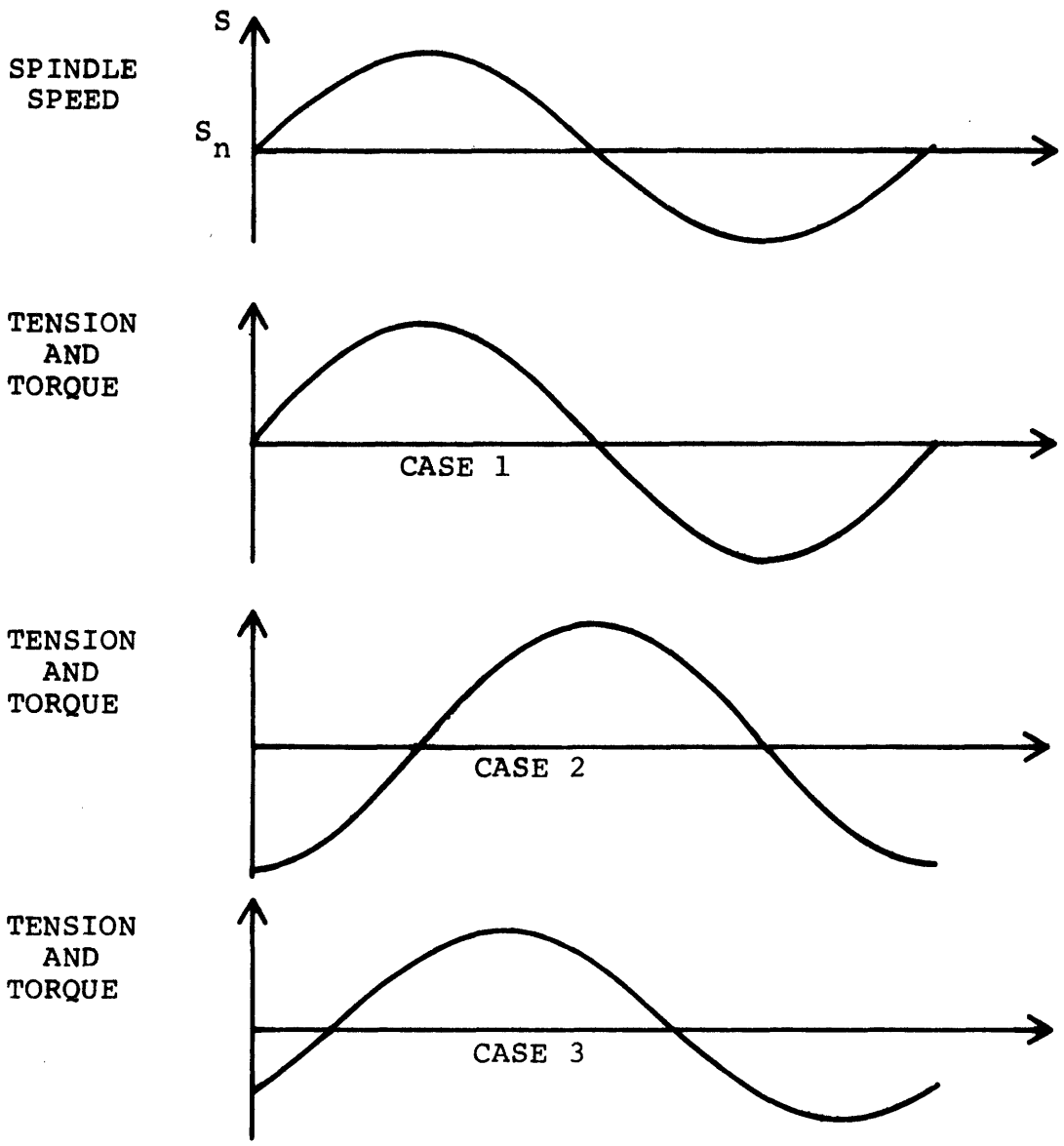

FIGURE 21 FORCE RESPONSE OF DIFFERENT THREADLINE MODELS TO HIGH FREQUENCY OSCILLATION OF THE SPINDLE SPEED

scheme for calculating filament tensions.

III.C. Cyclic Threadline Behavior

The transfer of rotational motion from texturing twisters to the translating filament bundle is one of the most interesting and complex aspects of the false twist texturing process. Twisters transfer motion to the yarn while the contacting yarn and twister surfaces are in continuous high speed relative motion. The total torque which can be transferred to the yarn is a function not only of the friction generated at the outer surface of the yarn, but also of internal yarn friction, or non-elastic resistance to deformation. This latter torque generating component appears to be highly advantageous in terms of the torque generating capability of a pin twister compared with the friction twister due to the deformation imposed by the full 360° excursion of the threadline around the spindle pin; but to what extent internal friction affects the torque-generating capability of either twister type remains to be determined. Regardless of the mechanism of torque transfer, however, there is no question that in order for a twister to be able to maintain a certain number of turns of twist in the threadline between roller 1 and the twister, for a given machine operating condition and feed material, a level of torque equal to or greater than that required by the threadline must be transferable from the twister to the yarn. If the level of torque called for by a designated machine twist cannot be supplied by the twister, then the texturing machine simply cannot operate at the designated twist level and rotational

slippage will occur between the yarn and the twister.

Interesting transient phenomena have been shown to occur in the threadline of the MITEX machine under such conditions, when the torque demanded by the threadline reaches a point where it is larger than that which can be supplied by the spindle twister. As was predicted by Brookstein [2], a mode of texturing system operation has been discovered where the usual constant machine roller and spindle speed conditions result in a regular oscillation of threadline torque, tension, and twists with a period of several machine lengths. This oscillating behavior results from unsteady rotational velocity of the yarn at the twister due to rotational slippage around the pin. Hence, the texturing system is observed to operate at a limit cycle under certain ranges of operating conditions. Experimentation has shown that for a given set of feed material and machine parameters, the system will always arrive at the same limit cycle regardless of system initial conditions (i.e. all initial conditions which do not cause threadline breakage), but that feed material with slightly different physical properties or surface finish, for instance, may reach a very different limit cycle under the same machine parameters in terms of amplitude and period of forces and twist. In all cases, sections of severe tight spots occur in the resulting textured yarn.

Figure 22 shows the time varying tension and torque curves occurring in the texturing zone during conventional texturing of commercial drawn feed yarn at operating Condition E [1.% OF; 60 TPI; 3.9 IPS] where the temperature of the heater is lowered

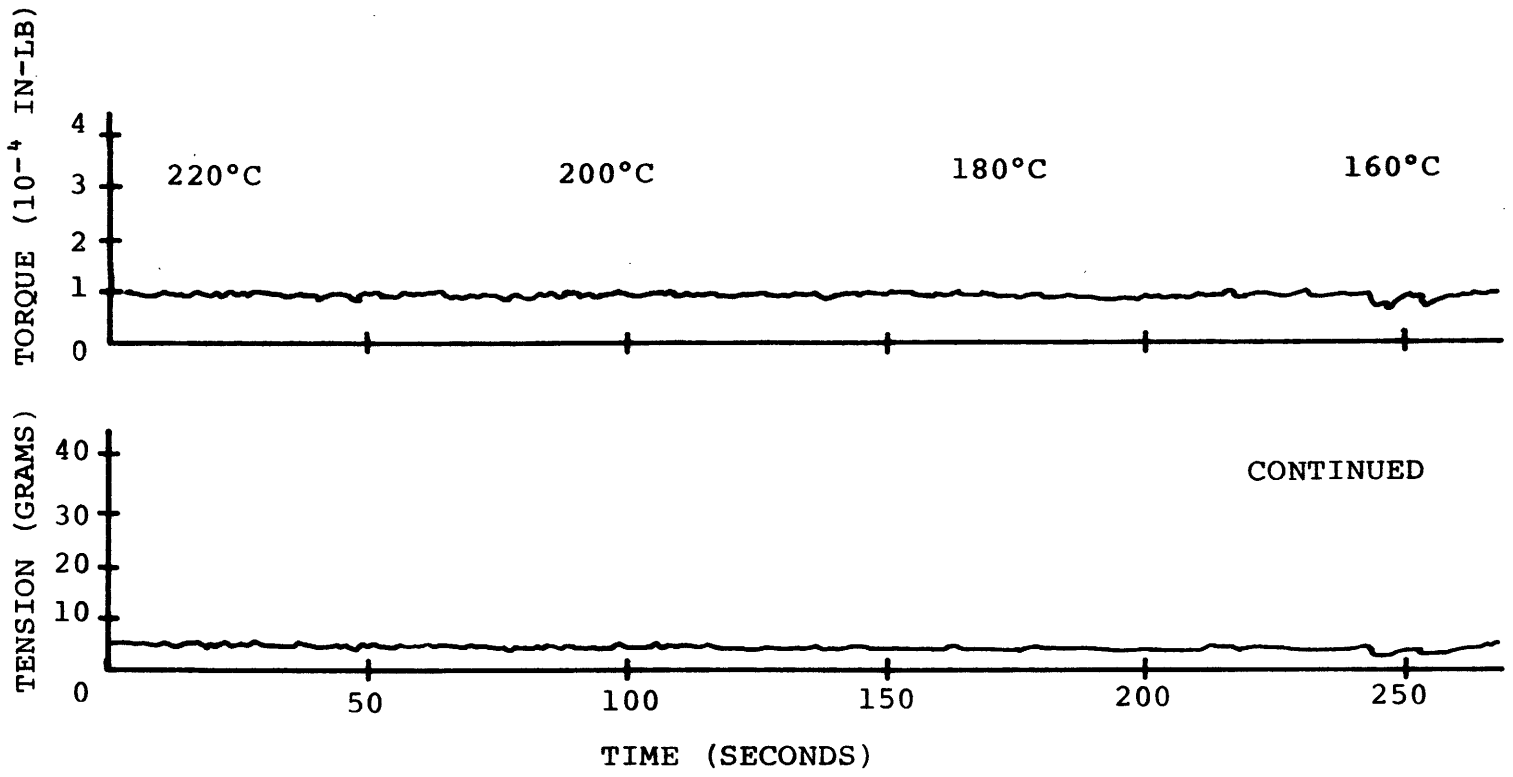

FIGURE 22 THREADLINE FORCES SHOWING THE DEVELOPMENT OF CYCLIC BEHAVIOR WITH DECREASING HEATER TEMPERATURE DURING CONVENTIONAL TEXTURING [1.0% O.F.; 60 TPI; 3.9 IPS]

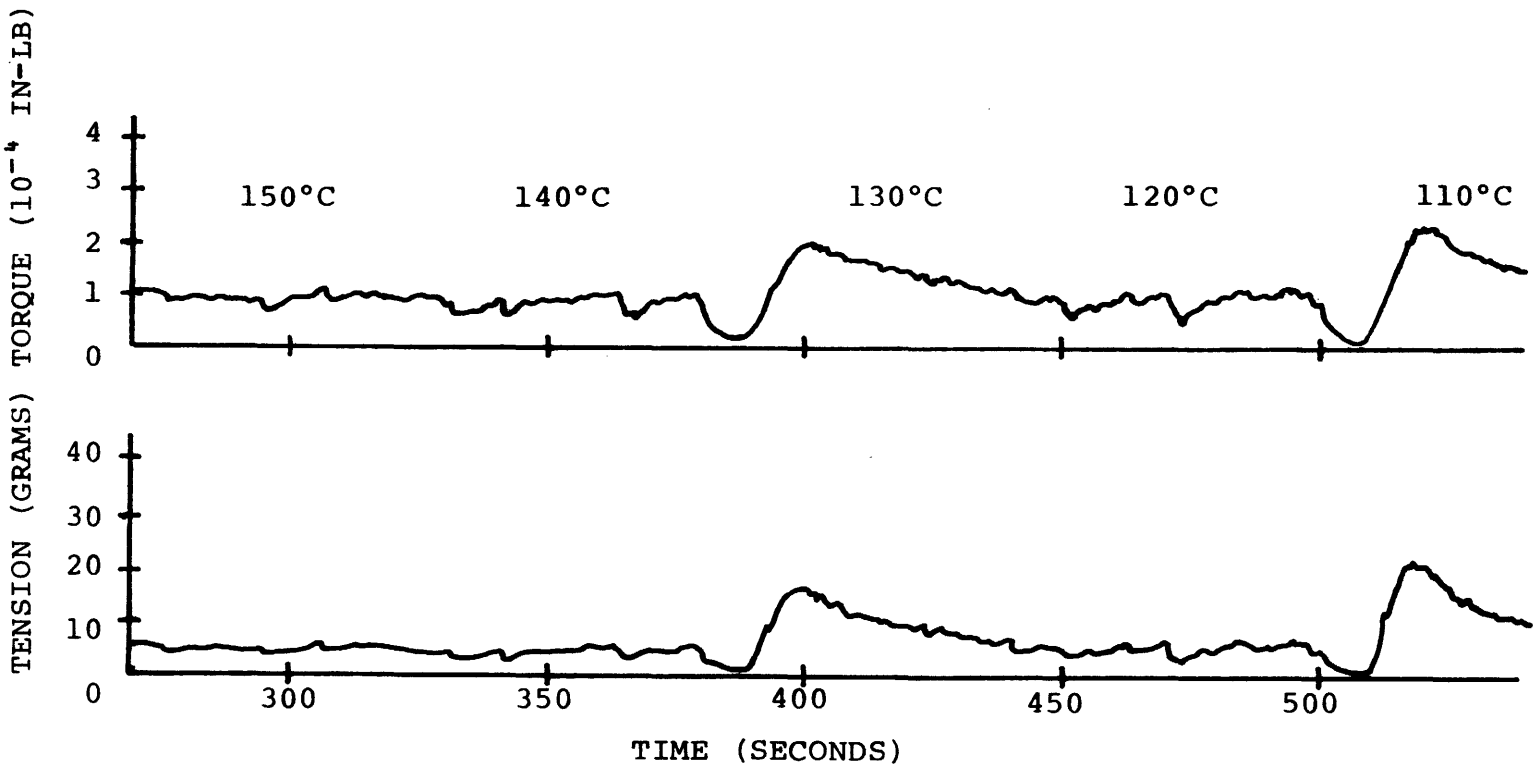

FIGURE 22 (CONTINUED -- 2 of 3)

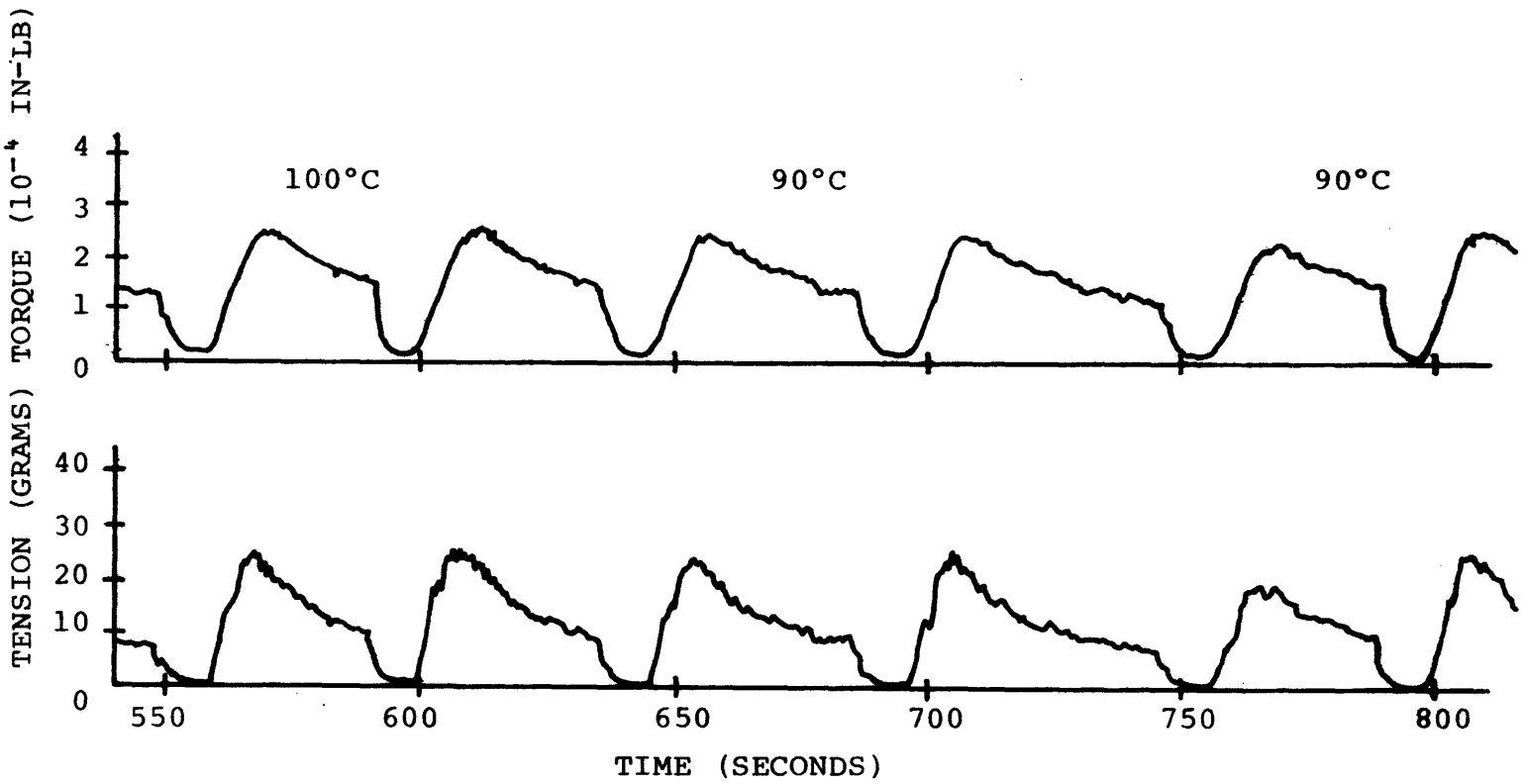

FIGURE 22 (CONTINUED -- 3 of 3)

from 200°C to 90°C in a sweep fashion. It can be seen that at this operating condition, the threadline becomes unstable at lower heater temperatures, and a very regular periodic cycling behavior develops. The total number of turns of twist in the texturing zone threadline is dropping by about 50% during the rotational slippage phase of each of the 90°C cycles, from a maximum value of about 100 turns per twisted inch to a minimum of about 50 turns per twisted inch. When the torque transferred from the spindle to the yarn once becomes equal to or greater than the threadline demanded torque, rotational slippage is prevented and threadline twists begin to increase. A tension and torque overshoot (i.e. above the steady state value) is then observed, which is similar to that seen in startup from zero twist (Section III.B.).

Further discussion of the role of heater temperature in threadline stability will follow the presentation of additional limit cycle data.

Figures 23a and b show the unsteady texturing zone tension and torque during a second texturing of commercial produced set textured yarn at operating Condition F[2.8% OF; 60 TPI; 3.9 IPS; 180°C]*. When textured yarn is used as feed material in the MITEX texturing machine in this manner, very pronounced and regular cycling behavior results. Unlike the plain feed yarn, which is unstable only at very low heater

---

*Retexturing of textured yarns is not done commercially, but offers an interesting case of study in the laboratory.

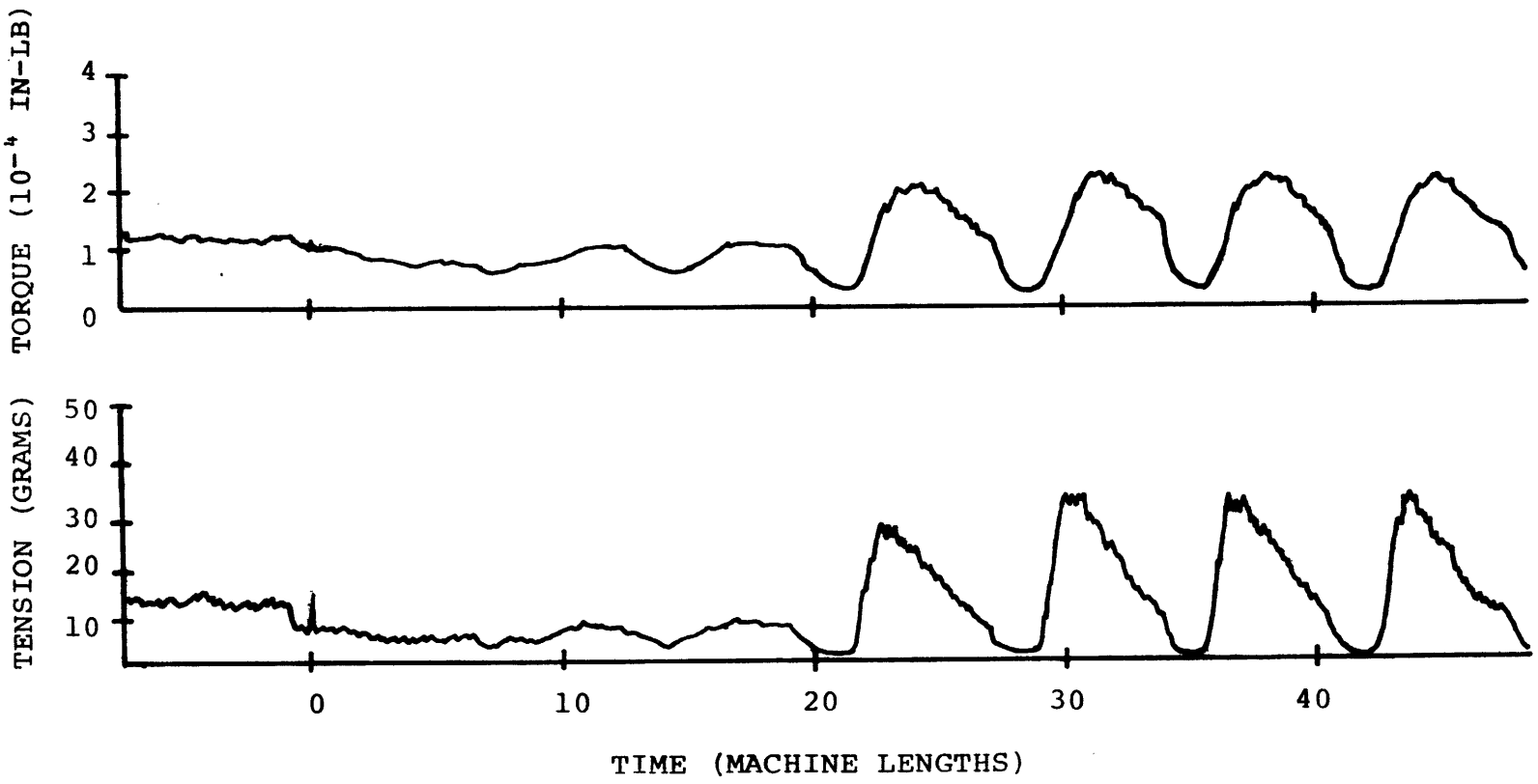

FIGURE 23a THREADLINE FORCES SHOWING THE DEVELOPMENT OF CYCLIC BEHAVIOR OF PRE-TEXTURED YARN FROM STEADY STATE TEXTURING CONDITIONS [2.8% O.F.; 60 TPI; 3.9 IPS; 180°C]

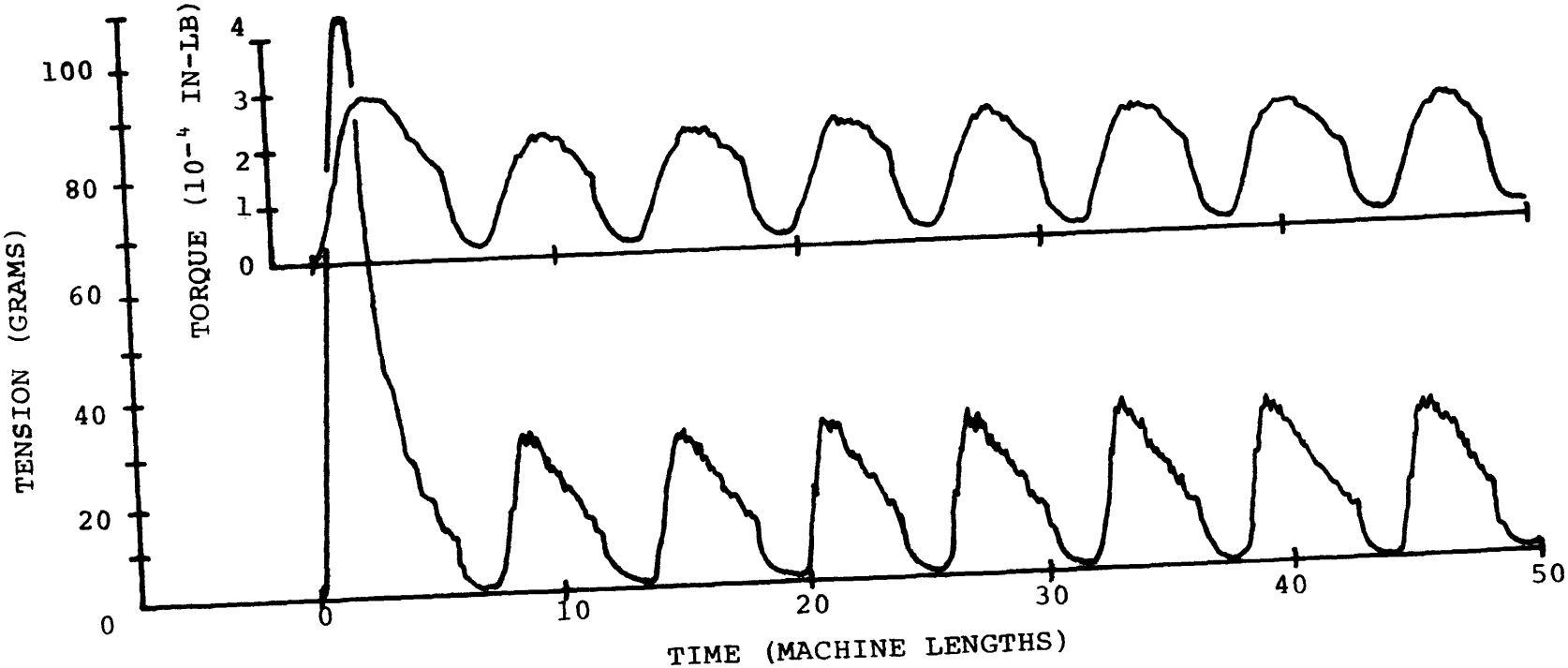

FIGURE 23b THREADLINE FORCES SHOWING THE DEVELOPMENT OF CYCLIC BEHAVIOR OF PRE-TEXTURED YARN FROM STARTUP CONDITIONS [2.8% O.F.; 0-60 TPI; 3.9 IPS; 180°C]

temperatures, the pre-textured feed yarn shows instability up to about 200°C heater temperature at the same machine conditions above which steady state operation is achieved. Further, if an identical pre-textured yarn is used to which 2 to 3% finishing oil has been applied, unsteady behavior will persist to heater temperatures above 220°C. Thus, the threadline stability is influenced by yarn material and structural properties and finish, as well as the machine settings of machine TPI and heater temperature.

A fifth important parameter is that of overfeed, or the difference between the speeds of roller 1 and roller 2 expressed as a percentage of roller 2 speed. Positive overfeeds represent a faster roller 1 and thus a lower filament and threadline tension in the texturing zone than negative overfeeds. It has been observed that the unstable limit cycle behavior will only occur over the range of overfeeds from 0 to +2% for the plain commercial feed yarn, and over the range of 0 to +3%, or more, for pre-textured feed material. The upper limits of overfeed represent machine conditions which are far from normal texturing conditions. On the other hand, when the MITEX machine is set to operate at an underfeed, the tension in the threadline is higher and cycling behavior is suppressed, presumably because the greater normal force of the yarn against the pin allows for the generation of a greater torque in the yarn; although a greater tension in the texturing zone also means a greater torque which must be supported at the twister, due to the helix angle of the filaments, and it is not clear which effect

dominates.

It is significant that to date cycling behavior has been observed at machine conditions representing conventional texturing only, where lower threadline tensions are possible. At the relatively high threadline tensions found in draw texturing, spindle slippage is not observed. Instead of becoming unstable when twist is increased to abnormally high levels in draw texturing (above 70 TPI, for instance), the threadline develops very pronounced buckling as discussed in Section III.A, and continues to operate at a steady state condition over the full range of heater temperatures.

Returning to the case of limit cycle behavior under conditions of conventional texturing using pre-textured feed yarn, it is interesting to observe qualitatively the initiation of cycling behavior starting at initial conditions of steady state running (Fig. 23a). Steady state running conditions were established using conventional commercial feed yarn. The pre-textured yarn had been tied onto the tail end of the plain feed segment, and the transfer knot can be seen passing the inlet twist trap at time zero, as evidenced by the small tension spike at time zero. With the new material in the machine, gradually the instability develops and grows in amplitude until the system settles into its characteristic limit cycle behavior.

This gradual attainment of full cycling amplitude for the case of pre-textured feed material can be contrasted with the case of conventional feed yarn which was seen in Fig. 22, where the full amplitude of cycle behavior was attained with the first

major occurrence of spindle slip. Although, prior to the first full cycle, several instances can be seen where the yarn started to slip around the pin (as evidenced by slight reductions in tension and torque), but was arrested before excessive twist could be lost from the texturing zone. These small rotational slippages are interesting since they suggest the possibility of constant rotational slippage around the pin such that the threadline can operate steadily at a lower level of twist than is designated by the machine TPI.

Although the low heater temperature necessary for this borderline behavior at slow speed texturing on the MITEX machine is abnormal, it is possible that in the case of high speed industrial machines the same case of borderline stability could exist at higher heater temperatures. It is also possible in this connection that certain rate dependent parameters in the draw texturing process will allow spindle slippage at high speeds but not at slow laboratory speeds, although no direct evidence for this exists.

The difference between the random low magnitude and duration "slips" which are seen in the range of 160°C to 140°C in Fig. 22, and the gross "slips" seen between 140°C and 90°C is that at the slightly higher temperature, the threadline torque which could be supplied by the spindle was below that demanded by the threadline for only a very short time. In contrast, at the lower temperatures, the torque discrepancy remained for a sufficient time to allow a significant number of turns of twist to be lost from the texturing zone. The

exact mechanism which causes this difference is not known, but heater temperature definitely plays an important role. It appears as though the amount of torsional energy stored in the texturing zone threadline may dictate whether a slight rotational slippage will arrest itself after only a few revolutions, or whether it will follow through and result in a major loss of twist in the texturing zone. In this regard, a higher heater temperature would tend to suppress torsional energy in the threadline by heat setting it in the twisted state, thus stabilizing the threadline against cycling. In all cases of limit cycle behavior observed on the MITEX machine, high heater temperatures caused the threadline to become stable. Although there is no clearcut explanation to account for the wide range of heater temperatures over which pre-textured feed yarn will cycle compared to the narrow range over which plain feed yarn will cycle, it is clear that the structural uniqueness of the pre-textured yarn plays a role.

Observation of Threadline Buckling during Cycling Behavior

As the twist level in the texturing zone threadline reaches a maximum value just before slippage of the yarn around the pin takes place, buckles are observed to form in the threadline. It is possible, although there is no direct supportive evidence, that the buckled threadline provides for less twister to yarn torque transfer, either because of reduced surface-friction generated torque or reduced bending losses, and thus enhances the possibility of spindle slippage.

In this connection, it is interesting to recall the well

known limitations of friction twisters in terms of their twist insertion capabilities. For reasons which apparently have not been established, disc type friction twisters are incapable of inserting twists beyond about 60 TPI machine twist, as opposed to the virtually limitless capability of pin twisters, which normally operate in the range of 65 to 70 TPI. The interesting question raised by this fact is whether threadline buckling has something to do with this limitation, since buckles just begin to become fairly pronounced at twist levels of about 60 TPI. Buckles may cut down on the surface friction which can be generated by the twister discs against the yarn surface. There is already a significant speed difference between the yarn surface and the twister disc surface, the disc surface running roughly twice as fast as the yarn surface in the same plane. The irregular surface of buckled twisted yarn may be enough to disrupt the delicate frictional balance which represents the steady state operating condition of the twister. The frictional properties of a yarn surface and of yarn bending properties are prime topics for further study related to unsteady twister slippage.

Computer Simulation of Cycling Behavior

In order to study cycling behavior on the kinematic computer model, several simplifying assumptions or spindle slip criteria were included in the statement of the analytical model. These criteria are based on observations made during cycling behavior on the MITEX machine and they are not intended to represent a fundamental analysis of the physical interactions

taking place at the twister and along the threadline:

(1) Angular velocity of the yarn at the twister is equal to the twister (spindle) speed as long as the total torque required to twist the threadline to the required level and to untwist the yarn downstream of the spindle is less than the maximum torque which the spindle can supply. (Torques are calculated as shown in Appendix 7 on the basis of an effective coefficient of friction. Internal yarn friction is not considered separately.)

(2) If the total threadline torque requirement becomes greater than the torque which the spindle can supply, then the yarn at the twister will slip with a constant rotational velocity relative to the spindle until the maximum pin suppliable torque again exceeds the total threadline torque.

(3) Since high slip velocities can cause corresponding reductions in draw ratios for short periods, the filament tension is given a near zero positive quantity whenever this condition occurs. This assumption is based on observed threadline behavior and it is intended to avoid problems in the polynomial tension expression.

(4) Coefficient of friction is assumed to be a linear function of twist; and yarn contact angle around the pin is assumed to be 2π radians.

(5) A component of torque proportional to θ_2 (helix angle in Zone 2) is assumed to be present in the

threadline in such a way that the equilibrium equation of the kinematic model [Eq. (1)] still holds.

By implementing the above criteria as described under Input Parameters"e",cycling behavior was simulated as shown in Figs. 24 and 25. It was found that slight differences in the effective coefficient of friction had a strong influence on computed cycle period as illustrated by the differences between the two figures. The expression for coefficient of friction was changed from $.22 - .15\ \theta_2$ in Fig. 24 to $.25 - .15\ \theta_2$ in Fig. 25, while all other expressions remained the same.

Clearly, such a change in coefficient of friction should also influence the rate of rotational slippage around the pin, but implementation of some assumed expressions describing rotational slip velocity as a function of threadline forces and coefficient of friction would add complexities not warranted within the context of the kinematic model.

It is interesting to note the general similarity between the experimental cycling force curves of Figs. 22 and 23 and the computed cycling force curves of Figs. 24 and 25. In both cases, tension is seen to attain a peak value before torque, and then to drop off more steeply than the torque curve in seeking a steady state value before slippage occurs. Just before the spindle slippage occurs, therefore, torque is still at a relatively high value, while tension has dropped to a relatively low value. This low value of tension corresponds to a small pin suppliable torque, which results in

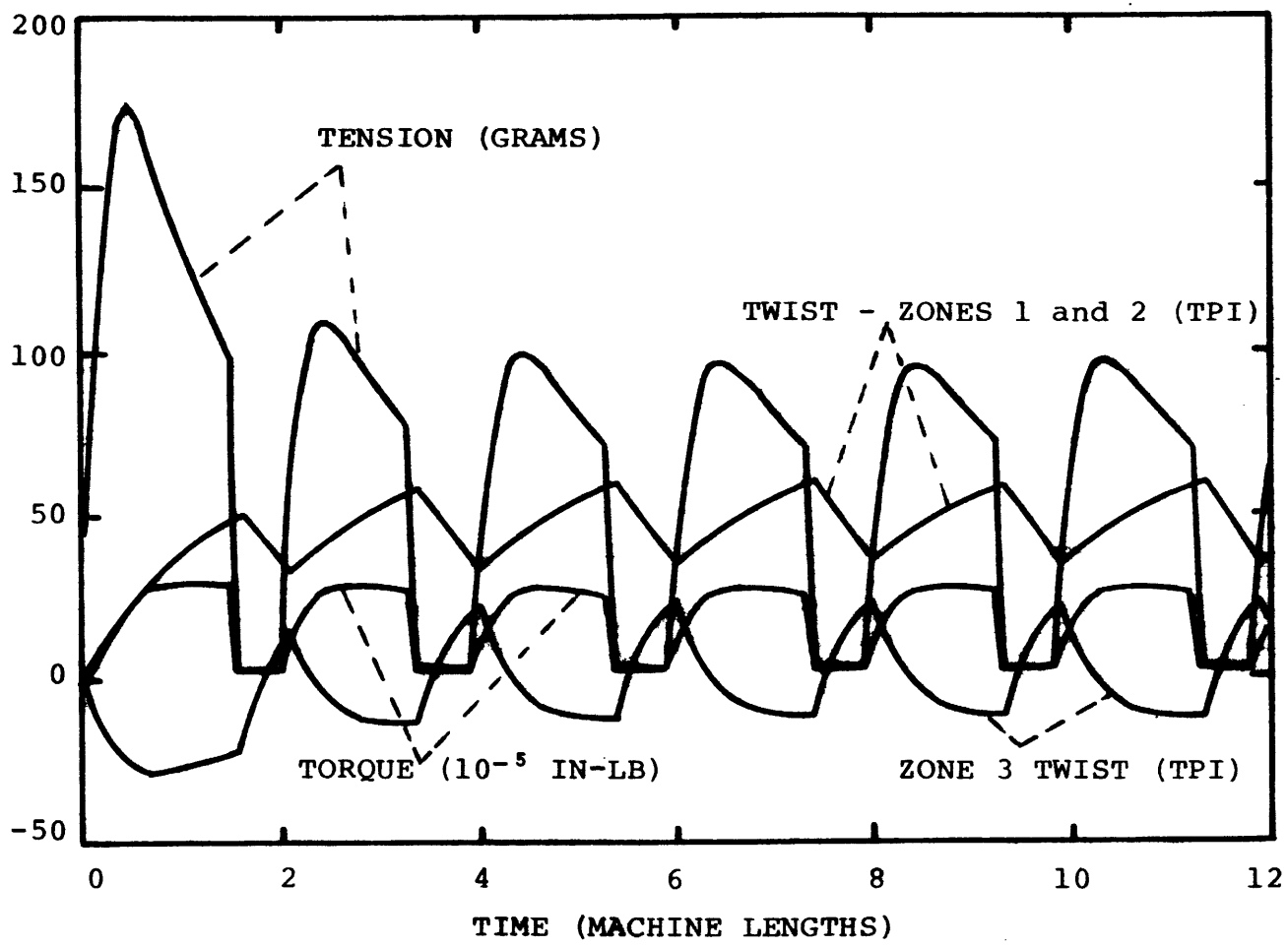

FIGURE 24 COMPUTED CYCLIC THREADLINE BEHAVIOR FROM STARTUP CONDITIONS (COEFFICIENT OF FRICTION = .22 - .15 θ_2)

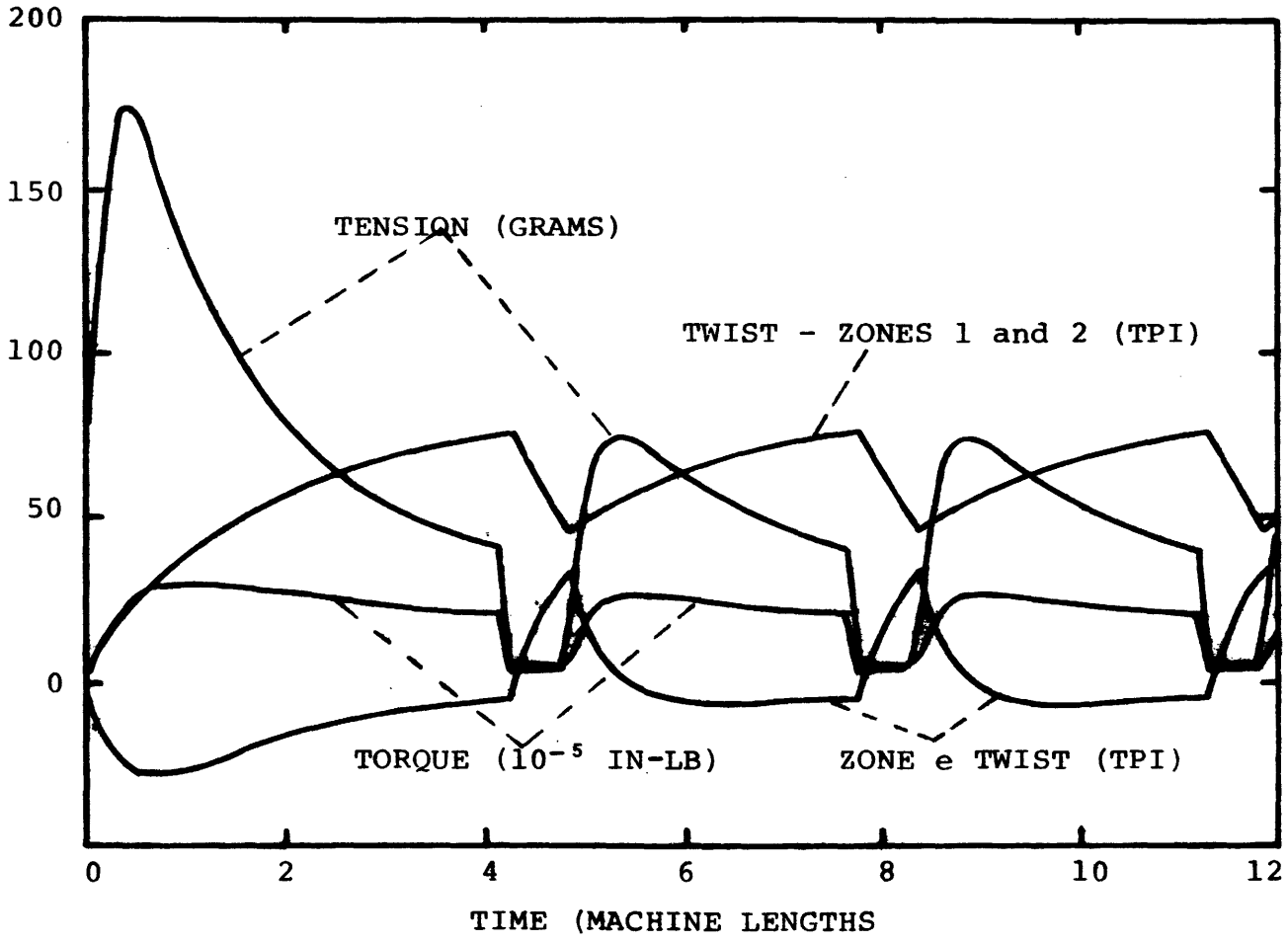

FIGURE 25 COMPUTED CYCLIC THREADLINE BEHAVIOR FROM STARTUP CONDITIONS (COEFFICIENT OF FRICTION = .25 - .15 θ_2)

rotational slippage.

The role that assumption 5 would play in the computer simulation of cycling behavior was not realized until several simulation attempts had been made using only assumptions 1-4. If no elastic component of threadline torque were included in the model statement, then spindle slip would occur only in very short, closely spaced spurts, resulting in an amplitude of twist variation in the threadline of only a few turns per twisted inch. Thus, the simulated texturing system would operate in a pseudo steady state, at a twist level below that called for by the spindle speed. Interestingly, this condition is similar to the borderline stability conditions observed earlier in this section, where the spindle slippage behavior of plain feed yarn was studied on the MITEX machine. The shortlived dips in tension and torque seen in the 150°C range of Fig. 22 undoubtedly represent short term rotational slippage around the pin, which is arrested either because insufficient torsional energy exists in the threadline to maintain the slippage once filament tensions have dropped, or because the variation of friction with twist is flatter than supposed.

The elastic torque component included in the kinematic model statement represents less than 20% of the total threadline torque at normal steady state operating conditions of texturing, but when filament tensions drop due to spindle slippage, the elastic component becomes the dominating threadline torque component and does not allow for correction of torque transfer inadequacy of the pin spindle until significant twist has been lost from the texturing zone, constituting

full cycling behavior. The effective torsional spring constant in the texturing zone thus appears to be an important parameter governing unsteady spindle slippage as observed on the MITEX texturing machine.

Cycling frequency in computer simulation can be varied greatly by making small changes in the effective pin-to-yarn coefficient of friction, and can thus be adjusted to correspond quite closely to experimental cycling frequency. Also controlling computed cycling frequency to some extent, however, is the relative slip velocity between the pin and the yarn, which is supplied as an input. For instance, as was mentioned previously, high relative slip velocities at the pin can cause such rapid changes in threadline geometry that the computed draw ratio is significantly reduced. In the real system, this would represent a situation of low threadline tension where a change in threadline geometry would take place in order to accommodate the excess filament length present in the texturing zone after spindle slip. The tension would then remain low for a period of time while the excess filament length was transported out of the machine; and, in fact, this behavior can be seen on the MITEX machine. The kinematic model is not able to handle this type of behavior and, instead, does away with excess filament length at the draw point. It is apparently for this reason that the computed low tension phase of each cycle is too short.

Thus, the kinematic computer model has served as a tool toward developing an understanding of cycling behavior as observed on the MITEX texturing apparatus.

III.D. Draw Point Motion in Draw Texturing

As was mentioned in Section III.A, attempts to correlate the random tension and torque fluctuations observed during normal steady state conditions of draw texturing with the occurrence of threadline buckles were unsuccessful. Since then, further investigation of these force fluctuations has led to the conclusion that they are more likely connected with random motion of the draw point with respect to the texturing machine, due either to variation in feed yarn properties along the yarn length, or variation in the amount of heat transferred to the yarn over the portion of the heater prior to the draw point, or both.

Ironically, drawing of the filaments results in the most drastic change in material properties which occurs in texturing, and yet it is perhaps the least controlled aspect of the entire process. The draw ratio which a given filament in the twisted bundle experiences at the draw point is determined by a number of variables including:

(1) Machine draw ratio.

(2) Threadline yarn properties.

(3) Radial position of the filament in the yarn at the draw point.

(4) Motion of the draw point.

Consider a condition of steady state draw texturing with variables (1) and (2) held fixed. Due to radial filament migration which takes place primarily as the yarn enters the texturing zone, variable (3) is constantly changing as a given filament passes through the draw point. Thus, the draw ratio of the filament varies along its length as it leaves the draw point, since draw ratio is a function of radial position in the twisted yarn. However, the average draw ratio experienced by all of the filaments in any yarn cross section leaving the draw point should remain constant, provided that the position of the draw point is stationary with respect to the texturing machine [i.e. variable (4) is zero]. If the draw point is in motion, variation in average draw ratio along the yarn will result.

Random Draw Point Motion

The following discussion relates to observations of draw point motion made on the MITEX machine, and how draw point motion affects the overall texturing system in terms of threadline forces.

Initially, microscope observation of the draw point was made on non-twisted yarn at MITEX operating Condition G [1.6 DR; 0 TPI; .34 IPS; 210°C] (where the yarn was not wrapped around the spindle pin). A distinct draw point was visible on each filament as illustrated in Fig. 26a and it was noticed that the central filaments were drawing slightly later than the peripheral filaments, as depicted in the figure by the curved profile of individual draw points across the yarn. The curved profile of draw points presumably reflects a temperature

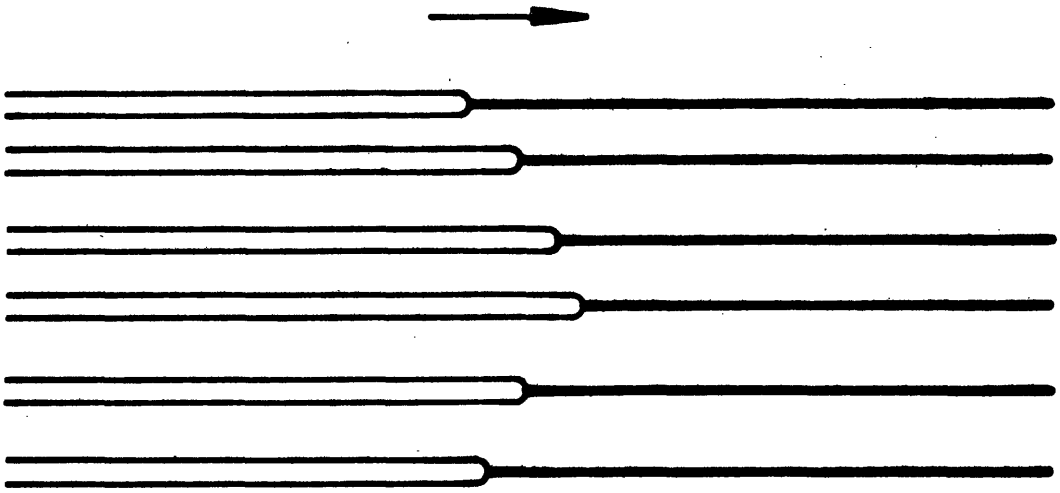

(a) SLOW SPEED [1.6 DR; .34 IPS; 210°C]

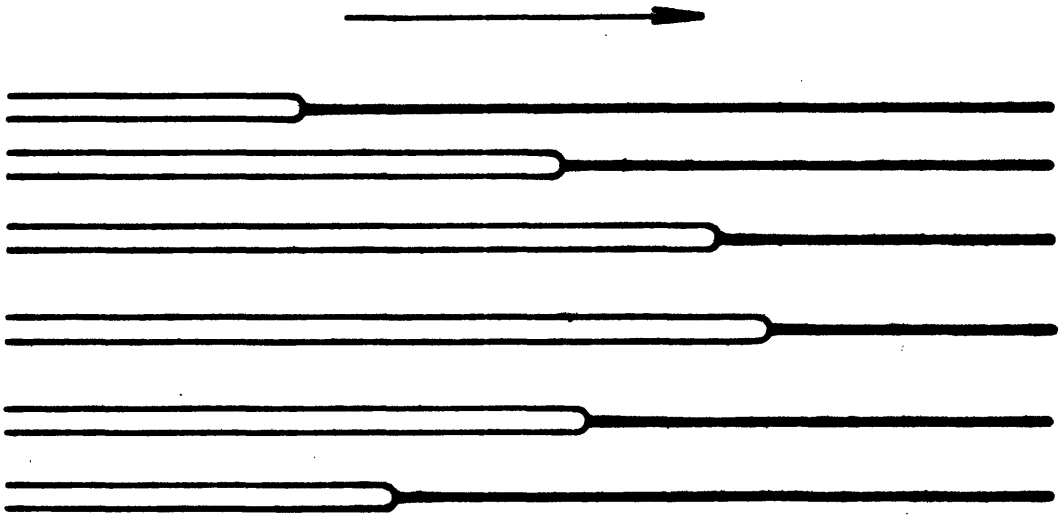

(b) HIGHER SPEED [1.6 DR; 3.1 IPS; 210°C)

FIGURE 26 DRAW POINT PROFILE ACROSS YARN DURING STRAIGHT DRAWING AT TWO SPEEDS (34 FILAMENT YARN)

gradient across the yarns. As a result of the slow roller velocities of this operating condition, it was also observed that all drawing took place prior to actual yarn contact with the heater, indicating a less direct heat transfer path to the draw point than would be expected when the draw point occurs in a segment of yarn which is in direct contact with the heater.

Although the individual draw points of all filaments consistently remained within a very short segment of yarn relative to each other, they were seen to move about considerably as a group relative to the texturing machine. It was then discovered that this motion of the yarn draw point correlated well with the random threadline tension variation observed during steady state yarn drawing. Such a correlation can be observed in Fig. 27 where the dark bars above the torque curve (which remains at zero during straight drawing) mark occasions when the draw point of the yarn was observed to be moving upstream or toward roller pair 1. The marks coincide quite well with incidents of low threadline tension.

This observation is in agreement with expected behavior based on the simple representation of draw point motion shown in Fig. 28, which leads to the following expression for draw ratio DR as a function of velocity of draw point motion V_{dp}, where velocities are normalized with respect to V_{out} by use of a prime:

$$DR = (1 - V'_{dp})/(V'_{in} - V'_{dp}).$$

The draw ratio is thus equal to the relative filament velocity moving away from the draw point divided by the relative filament velocity moving toward the draw point. Draw ratio is

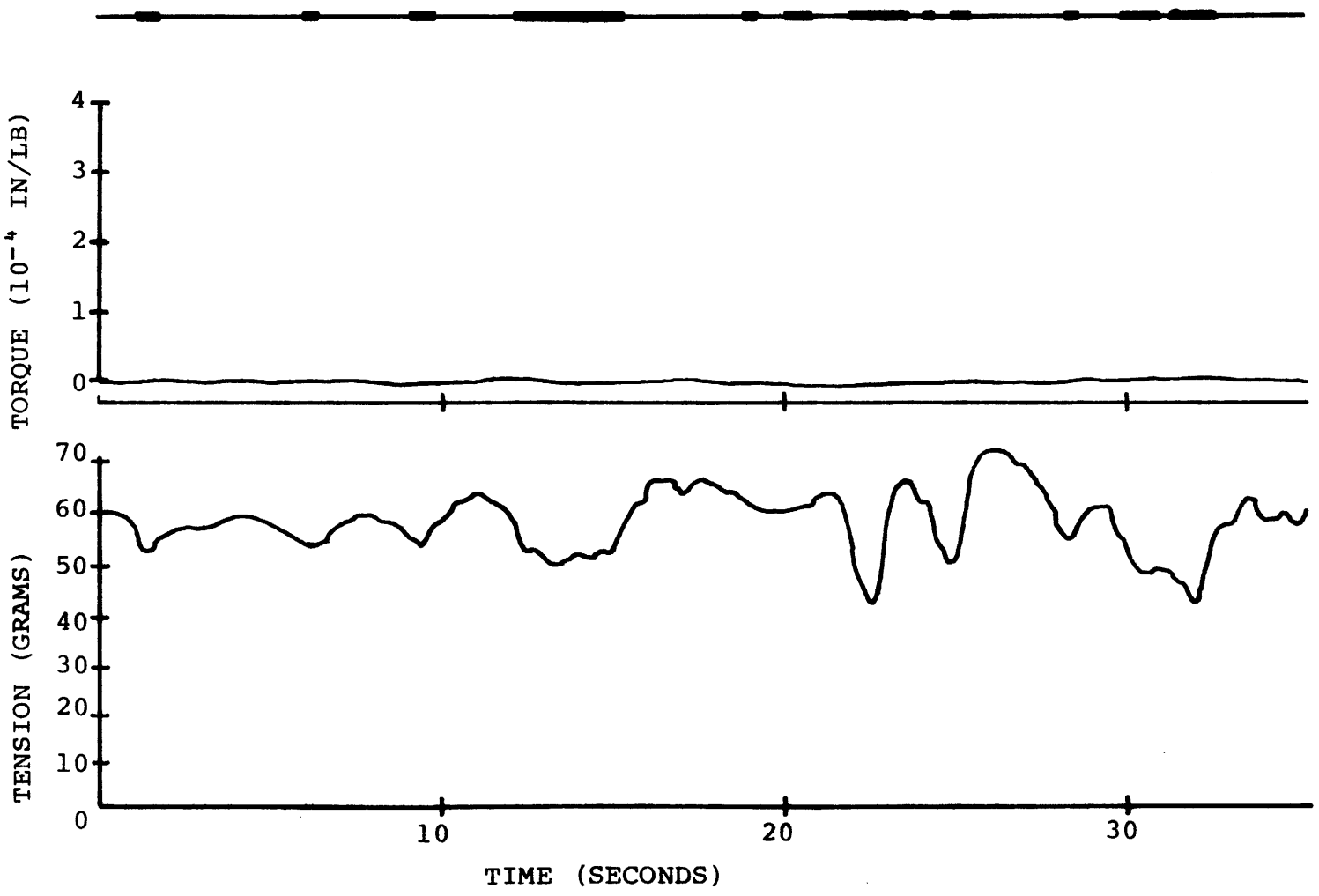

FIGURE 27 CORRELATION OF UPSTREAM DRAWPOINT MOTION WITH THREADLINE TENSION DURING STRAIGHT DRAWING [1.6 DR; NO SPINDLE; .34 IPS; 210°C]

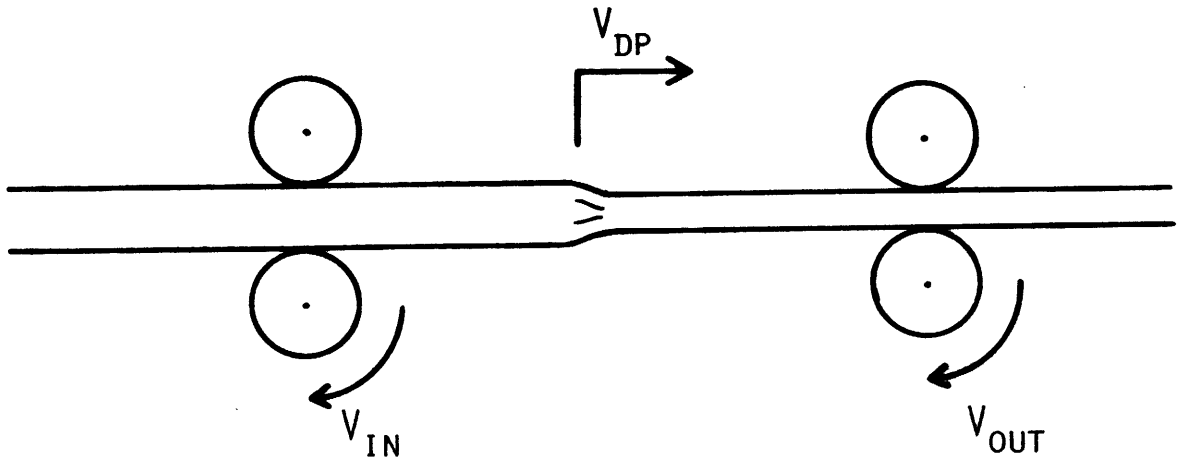

FIGURE 28 SIMPLE REPRESENTATION OF DRAW POINT MOTION

plotted against normalized velocity of draw point motion in Fig. 29 for a machine draw ratio of 1.6. The intercept on the ordinate represents steady state operation with a stationary draw point. If the draw point moves upstream, toward roller 1, draw ratio will decrease, while if the draw point moves downstream, draw ratio increases sharply. Since a lower tension is associated with a lower draw ratio, the above analysis agrees with the experimental results of Fig. 27, although it would require more thorough experimental techniques to make an accurate estimate as to the velocity of draw point motion as observed in the MITEX threadline. The position of the draw point was seen to remain with $\pm$.1 inches of its nominal position.

It seems likely that the draw ratio expression shown above would overpredict the actual draw ratio seen by the filaments for rapid draw point motion, due to the elasticity in the threadline which is not included in the representation of Fig. 28. Furthermore, this overprediction would be more severe the longer the threadline. Thus, the draw ratio expression can be used as a qualitative guideline only, since it represents the limiting case of very short threadlines.

Regarding the question of the cause of random draw point motion, it was observed during the course of the above experiment that blowing a puff of air against the draw point would cause it to move rapidly downstream and on to the heater, resulting in a threadline tension spike with a magnitude similar to that of the larger random tension spikes. The draw point would then drift quickly back upstream to its nominal

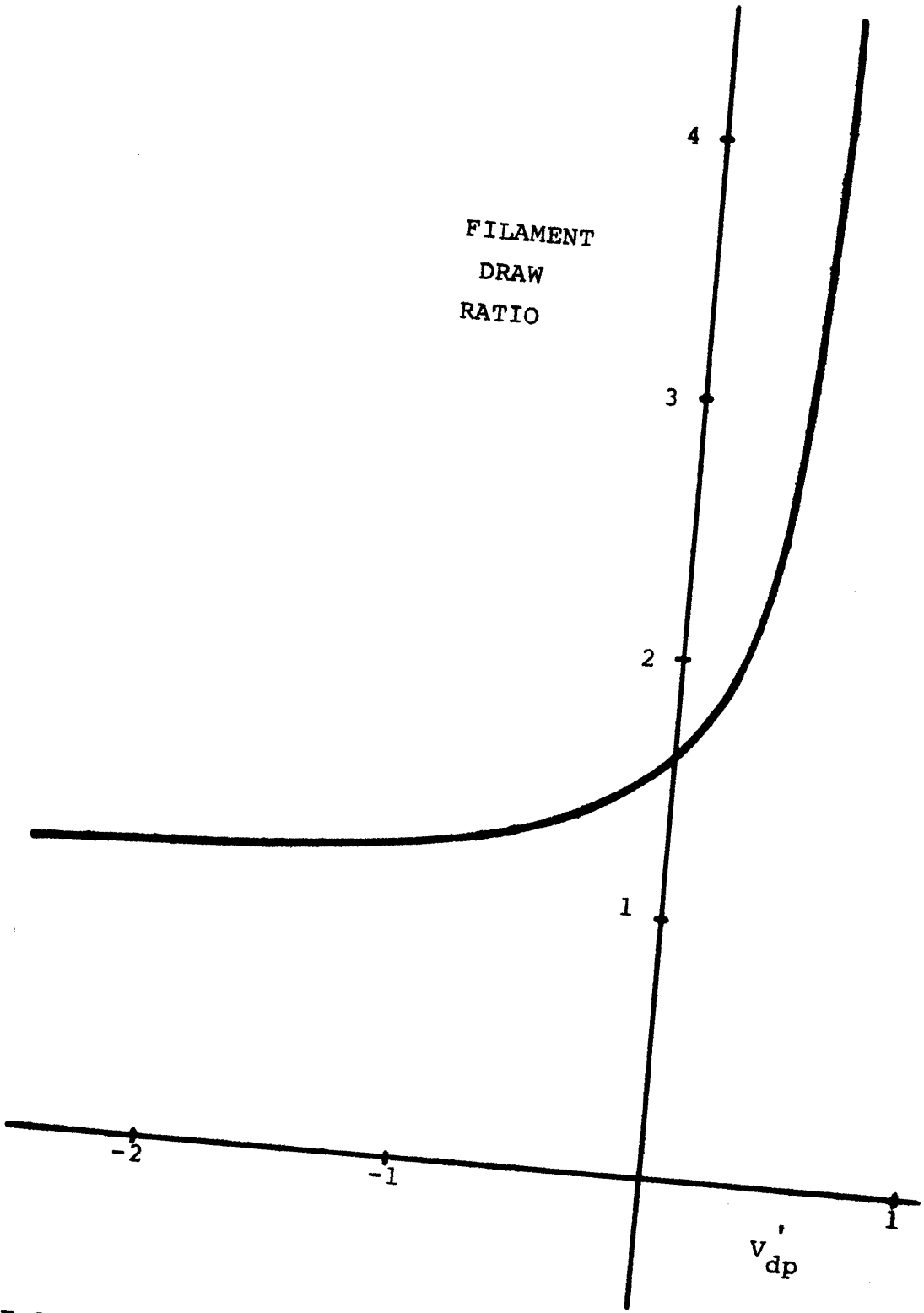

FIGURE 29 FILAMENT DRAW RATIO VS. VELOCITY OF DRAW POINT FOR STRAIGHT DRAWING AT A MACHINE DRAW RATIO OF 1.6

position, causing tension to dip slightly below normal in its return to a nominal value. This behavior illustrates the role of varying heat transfer in motion of the draw point. In addition, it may be true that yarn denier variations and therefore heat capacity variations along the yarn cause draw point motion and thus influence threadline tension. Such denier variations may also influence tension directly while causing negligible draw point motion, a topic which will be discussed following the presentation of further data.

Observations similar to those described above have been made at machine Condition B [1.6 DR; 60 TPI; .34 IPS; 210°C] during draw texturing, still at slow roller velocities. In the twisted filament structure, the yarn draw point is seen as a necking, or reduction of yarn diameter over a short yarn segment, but individual filament draw points are not observed as they had been in the case of straight drawing. The draw point occurs at a spot slightly further in front of the heater than in the case of straight drawing. Figure 30 shows correlation between upstream velocity of draw point motion and low values of tension and torque. Motion of the draw point in this case was determined by watching for changes in yarn radius while observing the nominal draw point location on the yarn. In Fig. 30, the marker pen was triggered at the sight of a reduction in yarn radius. (It is apparent from this figure that tension and torque are varying in nearly perfect unison. Thorough checking of this result leaves little doubt that Fig. 30 represents accurate threadline behavior and not electrical

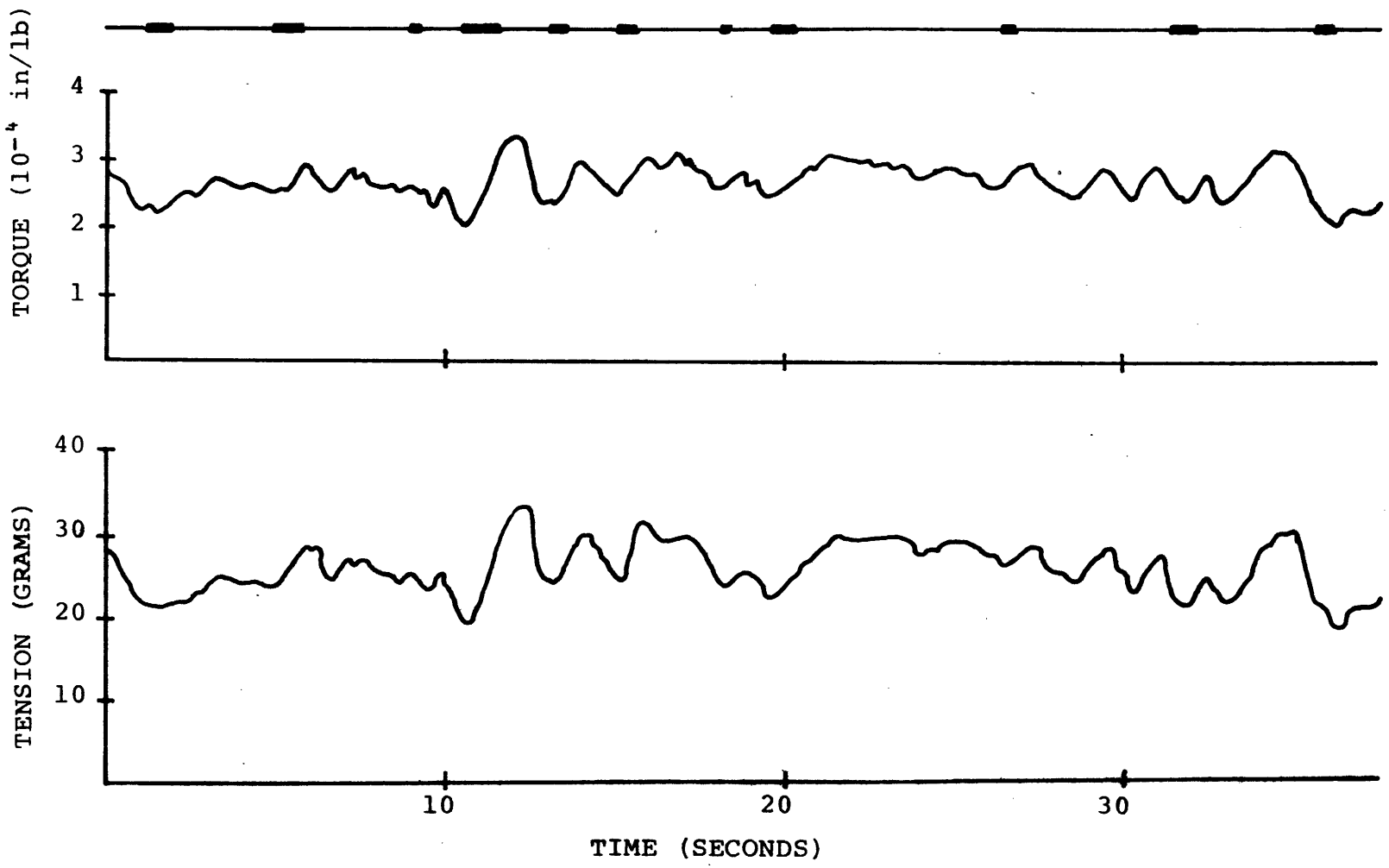

FIGURE 30 CORRELATION OF DRAW POINT MOTION (UPSTREAM) WITH LOW THREADLINE FORCES DURING SLOW SPEED TEXTURING [1.6 DR; .34 IPS; 60 TPI; 210°C]

or mechanical coupling in the instrumentation which might be suspected in observing the force traces.)

In order to determine the effect of machine speed on the draw point behavior observed above, similar experiments were run with machine speed increased by a factor of about 10. Comparison between the slow speed cases of straight drawing and draw texturing and the corresponding higher speed cases at operating Conditions H [1.6 DR; 0 TPI; 3.1 IPS; 210°C] and D [1.6 DR; 60 TPI; 3.1 IPS; 210°C], are listed below:

(1) The draw point of the yarn in the higher speed case occurred at about .1 inch onto the heater in both straight drawing and texturing, instead of prior to the heater, as in the slow speed case.

(2) A steeper draw point profile in the untwisted yarn implied a higher temperature gradient across the yarn than was present in the slow speed case (Fig. 26).

(3) Little random draw point motion occurred in straight drawing or texturing at the higher machine speed and manual, real-time recording of draw point motion was very difficult. The apparent increased stability of the draw point in the higher speed case could be due to the more direct heat transfer path between the heater and the draw point when drawing occurs over the heater.

(4) Draw point position was barely affected by puffs

of air blown directly on the yarn at the heater, in the higher speed case, compared to the large effect that such turbulences in the heater area had in the slow speed case.

(5) A periodic variation in threadline tension was seen in straight drawing at the higher speed, but it correlated directly with the speed of roller 2, and did not appear to cause draw point motion. (This variation can be seen in Fig. 36 of Section III.E at a period of about 1.6 seconds).

(6) The periodic tension peaks observed in (5) were far less evident in the corresponding tension and torque curves for steady state texturing.

Forced Variation of the Draw Point

A cam and slider arrangement has been devised for the MITEX machine which provides for sinusoidal movement of the heater relative to the texturing machine during straight drawing or draw texturing (see Fig. 6). Observation has shown that the draw point follows the motion of the heater very closely when the maximum speed of the heater is less than the translational speed of the yarn in the cold zone. Thus, draw point position is essentially being controlled directly. The motor/cam selection used on the MITEX machine led to the following approximate expression for oscillation of draw point position, which is appropriate for use with operating Conditions H and D [1.6 DR; 0 TPI; 3.1 IPS; 210°C] and [1.6 DR; 60 TPI; 3.1 IPS; 210°C]:

$$X = 0.172 \sin (1.05t) \text{ [inches]}$$

Differentiating the above we obtain:

$$V_{dp} = .181 \cos (1.05t) \text{ [inches/sec]}.$$

The maximum velocity of draw point motion with this arrangement is about .18 inches per sec, which is about 9% of the roller 1 (feed) velocity. Similarly, the amplitude of draw point motion is about $\pm$1% of the texturing zone length.

The threadline force variations resulting from oscillating draw point position at the operating Conditions listed above are shown in Figs. 31 and 32. It can be seen that the maximum and minimum threadline forces correspond roughly to the maximum heater velocity downstream and maximum heater velocity upstream, respectively. It is also quite evident that the amplitude of the tension and variation in straight drawing is much greater than the amplitudes of force variations in texturing, for the given draw point motion, even when amplitudes are taken in terms of percentages of the nominal force values. Apparently, the highly twisted yarn in the texturing threadline has a lower effective elastic constant than the straight yarn, which results in a smaller range of filament draw ratio variation at the draw point than with the straight yarn.

It would be of great value in this regard to be able to monitor the denier of the yarn in the post-spindle zone for both straight drawing and draw texturing while simultaneously imposing the known oscillation of the draw point position, although it might be difficult to isolate any simultaneous influence on local yarn denier due to feed yarn variation or threadline buckling.

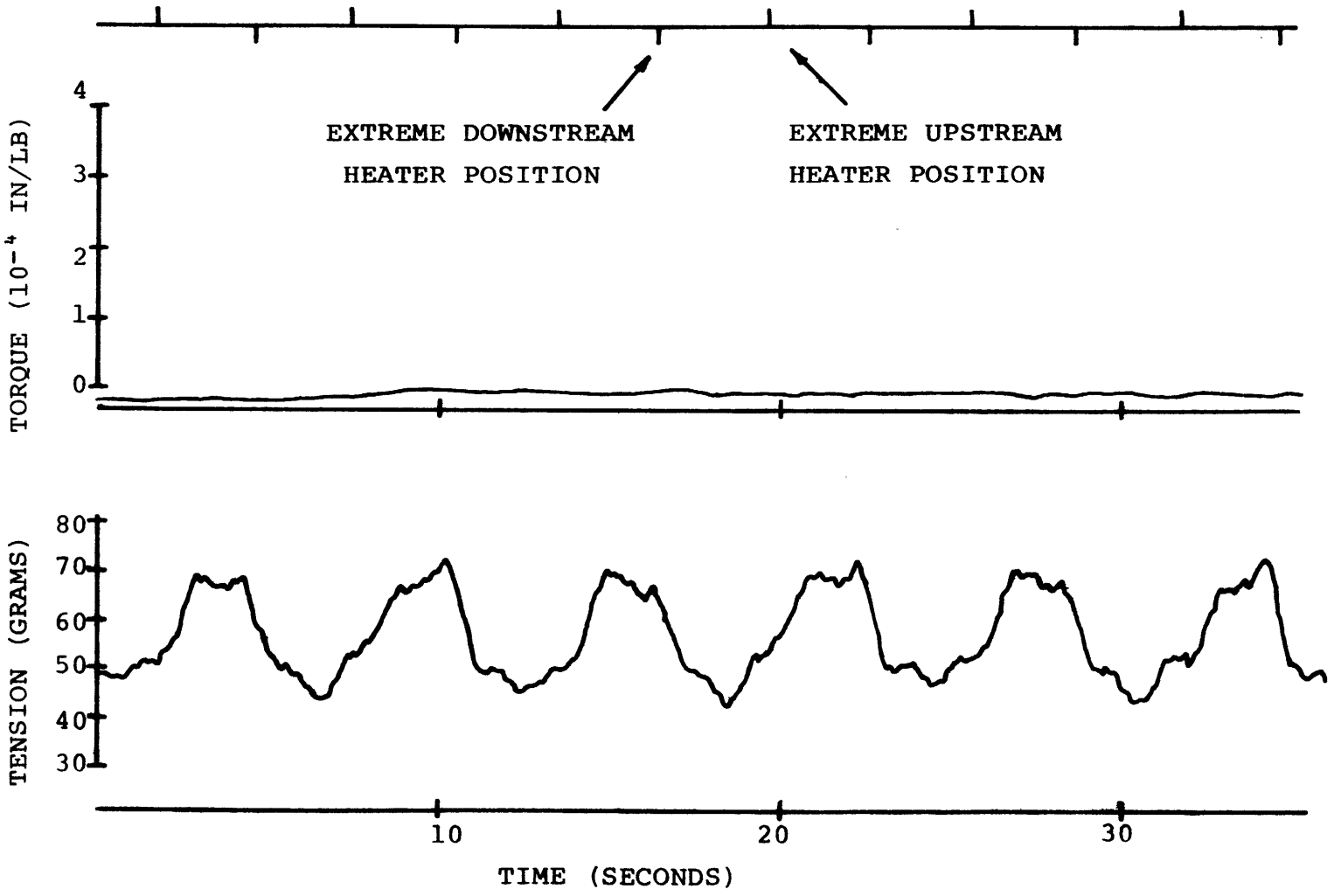

FIGURE 31 THREADLINE TENSION IN RESPONSE TO OSCILLATING DRAW POINT POSITION DURING STRAIGHT DRAWING [1.6 DR; NO SPINDLE; 3.1 IPS; 210°C]

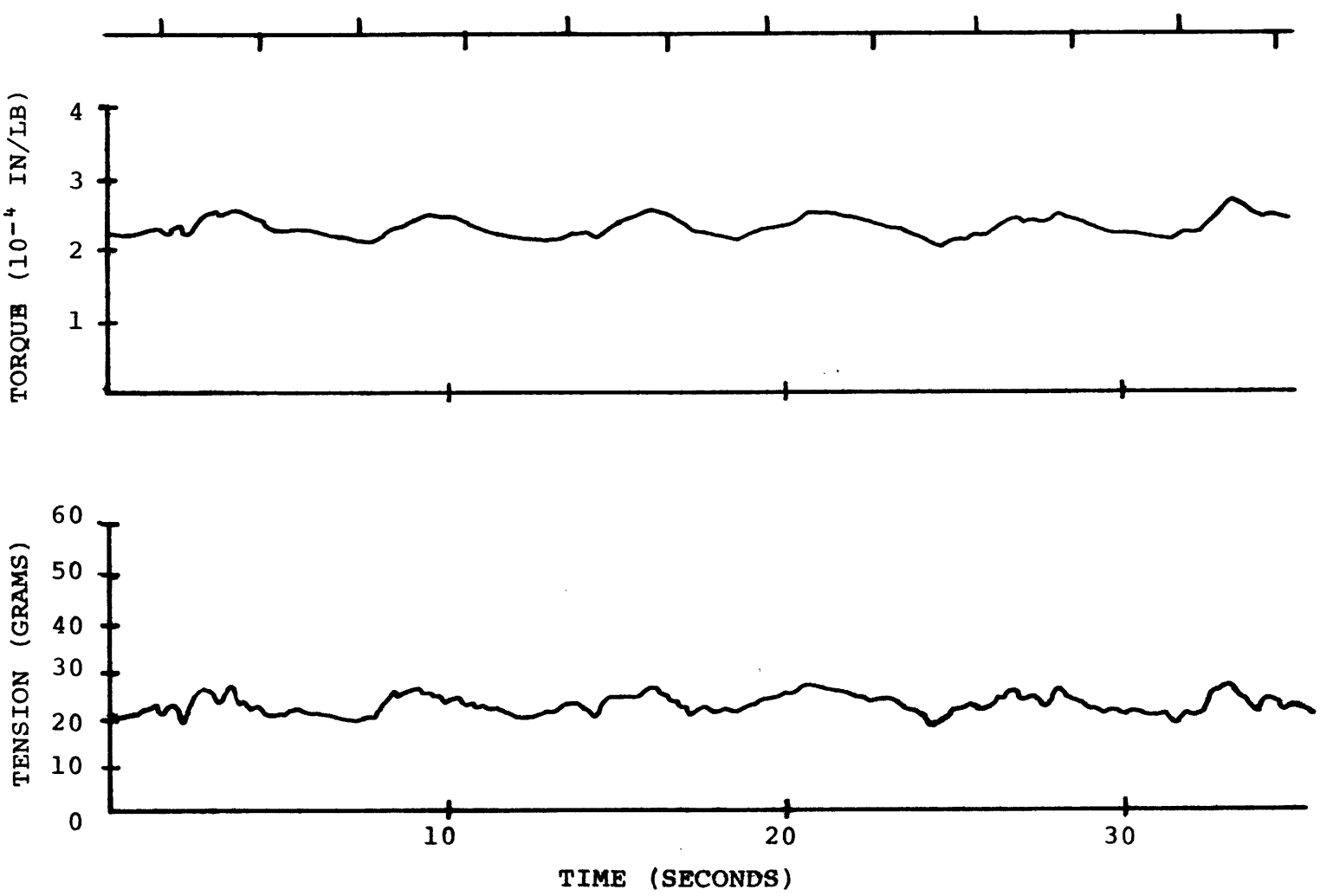

FIGURE 32 THREADLINE FORCES IN RESPONSE TO OSCILLATING DRAW POINT POSITION DURING DRAW TEXTURING [1.6 DR; 60 TPI; 3.1 IPS; 210°C]

Computer Simulation of Forced Draw Point Motion

Draw point motion can be simulated in the kinematic computer model by varying the lengths of Zones 1 and 2 such that the sum of the two zone lengths (the total texturing zone length) remains constant, as shown under Input Parameters (d) in Appendix A-3. Using inputs corresponding to the draw point position and velocity expressions along with the machine conditions used on the experimental apparatus, the force vs. time curves of Figs. 33a and 33b result. In both the straight drawing and draw texturing simulations, the computer model has overpredicted the amplitude of force variation. This follows from the discussion in the early paragraphs of this section, since no elastic element has been included in the kinematic computer model threadline.

III.E. Feed Yarn Property Variation

It has been observed that when certain POY-PET feed yarns are drawn in the MITEX machine at operating Condition I [1.6 DR; 0 TPI; 3.1 IPS; 210°C], periodic variations in drawing tension occur as shown in Fig. 34. While two different frequencies of tension variation are evident in the data of Fig. 34, the higher frequency variation has a period corresponding exactly to one revolution of roller 2 on the MITEX, and reflects an out-of-round roller. The lower frequency variation, however, has a sufficiently long period that it is not likely to have been caused by any machine related periodicities, but rather by variation along the feed yarn and, indeed, it corresponds exactly to the distance traversed by the feed yarn in going from one end of the feed yarn package

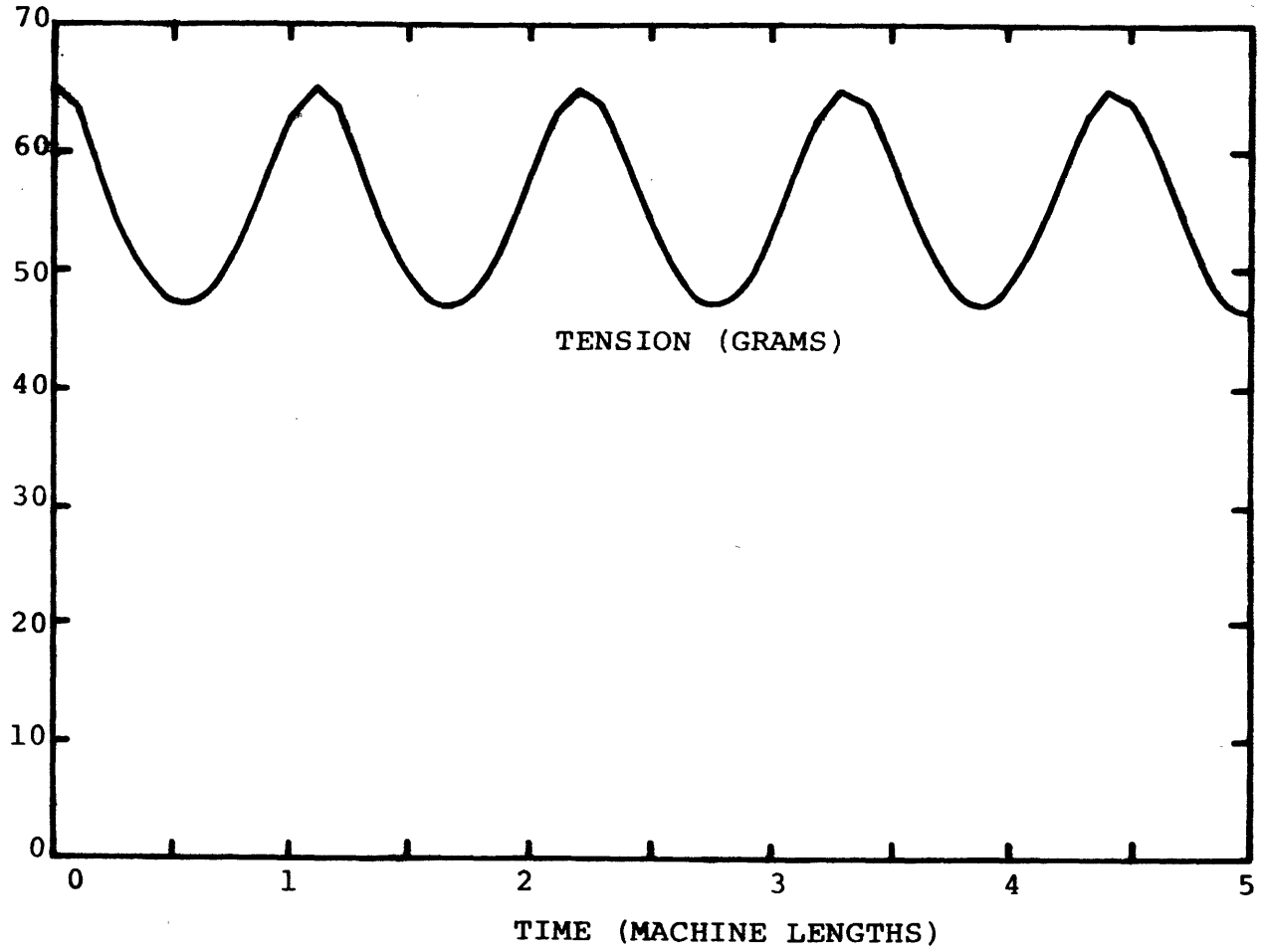

FIGURE 33a COMPUTED THREADLINE RESPONSE TO OSCILLATING DRAW POINT POSITION DURING STRAIGHT DRAWING

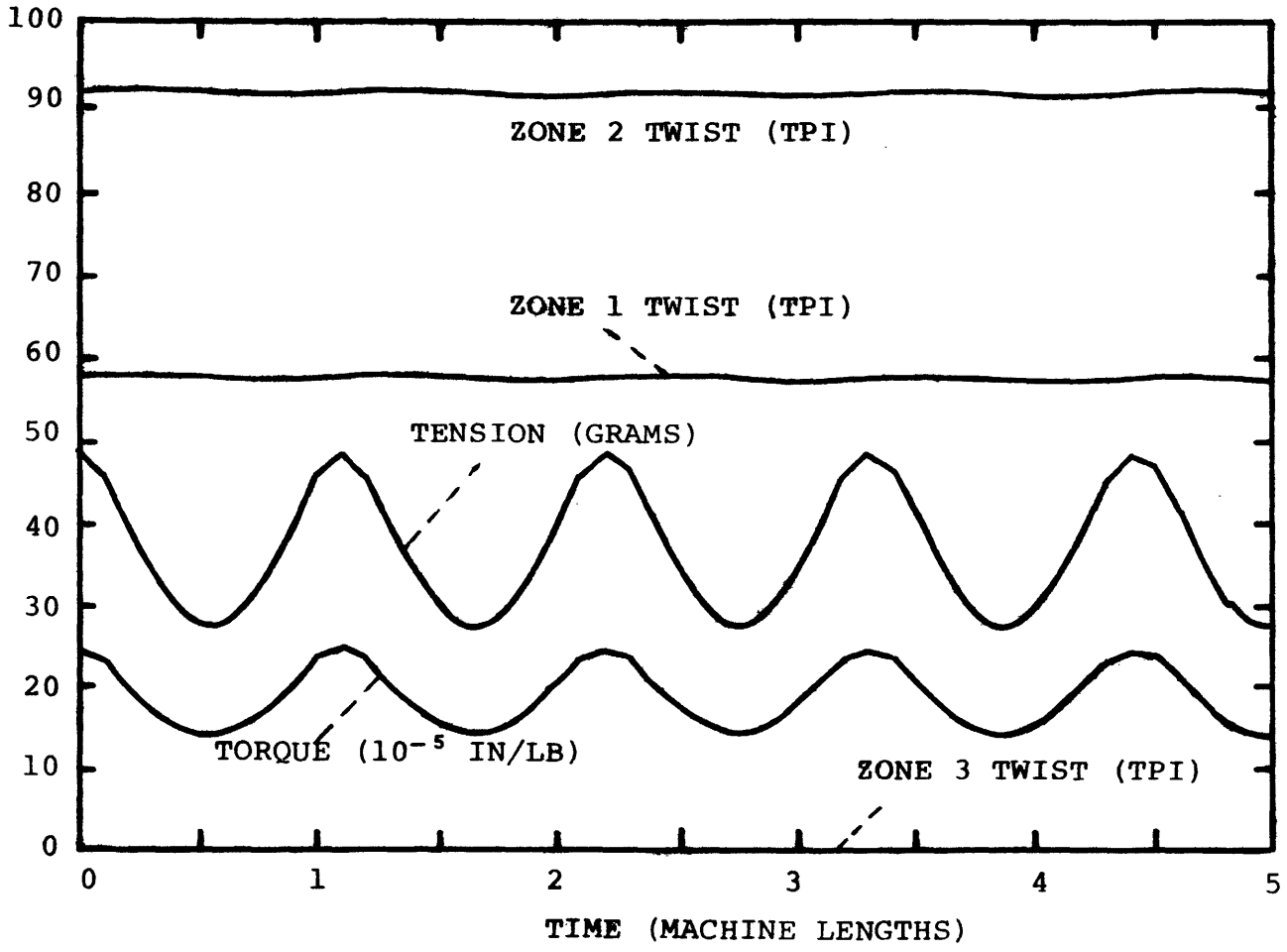

FIGURE 33b COMPUTED THREADLINE RESPONSE TO OSCILLATING DRAW POINT POSITION DURING DRAW TEXTURING

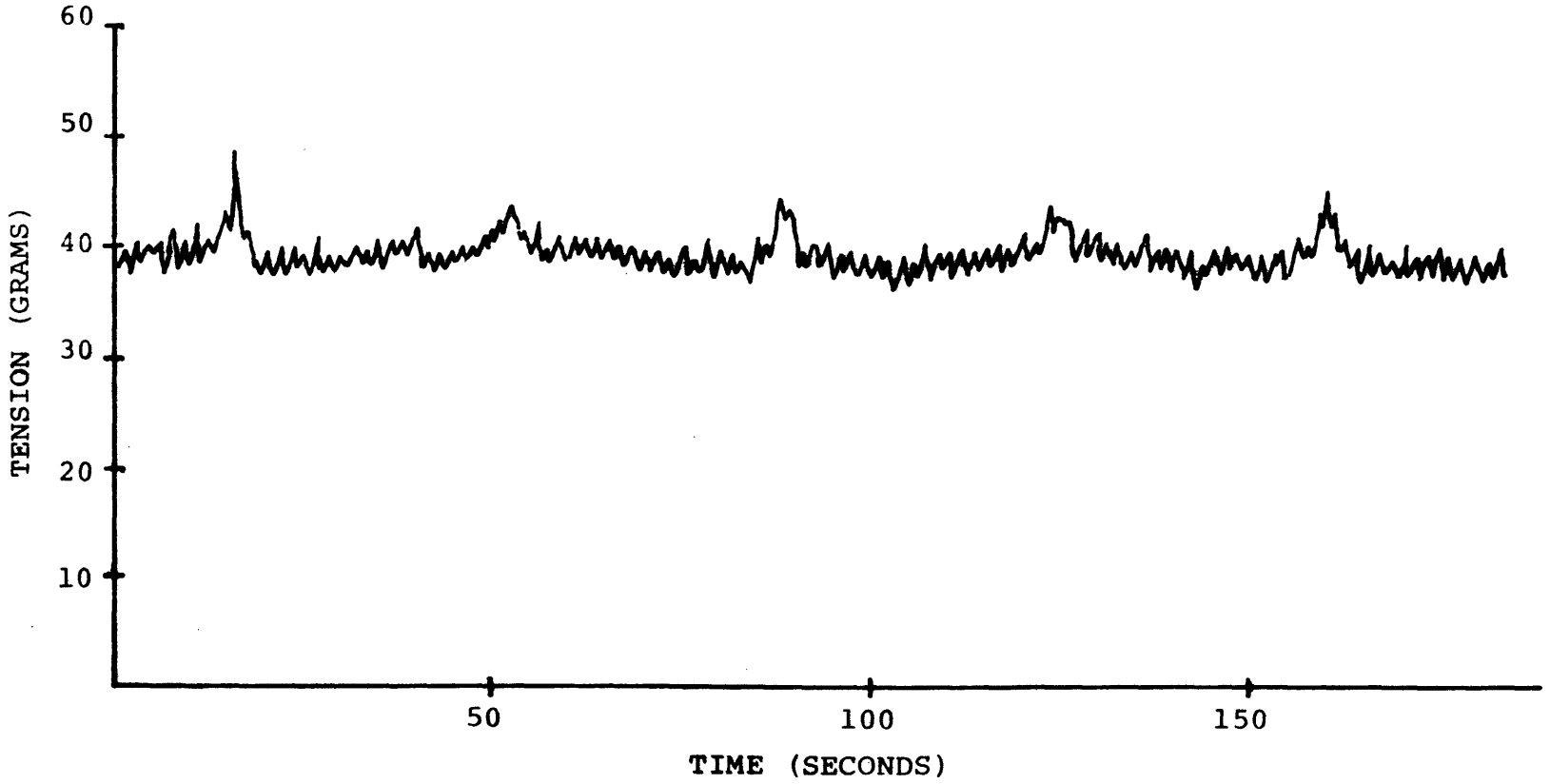

FIGURE 34 PERIODIC DRAW TENSION VARIATIONS IN POY-PET FEED YARN DURING STRAIGHT DRAWING AT 1.5 DR; 3.1 IPS; 210°C.

to the other (i.e. the package height multiplied by the secant of the wrap angle of the yarn on the package).

This observation provides strong evidence that certain POY-PET feed yarns contain property variations along their lengths which may interfere with normal steady state texturing machine operation. It cannot be stated as a result of the data in this section what the varying yarn property or properties are, but the variation seems to be associated with each end of the feed yarn packages, which suggests a variation in windup tension caused by winding devices during feed yarn spinning. Such non-uniform windup tensions could cause fine structure variations in the yarn as package stresses relax over a period of time after the winding operation.

A number of commercial POY-PET feed yarns from different manufacturers have been tested at operating Condition I [1.6 DR; 0 TPI; 3.1 IPS; 210°C] (straight drawing), and then subsequently at operating Condition J [1.6 DR; 65 TPI; 3.1 IPS; 210°C] (draw texturing), in order to investigate uniformity differences between feed yarns and to what extent yarn property variations might influence threadline forces during texturing. The results of these tests are tabulated in Table 1. It is evident that six of the nine feed yarns tested at both operating conditions showed force variations in texturing as well as in straight drawing, and only one of the eighteen yarns tested in straight drawing (yarn 3) failed to show a detectable force variation other than that attributable to the out-of-round roller. The period (λ) of property variation along each of these yarns seems to remain constant along the 200-inch

TABLE 1

FORCE PERIODICITIES

	DRAWING TENSION			TEXTURING TENSION			TEXTURING TORQUE		
Yarn	Avg. Amplitude (g)	% S.S. Value	λ (Feed Yarn) (in.)*	Avg. Amplitude (g)	% S.S. Value	λ (Feed Yarn) (in.)	Avg. Amplitude (g)	% S.S. Value	λ (Feed Yarn (in.)
A	8.0	20	68.7	2.7	11	69.7	.2	8	69.7
B	4.7	14	60.6	1.8	8	60.2	.10	4	60.2
C	5.0	15	----	1.8	8	----	.15	7	----
D	3.9	13	75.0	2.3	10	75.6	.15	7	75.6
E	4.7	15	70.7						
F	4.6	13	75.2	2.3	10	----	.20	9	----
G	5.4	15	75.5						
H	5.1	15	75.0	1.8	8	----	.10	4	----
I	5.4	16	76.2						
J	6.5	17	71.0	2.7	11	69.6	.05	2	----
K	6.5	17	70.3						
L	8.1	20	69.5						
M	6.5	17	71.5						
N	6.0	16	70.6						
O	6.4	17	70.3	2.7	11	70.2	.05	2	70.2
P	7.2	22	59.9						
Q	4.0	13	60.5						
R	3.9	13	66.7	1.4	20	67.7	.15	13	67.7

NOTES: 1. Where no periodicity is seen, "amplitude" represents random disturbance.

2. Blank spaces indicate yarn not tested.

*Along the original, i.e. undrawn feed yarn.

samples tested, but between yarns it ranges from 60 to 72 inches. The differences in period of property variation between different yarn packages may be due to differences in the spinning machine windup settings used by the various feed yarn manufacturers.

It appears as though the type of feed yarn variation observed in these tests is fairly common in commercial POY-PET feed yarns, and there is a good chance that the variations can cause threadline forces to fluctuate periodically during commercial texturing. Any fluctuation occurring in the texturing zone could conceivably disrupt the operation of the twister or affect the average yarn draw ratio, thus causing texturing yarn variability.

Once equipment for continuous evaluation of both feed and textured yarns is available in the laboratory, more thorough investigations can be conducted to determine the response of the texturing system to a range of feed yarn non-uniformities.

III.F. Transient Threadline Behavior in Industrial Texturing Machines

During the course of one of our texturing research programs at M.I.T., this author was very fortunate in having the opportunity to spend a few days at a large industrial texturing plant. Activities during this time included a brief experiment performed on three different types of full scale texturing machines, with the following objectives in mind:

(1) Determine the threadline tension behavior and settling time in industrial machines following a reproducible threadline disturbance.

(2) Compare the structure and dyeability of fabric knitted from yarn which had been textured under the disturbed condition with fabric knitted from normal textured yarn.

(3) Observe differences in behavior between the three different machines, each subjected to a similar disturbance.

It was discovered that the hand held tension measuring unit available at the plant could serve a convenient dual purpose. Aside from the usefulness of this device for measuring tension in the running threadline, it was found to provide an ideal threadline disturbance by virtue of the design of its measurement prongs, which apply tangential forces to the yarn through surface friction. As shown in Fig. 35, the three rigid prongs are pushed against the threadline until the threadline slips between them and rides in shallow grooves. The center

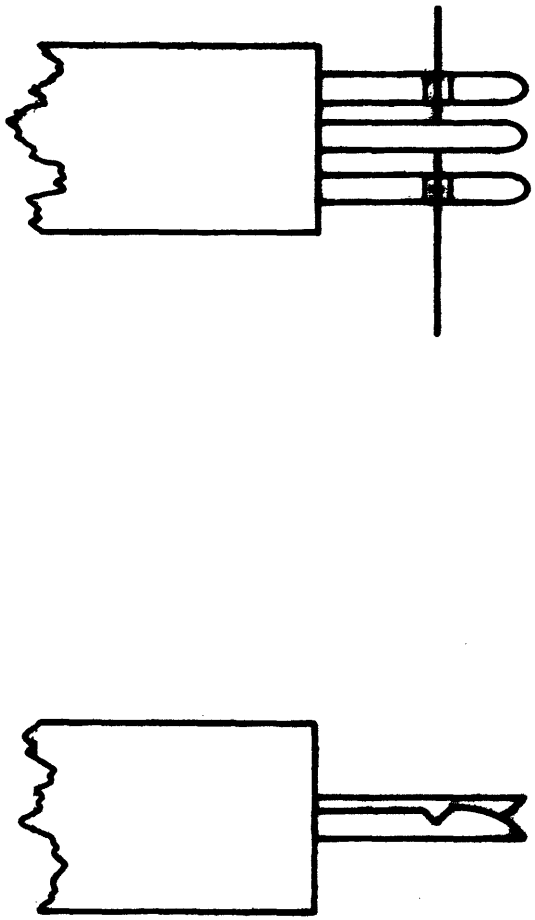

FIGURE 35a TENSION MEASURING PRONGS OF HAND HELD TENSION DEVICE

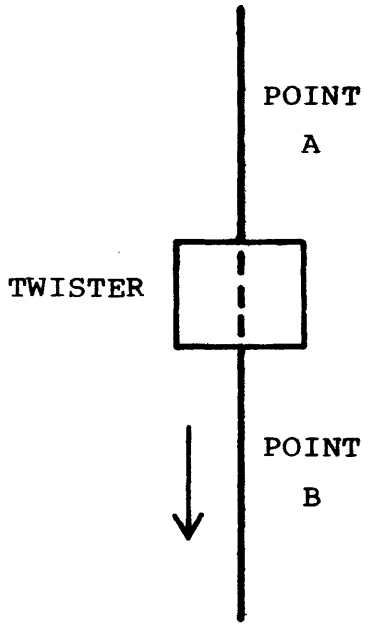

FIGURE 35b TENSION PRONGS WERE APPLIED AT POINTS A AND B, BEFORE AND AFTER THE TWISTER

prong has a strain gauge buried in its base, supplying the tension signal which is displayed on a meter.

In performing the experiment, one such tension device was held continuously in position in the post-spindle zone (point B), while another was imposed in front of the spindle (point A) periodically, on a predetermined schedule. The resulting time varying tensions displaced on both meters were recorded in approximate form, and following each test, the package of textured yarn was removed from the machine and used to produce a circular-knit fabric sample containing yarn textured during the imposed disturbances. This test fabric was then dyed in a similar manner as is used for commercial fabrics, and was evaluated in terms of fabric structure and the variation in apparent darkness of the dye color along the sample.

The texturing machines at the plant consisted of three different models--one pin twister model and two disc type friction twister models. The windup roller speeds of the machines are listed below, along with schedule of application of the pre-spindle (point A) tension measuring device.

Machine 1 (pin): 175 m/min
Disturbance: 30 secs on,
30 secs off,
10 cycles

Machine 2 (disc): 300 m/min
Disturbance: 20 secs on,
20 secs off,
10 cycles

Machine 3 (disc): 374 m/sec

Disturbance: 15 secs on,

15 secs off,

10 cycles.

The resulting tension traces are shown in Figs. 36a, b, and c. Smooth tension lines are used here, but actual tension was observed to jump around randomly by roughly $\pm$1.5 grams at high frequencies.

An immediate similarity can be noticed between the tension trace at point B in machine 1 and that for the step change in spindle speed observed in Section III.B. Apparently, introduction of the tension prongs at point A has a similar influence on the threadline as a step reduction in spindle speed, i.e. the propagation of a lower twist level into the texturing zone. Similarly, when the tension measuring device is removed from point A after a steady state threadline condition has been reached with the device in place, the threadline behaves as though spindle speed undergoes a step increase.

The mechanism by which this twist change occurs is not clear, although it is possible that spindle slippage is taking place upon the insertion of the prongs. If spindle slippage were found not to occur, however, it would be difficult to explain why the twist level in the yarn upstream from point A decreases upon the insertion of the prongs, except to say that somehow torque is reduced in the threadline upstream of point A such that only a lower level of twist can be inserted into the yarn entering the machine.

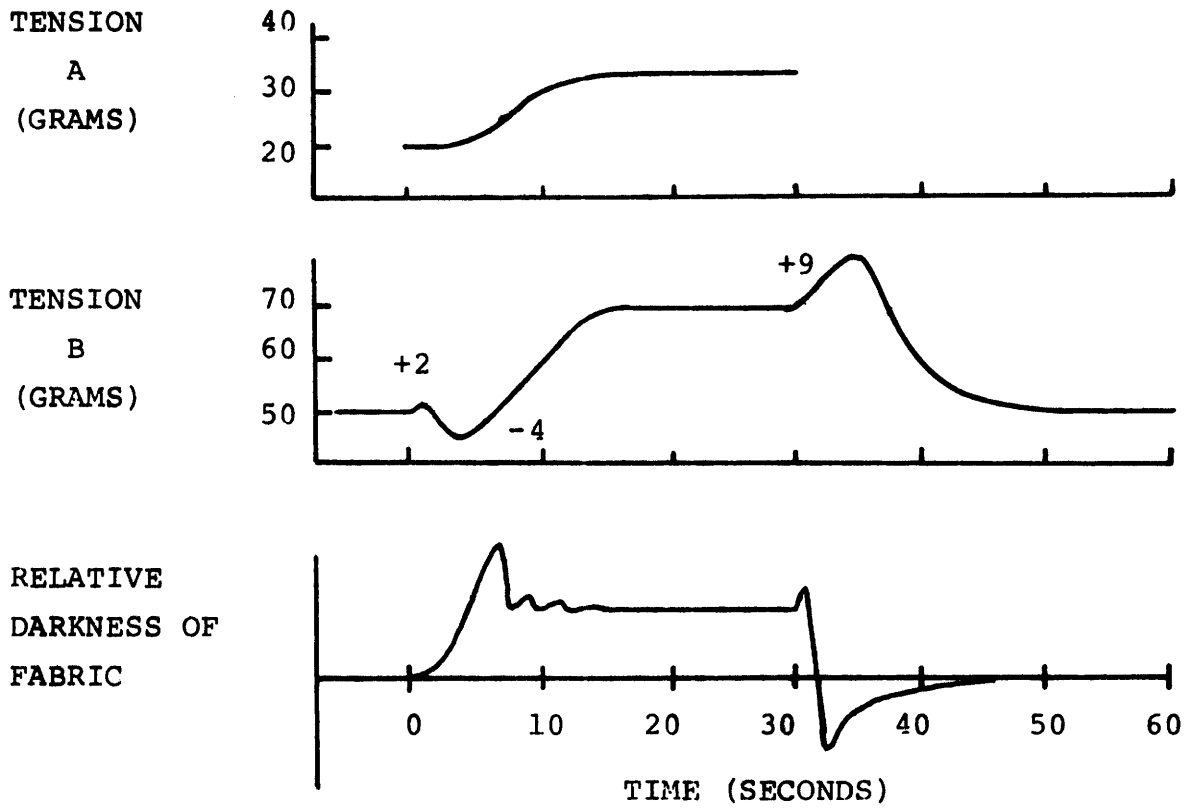

FIGURE 36a MACHINE 1--THREADLINE TENSION AT POINTS A AND B AND APPARENT DYED FABRIC DARKNESS VS. TEXTURING MACHINE TIME

In comparing the threadline tension response of the pin twister machine to that of the disc twister machines, an interesting fundamental difference can be observed. Apparently little or no twist change occurred in the texturing zone of the disc twister machines upon the insertion of the tension measuring prongs, as evidenced by the constant tension measured at point A. It is possible that a very rapid tension change took place at point A before the tension device could be read, but this appears unlikely since twist changes require times on the order of several machine lengths to be completed.

Thus, it appears that the friction twisters are in a sense self-compensating, since the tension/torque jump across the prongs shows up as an increase in the tension measured at point B, but does not seem to affect the texturing zone threadline upstream of point A.

Indeed, this difference in behavior between pin and disc machines is also seen quite clearly in the test fabrics knitted from the yarn textured during these tests. A subjective indication of the relative darkness of dyed fabric plotted against machine time for each sample is shown in Fig. 36 for one disturbance cycle. Both the tension traces and fabric color variations repeated very well for all 10 cycles in each test.

The darker-than-normal and lighter-than-normal sections in the dyed fabric from machine 1 have been related very closely to the twist changes which occurred as a result of the threadline disturbance. At the section of fabric corresponding to a transient reduction in threadline twist, a very dark stripe

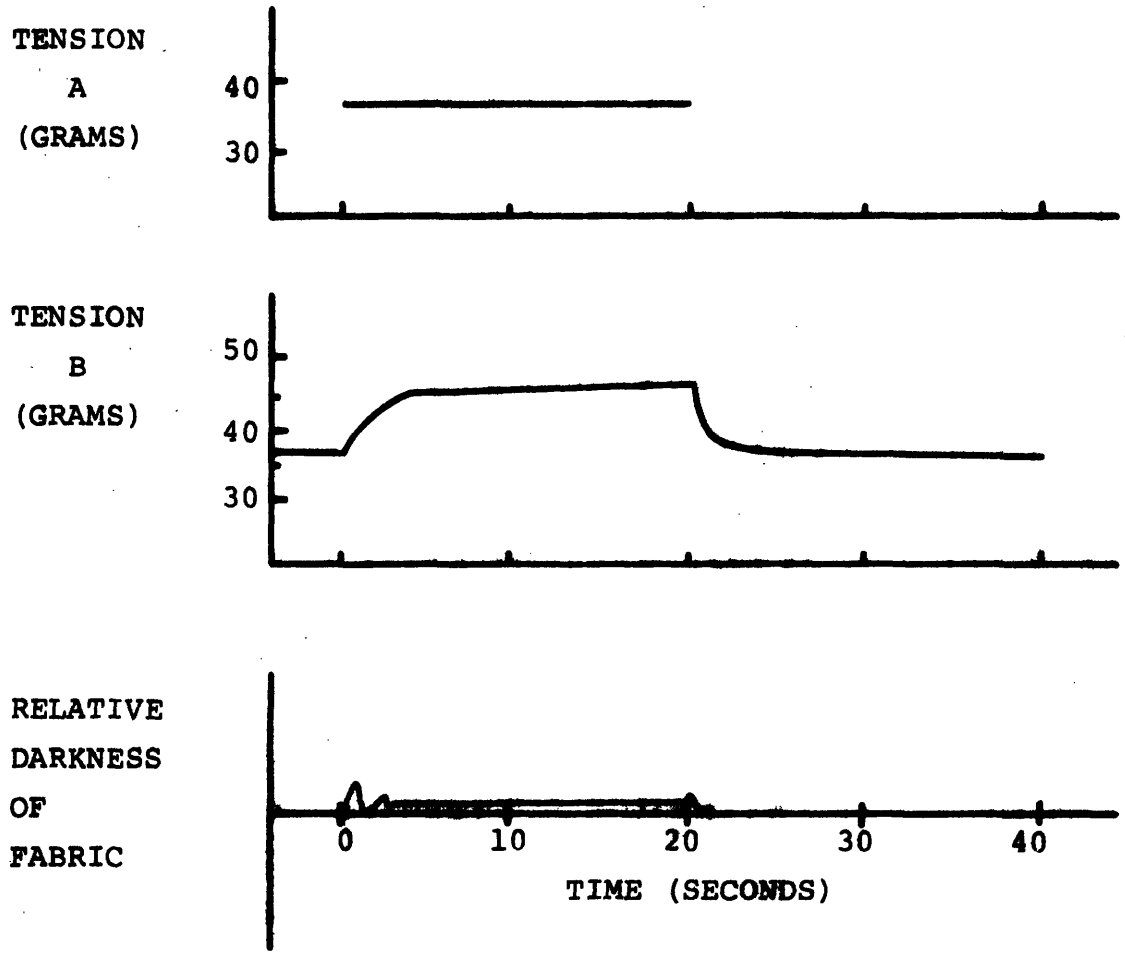

FIGURE 36b MACHINE 2--THREADLINE TENSION AT POINTS A AND B AND APPARENT DYED FABRIC DARKNESS VS. TEXTURING MACHINE TIME

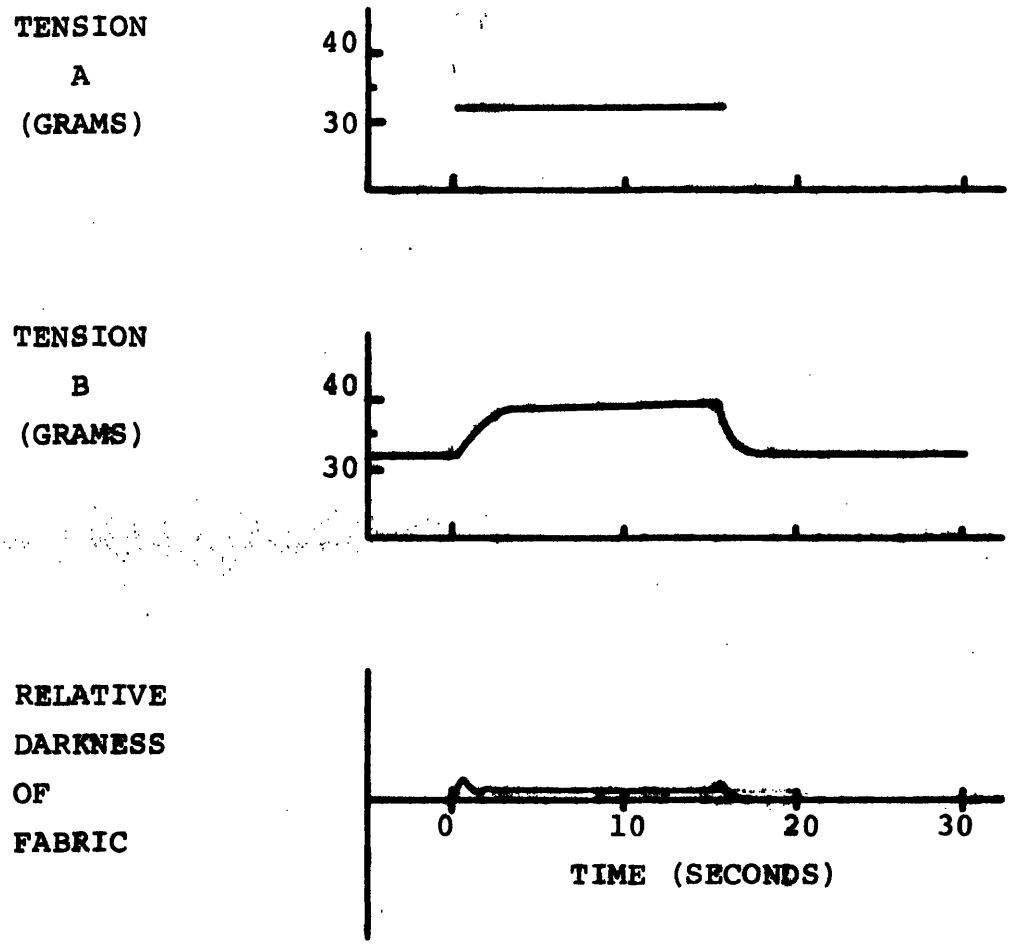

FIGURE 36c MACHINE 3--THREADLINE TENSION AT POINTS A AND B AND APPARENT DYED FABRIC DARKNESS VS. TEXTURING MACHINE TIME

is seen which is apparently due in part to improperly textured yarn containing many tight spots as indicated by the rough fabric texture in the dark segments. The evidence of tight spots in the fabric confirms observations made on the texturing machine threadline downstream of roller 2 immediately following the insertion of the prongs at point A. A significant reduction in the diameter of the yarn leaving rollers was observed which lasted a period of several seconds, indicating a long string of tight spots similar to that observed on the MITEX machine following a step decrease in spindle speed.

The darkness of this stripe could also be due in part to a lower average yarn draw ratio which would occur at the draw point during transient twist reduction. A lower yarn draw ratio would cause lower crystallinity and allow for greater dye accessibility to the filaments. Conversely, a light stripe is apparent in the segment of fabric, including yarn which had been subjected to a transient increase of twist level in the texturing zone, reflecting a higher (average) yarn draw ratio and therefore a lower dye accessibility to the filaments. Tight spots were not observed in the fabric at this point.

In contrast to the behavior of machine 1, the two disc machines were affected only slightly by the threadline disturbance, although stripes of fabric representing the actual instants of insertion or withdrawal of the tension prongs were readily evident, presumably due to temporary excessive disturbance of the threadline at those times. It is also worthy of note that in all three samples the fabric segments corresponding to steady state operation with the prongs in

place at point A exhibit greater light transmittance than the fabric segments corresponding to steady state operation without the prongs at point A, despite the darker appearance of the former segments under reflected light.

This experiment performed on commercial texturing machines has thus confirmed several observations which have been made on the MITEX pin twister machine and, at the same time, has allowed for an introduction to the mechanics of friction twister machines.

III.G. Conclusions and Recommendations

In this thesis, data have been compiled relating to several aspects of non-steady state threadline behavior in the false twist texturing process. Emphasis has been placed on threadline force response to variation in spindle speed, unsteady spindle slippage, motion of the draw point, and feed yarn property variations. In addition, a unique opportunity to visit a commercial texturing plant has allowed us to confirm, at least qualitatively, the relevance of some of our laboratory texturing observations to the case of full scale machines. At the same time it has provided a look at what effect certain controlled threadline disturbances can have on the textured yarn in terms of the structure and dyeing characteristics of a knit fabric made from the test yarns. The above studies have thus served to pinpoint some aspects of the texturing process conceivably responsible for types of variation in textured yarns of concern to the industry.

It is doubtful that such pronounced threadline instabilities as those observed in our laboratory cycling study, would be allowed to occur at industrial texturing conditions, but the possibility does exist that some amount of uncontrolled twister slippage could occur such that twist levels in the texturing zone of a pin spindle machine would vary with time. Twist variation in friction twisting is often a function of the specific twisting head, i.e. its geometry and materials. Such twist variation in draw texturing would cause subtle changes in local filament draw ratio and in the

crimp levels of the resulting textured yarn, and might be detectable in the dyed fabric.

Draw point motion, on the other hand, must be taking place to some extent in every draw-texturing machine position. Unfortunately, information as to the degree of fluctuation of the draw point in commercial machines has not been encountered but it remains a fascinating aspect of the texturing system which would seem to warrant further attention. The implications of drawpoint motion in the draw texturing threadline are two-fold. Not only would the resulting denier and draw ratio variations in the textured yarn cause local dye uptake differences along the yarn length, but also fluctuation in threadline forces which accompanies drawpoint motion could upset the steady state operation of the twister, causing changes in the rotational velocity of the yarn at the twister. As has been shown in earlier sections, changes in rotational velocity of yarn at the twister can, in turn, have a major influence on threadline forces; and hence a complicated chain of interactions between the twister and the draw-point can be envisaged.

In this regard, it has been shown in this thesis that forced motion of the draw point (occasioned by heater movement) will result in a tension variation, but the converse to this interaction has not been investigated as a part of the present studies. Observation of the draw point during oscillation of the spindle speed, for instance, could provide some useful information concerning the interactions between the draw point

and the twister.

Another source of texturing zone force variations has been shown to be variation in feed yarn properties along the yarn length. A broader characterization of property variations in commercial feed yarns would be desirable in any continuing study on the causes of textured yarn variability.

Once equipment for continuous testing of yarn properties is obtained, the effect of the texturing heater temperature variation can be explored more effectively than is presently possible. Heater temperature, like yarn draw ratio, is known to be of paramount importance in the texturing process, and can greatly affect yarn molecular structure and thus its dyeability characteristics. For this reason, commercial heater temperatures are maintained as accurately as is commercially feasible, usually to within $\pm 2°C$. However, the question of whether the twisted yarn attains the full temperature of the heater in its brief pass is difficult to resolve, particularly at today's high machine speeds. For this reason, studies of heater to yarn heat transfer are vital before a complete picture of the causes of textured yarn variability can be established.

Finally, the effect of threadline buckling on textured yarn properties has not been established in this thesis, as only qualitative observations concerning the origin and appearance of buckles have been discussed. Further study of the interaction of buckled yarn with both the heater and the twister appears to be highly desirable.

REFERENCES

1. Backer, S., Yarn, Scientific American, December, 1972, pp. 52-54.
2. Brookstein, D.S., On the Dynamics of Draw Texturing, Sc.D. Thesis, Department of Mechanical Engineering, M.I.T., Cambridge, Massachusetts, 1975.
3. Backer, S. and Yang, W-L, Mechanics of Texturing Thermoplastic Yarns, Part II: Experimental Observations of Transient Behavior, Textile Research Journal (in press).

BACKGROUND LITERATURE

Backer, S. and Yang, W-L., Mechanics of Texturing Thermoplastic Yarns, Part I: Experimental Observations of Steady State Texturing, Textile Research Journal, Vol. 46, pp. 599-610.

Brookstein, D.S. and Backer, S., Mechanics of Texturing Thermoplastic Yarns, Part III: Experimental Observations of Torsional Behavior of the Texturing Threadline for Pre-drawn PET Yarns, Textile Research Journal (in press).

Clements, J.L., The Relationship of Dye Uniformity of False Twist Textured Polyester Yarns to Fabric Streakiness, Knitting Times, Vol. 42, No. 15, April 10, 1972.

Denton, M.J., Twisting-Rate Variations in the False-Twist Threadline, Part I: Background and the Effect of a Step Change in the Twisting Rate, Journal of the Textile Institute, No. 8, 1975.

Denton, M.J., Twisting-Rate Variations in the False-Twist Threadline, Part II: The Effects of a "Rectangular-Pulse" Transient Change and a Sinusoidal Variation in the Twisting Rate, Journal of the Textile Institute, No. 8, 1975.

Thwaites, J.J., The Mechanics of Friction-Twisting, Journal of the Textile Institute, Vol. 61, No. 3, March 1970.

Thwaites, J.J., Mechanics of Texturing Thermoplastic Yarns, Part IV: The Origin and Significance of the Torsional Behavior of the False-Twist Threadline, Textile Research Journal (in press).

APPENDIX 1

Observations of the Torque-Tension Behavior of a Monofil Coil Spring

An experiment was performed early in the course of the present research which illustrates rate dependent behavior in polyester filaments.

A polyester coil spring was prepared from 16 monofil which had been wrapped in a closed "S" coil around a .25-inch diameter aluminum rod. After the coil was heated in a 215°C oven for about 20 minutes and allowed to cool in room air, it retained its closed coil configuration upon being removed from the rod. A portion of the coil was then stretched under a load of about 300-400 grams and subsequently allowed to return to zero load. This cycle was repeated several times until the coil would only return to a helix angle of about 70°, and a diameter of about .35 inches after sitting for several minutes under no load.

From this coil a sample containing 6 turns was cut and mounted in the apparatus shown in Fig. A1-a, under conditions of zero tension and zero torque. The lower grip/weight assembly had a total weight of about 100 grams. This sample was then subjected to the following schedule of events:

(1) Stretch the spring at a rate of 10 inches per second (while holding the twisting platform fixed) until the weight lifts off the platform. (This straightens the spring to a large extent, but not completely.)

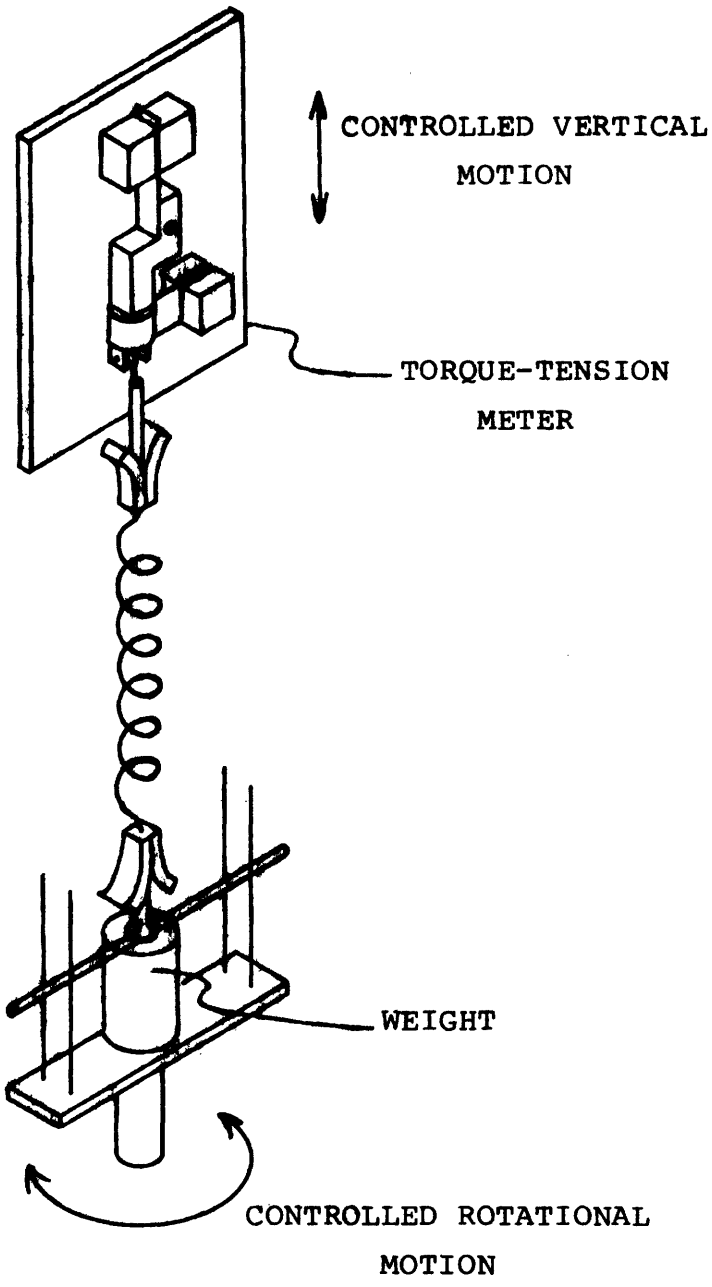

FIGURE A-1a MONOFIL COIL TESTING APPARATUS

(2) Unwind the twist from the sample at a rate of 100 RPM (6 revolutions of the twisting platform in the "Z" direction).

(3) Allow the spring to retract at a rate of 10 inches per minute while holding the twisting platform fixed.

Roughly a 5-second delay has occurred between each of the above steps.

The torque vs. tension trace resulting from these operations is shown in Fig. A1-b. The curve proceeds as follows:

A-B-C; Step 1

C-D ; 5 second delay

D-E ; Step 2

E-F ; 5 second delay

F-G-A; Step 3.

An interesting aspect of these curves is the drift of torque in the "S" direction between each of the steps 1, 2, and 3, the cause of which is not known. It appears to be a viscoelastic phenomenon within the PET coil material.

The same test was repeated, except that this time a 60-second delay was imposed between steps 2 and 3. The torque vs. tension plot for this second test is shown in Fig. A1-c. The striking difference between Figs. A1-b and A1-c is that in Fig. A1-b torque is seen to diminish monotonically during step 3, while in Fig. A1-c it is seen to increase steadily before beginning to decrease at a low value of tension.

It would be interesting to study these phenomena further to try and gain insight into the viscoelastic effects which

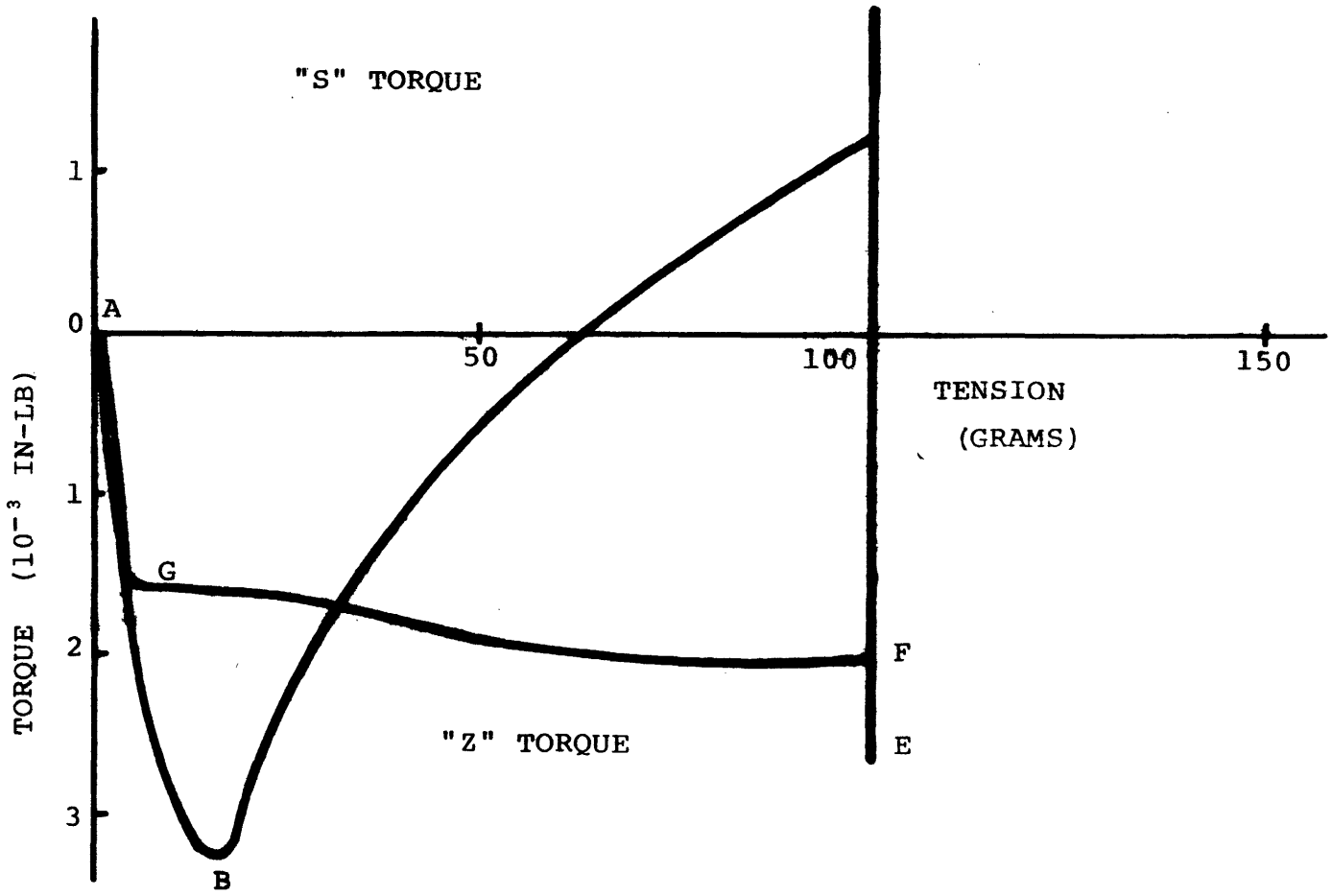

FIGURE A1-b TORQUE vs. TENSION BEHAVIOR OF A MONOFIL COIL SPRING

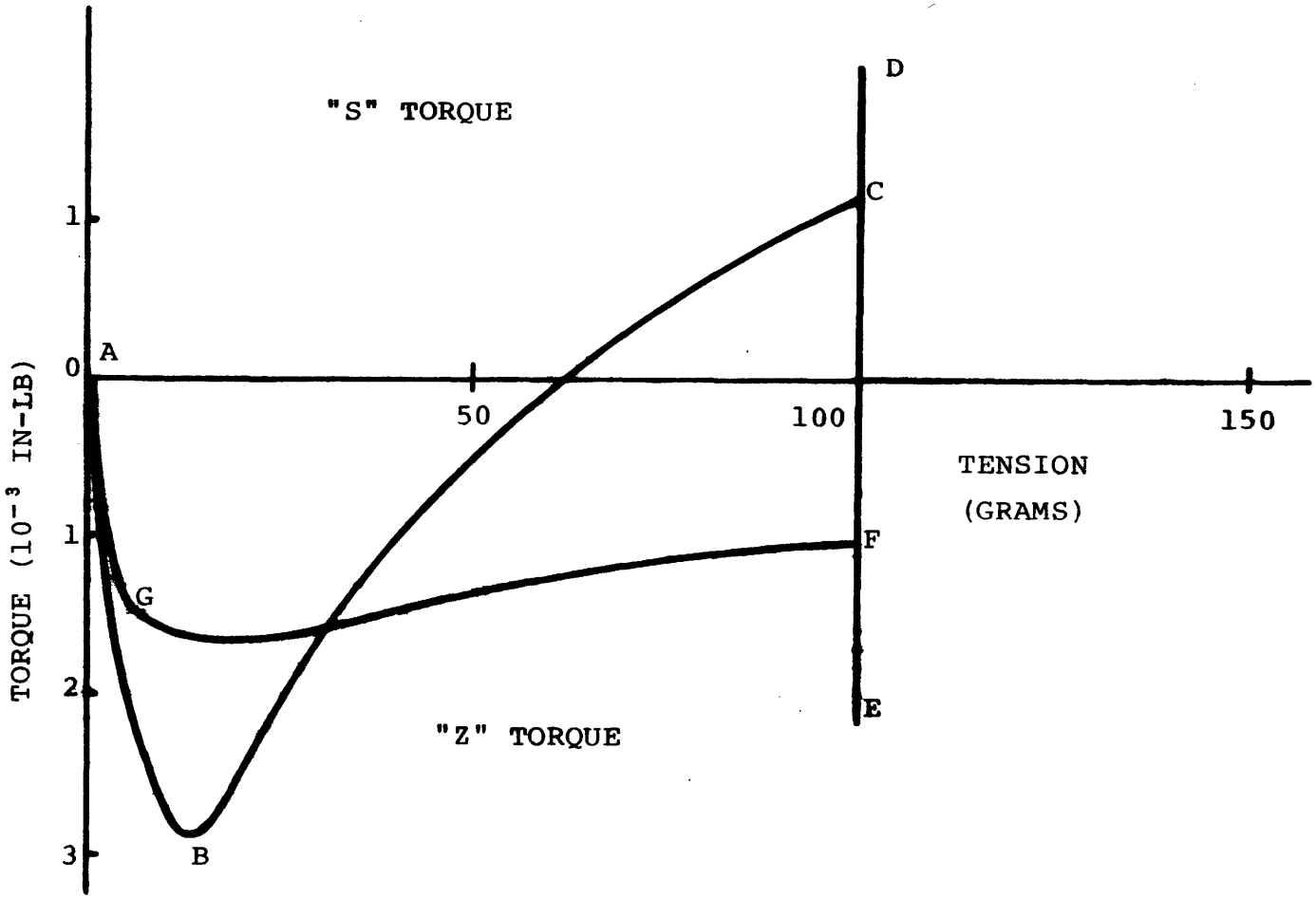

FIGURE A1-c TORQUE vs. TENSION BEHAVIOR OF A MONOFIL COIL SPRING

take place in the texturing process, particularly those which take place as yarn is untwisted at the twister. A start in this direction would be to compare the above force traces with those of filaments which are elastic in the range of deformations discussed.

APPENDIX 2

Examples of Steady State Analysis and Transient Analysis Results

1. Table A2-a: Threadline Tension and Torque during Steady State Draw Texturing of POY-PET.
2. Table A2-b: Steady State and Transient Computer Program Input Data.
3. Table A2-c: Threadline Tension and Torque during Draw Texturing of POY-PET.
4. Figure A2: Threadline Force Response to a Step Change in Spindle Speed (55 TPI to 65 TPI; DR = 1.5).

TABLE A2-a

Threadline Tension and Torque during Steady State Draw Texturing of POY-PET

Draw Ratio	Machine Twist	55 TPI	65 TPI	75 TPI	
1.50	Tension (g)	16.0	13.5	10.0	Experimental
		26.4	22.1	17.3	Computed I
		17.3	15.0	12.2	Computed II
	Torque (10^{-4} in-lb)	1.80	1.75	1.50	Experimental
		2.04	2.48	2.92	Computed I
		1.45	1.85	2.26	Computed II
1.60	Tension (g)	25.0	22.0	15.5	Experimental
		35.7	29.0	23.6	Computed I
		23.9	20.6	16.8	Computed II
	Torque (10^{-4} in-lb)	2.25	2.27	2.12	Experimental
		3.41	2.87	3.32	Computed I
		1.73	2.14	2.56	Computed II
1.71	Tension (g)	40.0	34.2	27.2	Experimental
		48.5	40.8	32.6	Computed I
		33.3	28.6	23.3	Computed II
	Torque (10^{-4} in-lb)	3.15	3.25	3.10	Experimental
		2.89	3.39	3.85	Computed I
		2.09	2.53	2.96	Computed II

TABLE A2-b

Steady State and Transient Computer Program

Input Data for Results in Table A2-a

Variable	I	II	Definitions and Units
AN	30.	30.	(total number fils)
AN0	1.	1.	(number fils in each
AN1	6.	6.	layer of the hot zone)
AN2	9.	9.	
AN3	14.	14.	
BN0	1.	1.	(number fils in each
BN1	6.	6.	layer of the cold zone)
BN2	12.	12.	
BN3	11.	11.	
RFIL	5.81×10^{-4}	5.81×10^{-4}	[in]
ECOLD	4.83×10^{5}	4.83×10^{5}	[PSI]
RR	3.	3.	(EI/GIp)
A	-37.70/AN	-33.0/AN	[g]
B	36.48/AN	28.5/AN	[g]
V1	1.0	1.0	Roller 1 vel [in/sec]
V4	1.5,1.6,1.71	1.5,1.6,1.71	Roller 2 vel [in/sec]
SPIN	55,65,75	55,65,75	[Machine TPI]

TABLE A2-c

Threadline Tension and Torque during Draw Texturing of POY-PET

Draw Ratio	Machine Twist / Yarn Sample	55 TPI (BASIC) A	55 TPI (BASIC) B	55 TPI (BASIC) J	55 TPI (BASIC) D	65 TPI (BASIC) A	65 TPI (BASIC) B	65 TPI (BASIC) J	65 TPI (BASIC) D
1.50	Tension (g)	18.0	15.0	20.0	13.5	15.0	12.3	16.7	11.5
	Torque (10^{-4} in/lb)	2.10	1.75	2.15	1.75	2.00	1.70	2.05	1.70
1.60	Tension (g)	31.5	25.0	30.5	24.0	27.2	21.7	25.5	19.5
	Torque (10^{-4} in/lb)	2.70	2.25	2.55	2.25	2.65	2.25	2.60	2.22

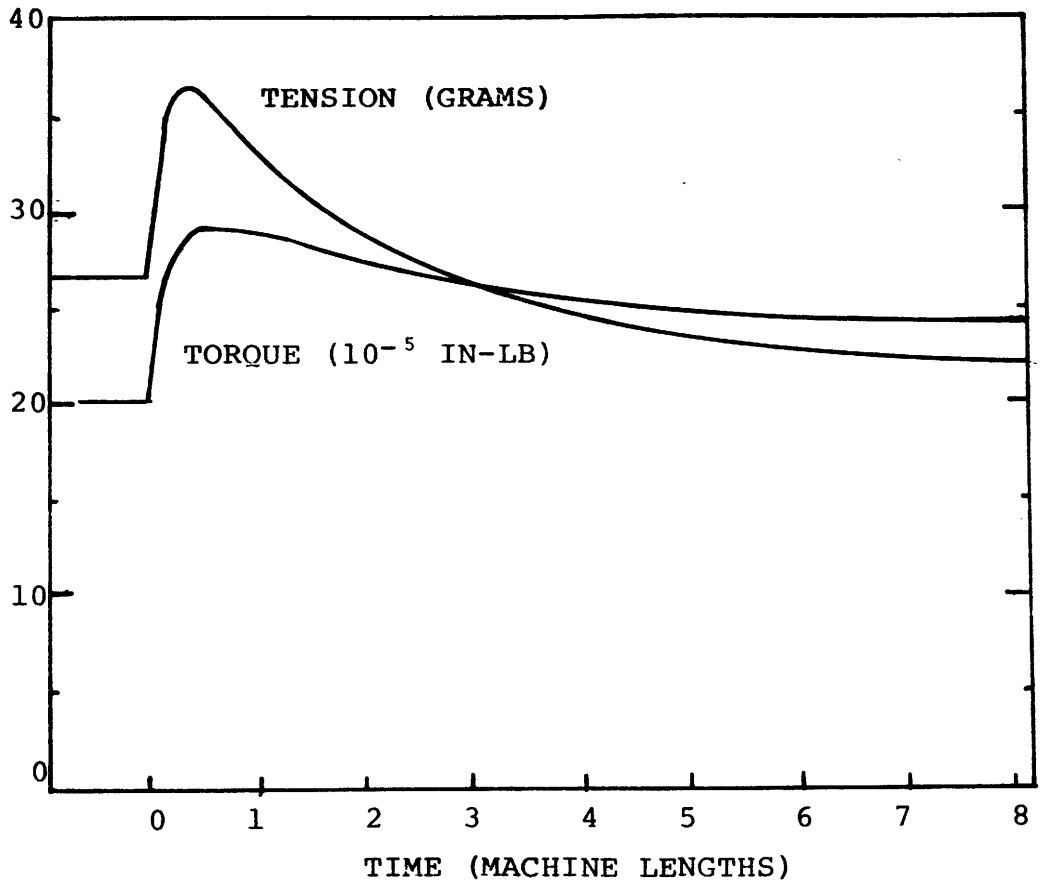

FIGURE A2 TRANSIENT ANALYSIS PREDICTION OF THREADLINE FORCE RESPONSE TO A STEP CHANGE IN SPINDLE SPEED (55 TPI to 65 TPI, DR = 1.5)

APPENDIX 3: Input Parameters and Subprograms for the Kinematic Computer Model

(a) Startup to 60 TPI

Roller Startup:

```
      If (T.LT.1.) go to 10
      Go to 20
   10 V_out = 0
   20 Continue
```

Spindle Speed Change:

```
      PAR 1 = _____
      PAR 2 = _____
      T1    = _____
      T2    = _____
      PAR   = PAR 1
      If (T.LT.T1) go to 30
      PAR   = PAR 2
      If (T.GT.T2) go to 30
      PAR   = PAR 1 * (1. + ((PAR2/PAR 1) -1.) * .5
                * (1. + sin (PI * ((T - T1)/(T2 - T1) - .5))))
   30 Continue
      WE = PAR
```

Input Parameters:

Characteristic length = 17. inches (one machine length)

Characteristic velocity = 3.14 inches/sec (roller 2 surface velocity)

Characteristic force = 293. grams (derivative of tension vs. draw ratio poly-

nomial at DR = 2;

Tension = $Ay(DR)^2 + By(DR)^3$)

PAR 1 = 10.

PAR 2 = 6409.

T1 = 2.0

T2 = 2.4

Rϕ = 1.49 E-4 (Note: placing the single

R1 = 1.49 E-4 filament layer of the model at

R2 = 1.18 E-4 about 80% of the estimated

R3 = 1.18 E-4 outer layer radius of the real

TL1 = .353 yarn seems to provide the best

TL2 = .647 results)

TL3 = .529

V_{in} = .625

V_{out} = 1.0

A = -.125)
)
(Ay = - 37.8)) (Yarn F)
)
B = .126)
)
(By = 37.0))

DTL1 = 0

DTL2 = 0

DTL3 = 0

THϕ = 0

Y = 0., 0. (Initial conditions; θ_2, θ_3)

TSTEP = .1

(b) Step Change in Spindle Speed.

Use "spindle speed change" program of (a). Input para-

meters: same as in (a) except,

65-55 TPI	55-65 TPI
PAR 1 = 6943.	PAR 1 = 5875.
PAR 2 = 5875.	PAR 2 = 6943.
Y = .9601, 0.	Y = .7656, 0.

(c) Oscillating Spindle Speed

Input Parameters:

Characteristic length = 17. inches

Characteristic velocity = 3.14 inches/sec

Characteristic force = 284. grams

$R\phi$ = 1.63 E-4

R1 = 1.63 E-4

R2 = 1.28 E-4

R3 = 1.28 E-4

TL1 = .305

TL2 = .765

TL3 = .459

VIN = .625

VOUT = 1.0

W = .0320 (.001 CPS)

= .0639 (.002 CPS)

= .160 (.005 CPS)

= .320 (.01 CPS)

= .639 (.02 CPS)

= 1.60 (.05 CPS)

= 3.20 (.1 CPS)

= 6.39 (.2 CPS)

= 63.9 (2. CPS)

c) Oscillating spindle speed--Input parameters (continued)

WE = 5969. (1. + .9 * SIN (W*T)

A = -.130

(Ay = -37.0)

B = .127

(By = 36.0)

DTL1 = 0.

DTL2 = 0.

DTL3 = 0.

THϕ = 0.

Y = .8736, 0.

TSTEP = .1 (.001-.02 CPI

= .05 (.05 and .1 CPS)

= .02 (2. CPS)

= .002 (2. CPS)

(d) Draw Point Motion

Zone Length Variation:

TL = TL1 + TL2

TL1 = TL1 + C1 * SIN (W*T)

DTL1 = C2 * COS (W + T)

DTL2 = -DTL1

---

*Note: Computer simulation was run at 56 TPI nominal vs. 60 TPI nominal in the MITEX experiments. Also, slightly different radii, machine lengths, and material parameters (A and B) happened to be used compared with other draw texturing runs.

(d) Draw point motion, continued

Input Parameters: same as in (a) except,

C1 = .0101

C2 = .0575

W = 5.68

WE = 0. (zero TPI)

= 6409. (60 TPI)

Y = 0., 0. (zero TPI)

= .8576, 0. (60 TPI)

(e) Cyclic Threadline Behavior

Spindle Slippage:

```
      If (NEWDT) 10, 50, 60
10    WS = _____
      Go to 30
      If (SMT-SMTX) 30, 30, 40
30    WE = WS
      Go to 50
40    WE = WE - WE * SLF
50    Continue
```

Threadline Tension Control:

```
      If (DFIL - 1.) 80, 80, 90
80    TDR = C
      Go to 100
90    Continue
      TDR = A * DFIL ** 2. + B * DFIL ** 3.
100   Continue
```

(e) Cyclic Threadline Behavior, continued

Elastic Component of Torque:

TORQ = TDR * SIN2 * R2 + TH2 * TK

Input Parameters:

Characteristic length = 17. inches

Characteristic velocity = 3.14 inches

Characteristic force = 2520. grams

$R\phi$ = 1.18 E-4

R1 = 1.18 E-4

R2 = 1.18 E-4

R3 = 1.18 E-4

TL1 = .353

TL2 = .647

TL3 = .529

VIN = .95

VOUT = 1.0

SLF = 1.

TK = 5. E-7

A = -.125

(Ay = -300.)

B = .129

(By = -310.)

DTL1 = 0.

DTL2 = 0.

DTL3 = 0.

TH0 = 0.

FMU = .22 - .15 * TH2 (first run)

= .25 - .15 * TH2 (second run)

C = .001

APPENDIX 4: An Alternate Method of Computing Threadline Forces in the Kinematic Computer Model

In Section II.C, and throughout this thesis, threadline forces in the kinematic computer model have been computed using a polynomial expression for filament tension vs. filament draw ratio, where draw ratio was obtained by considering the filaments inextensible, except at the draw point. It has become evident, as stated in Section III.B, that an improvement in modeling the threadline might be made by considering the filaments to be elastic in the texturing zone (while at the same time retaining the assumption of zero bending and torsional rigidities).

The following development leads to expressions for including elastic filaments in Zone 1 as a means for computing threadling forces in the kinematic computer model, as derived from a simple mass conservation equation:

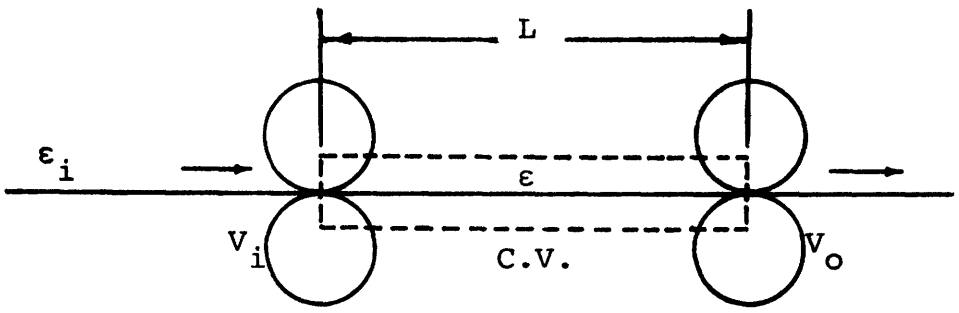

$$M_{cv} = M_{cv}(o) + \int_o^t (\dot{M}_i - \dot{M}_o),$$

where for a linear density equal to unity at zero strain,

$$M_{cv} = \frac{L}{1 + \varepsilon}$$

$$M_{cv}(o) = \frac{L(o)}{1 + \varepsilon(o)}$$

$$\dot{M}_i = \frac{V_i}{1 + \varepsilon_i}$$

$$\dot{M}_o = \frac{V_o}{1 + \varepsilon} \quad .$$

Differentiating this expression leads to

$$\frac{(1 + \varepsilon)\dot{L} - L\dot{\varepsilon}}{(1 + \varepsilon)^2} = \frac{V_{in}}{1 + \varepsilon_i} - \frac{V_o}{1 + \varepsilon}$$

which reduces to

$$\dot{\varepsilon} = \frac{1 + \varepsilon}{L} \left[\dot{L} + V_o - \frac{1 + \varepsilon}{1 + \varepsilon_i} V_i \right].$$

Applying this expression to Zone 1 in the kinematic computer model is done as follows:

L = TL1 * SEC1

$\dot{L}$ = DTL1 * SEC1 + TL1 * TAN1 * SEC1

V_o = DLDOT/DFIL

V_i = ALDOT

where DFIL is computed by solving the cubic polynomial expression,

Filament Tension = ε*EA = (A*DFIL**2. + B*DFIL**3.).

The following would be input parameters for the above expressions:

APPENDIX A-4

1. Pre-strain ε_i
2. Filament stiffness EA
3. A and B (same as in Section II.C).

APPENDIX 5

FEED YARN PROPERTIES AND IDENTIFICATION

1. Sample "F", which is a partially oriented polyester feed yarn of 245 undrawn denier and 34 filaments, was used in all draw texturing studies except for the steady state tests of Appendix 2, where sample C was used (POY-PET 255/30).

2. A 150 denier, 34 filament conventional feed yarn was used in the cycling experiments for conventional feed yarn. (M.I.T. sample B-1.)

3. A 150 denier set textured yarn was used in the cycling experiments for pretextured yarn. (M.I.T. sample D-20.)

TABLE A5

POY FEED YARN PROPERTIES

	A	B	C	D	F	H	J
Ay* (grams)	-40.20	-37.10	-37.70	-34.25	-37.75	-39.37	-42.91
By (grams)	40.56	45.60	36.48	33.22	36.96	37.80	41.89
Filament Radius (in)	---	---	5.81×10^{-4}	---	5.35×10^{-4}	5.35×10^{-4}	---
Young's Modulus (E)	---	---	4.38×10^{5}	---	4.71×10^{5}	4.68×10^{5}	---
Denier**	255	---	255	---	245	245	---

* Tension 210°C = $Ay \cdot DR^2 + By \cdot Dr^3$

** Grams per 9000 meters

APPENDIX 6

Calibration of the Instruments

1. Torque-Tension Meter:

   (a) A 7.3-inch length of thin music wire ($K_t = 3.63 \times 10^{-2}$ in • lbf/in • turn) is used to calibrate the torque meter without removing the apparatus from its in-line position. This wire provides $5. \times 10^{-4}$ in • lb of torque per turn of 360°. The torsional spring constant of the wire was determined using the torsional pendulum method.

   (b) Tension is calibrated by hanging known weights on a free end of the yarn which has been threaded through the meter and then draped over a frictionless pulley which is aligned with the height of the threadline.

2. Heater:

   A group of solid chemical flakes with known melting points are used to calibrate the heater temperature readout (for instance, DICYANDIAMID melts at exactly 210°C)

3. Tachometer:

   The speed of the spindle is adjusted to multiples of the 60-cycle line

frequency with a strobe in order to establish the exact corresponding voltage outputs of the tachometer.

APPENDIX 7

Breakdown of Kinematic Computer Model

Input Initial Conditions

$Y(1)_{t=0}$, $Y(2)_{t=0}$, $Y(3)_{t=0}$, $Y(4)_{t=0}$.

Initialize State Variables

TH2 = Y(1)	Helix angle in Zone 2
TH3 = Y(2)	Helix angle in Zone 3
T4 = Y(3)	Total radians of twist in Zone 4
T5 = Y(4)	Total radians of twist in Zone 5

Input Constant Parameters

PI	Π
R0, R1, R2, R3	Helix radius in respective zones
TK	Torsional spring constant

Input Variable Parameters (Functions of time and/or state variables)

TL1, TL2, TL3, TL4, TL5	Lengths of respective zones
DTL1, DTL2, DTL3	Time derivatives of the zone lengths
VIN, VOUT, VOUT4, VOUT5, WE	Roller velocities and yarn angular velocity at print e
A, B	Tension vs. draw ratio curve-fit coefficients
FMU	Coefficient of friction
TH0	Helix angle in input.

Calculate $\sec(\theta_i)$, $\sin(\theta_i)$, $\tan(\theta_i)$, $i = 0, 2, 3$

```
SECi = 1./COS(THi)

SINi = SIN(THi)

TANi = SINi * SECi
```

Calculate Helix Angle in Zone 1

```
TH1 = ATAN(TAN2 * R2/R1)
```

Calculate $\sec(\theta_1)$, $\sin(\theta_1)$, $\tan(\theta_1)$

```
SEC1 = 1.COS(TH1)
SIN1 = SIN(TH1)
TAN1 = SIN1 * SEC1
```

Calculate $\dot{\theta}_3$

```
X1   = SIN2 * SEC3 * (R3/R2) - TAN3
X2   = SIN2 * SIN3 * (R3/R2)
X3   = SEC3 * SEC3 * (TL3
DTH3 =  (X1 * (VOUT + DTL3) - WE * R3)/(1. -X2) * X3)
```

Calculate Filament Length per Unit Time passing Point f

```
GLDOT = VOUT * SEC3
FLDOT = GLDOT + TL3 * SEC3 * TAN3 * DTH3 + DTL3 * SEC3
```

Calculate $\dot{\theta}_2$

```
Z1   = TAN0 * VIN * R2/R0
Z2   = TAN1 * DTL1 * R2/R1
Z3   = TAN 2 * (DTL2 + (ELDOT/SEC2))
Z4   = SEC2 * SEC2/((R1 * R1/(R2 * R2)) + TAN2 * TAN2)
Z5   = SEC1 * SEC1 * TL1
Z6   = SEC2 * SEC2 * TL2
DTH2 = (Z1 - Z2 - Z3 + WE * R2)/(Z4 * Z5 + Z6)
```

Calculate $\dot{\theta}_1$

```
DTH1 = Z4 * DTH2 * R1/R2
```

Calculate Filament Length per Unit Time Passing Points c and d

```
ALDOT - VIN * SEC0
CLDOT = ALDOT - TL1 * SEC1 * TAN1 * DTH1 - DTL1 * SEC1
DLDOT = ELDOT + TL2 * SEC2 * TAN2 * DTH2 + DTL2 * SEC2
```

Calculate Tension and Torque from Tension vs. Draw Ratio Curve

```
DFIL = DLDOT/CLDOT

TDR  = A * DFIL * DFIL + B * DFIL * DFIL * DFIL

TEN  = TDR/SEC2

TORQ = TDR * SIN2 * R2 + TH2 * TK
```

Calculate Tension in Zone 3 (for a pin spindle)

```
TEN3 = TEN * EXP (2. * PI * FMU)
```

Calculate Total Torque on the Twister in the Threadline Direction

```
SMT = TORQ - TEN3 * TAN3 * R3
```

Calculate Maximum Torque which the Twister can Supply

```
SMTX = R2 * (TEN3 = TEN)
```

Specify Outputs

•

•

•

•

Example:

CL = 24 [inches] characteristic length

Y(10) = TAN1/(2. * PI * R1 * CL) [turns/twisted inch]

•

•

•

•

Integrate Differential Equations

F(1) = DTH2 ---------- $\frac{dY(1)}{dt}$

F(2) = DTH3 ---------- $\frac{dY(2)}{dt}$

F(3) = (TAN3/R3) * VOUT - (Tr/TL4) * VOUT4 ------- $\frac{dY(3)}{dt}$

F(4) = (T4/TL4) * VOUT4 - (T5/TL5) * VOUT5 ------- $\frac{dY(4)}{dt}$

RETURN

Return to "Initialize state variables" with the new values of the state variables, Y(i).